Functional characterization of the *Trypanosoma brucei* polyadenylation complex

Dissertation

Vorgelegt von

Henrik Koch

(M.Sc. Biologie)

zur Erlangung des akademischen Grades

doctor rerum naturalium

(Dr. rer. nat.)

Eingereicht am Fachbereich Biologie und Chemie

der Justus-Liebig-Universität Gießen

Gießen, Juli 2016

Die vorliegende Arbeit wurde am Institut für Biochemie des Fachbereichs 08 der Justus-Liebig-Universität Gießen in der Zeit von September 2012 bis Juli 2016 unter der Leitung von Prof. Dr. Albrecht Bindereif angefertigt.

Dekan:	Prof. Dr. Volker Wissemann Institut für Botanik (FB08) Justus-Liebig-Universität Gießen
1. Gutachter:	Prof. Dr. Albrecht Bindereif Institut für Biochemie (FB08) Justus-Liebig-Universität Gießen
2. Gutachter:	Prof. Dr. Roland K. Hartmann Institut für Pharmazeutische Chemie (FB16) Philipps-Universität Marburg

Table of contents

1 Summary

All protein-coding genes in the protozoan parasite *Trypanosoma brucei* are arranged in long clusters and are transcribed into polycistronic precursor RNAs. These pre-mRNAs require further processing by coupled *trans* splicing and polyadenylation to generate mature mRNAs. Although studies in the last decade have identified numerous spliceosomal components, we still know very little about the components, mechanisms, and dynamics of the 3´ end-processing machinery in trypanosomes. Moreover, most genes in trypanosomes contain one to three *trans* splice and even more dispersed polyadenylation sites, indicating that the regulation of both processes provides another, still not very well explored level of post-transcriptional gene regulation in trypanosomes: In terms of polyadenylation, factors regulating the polyadenylation efficiency of a primary transcript with a single poly(A) site directly affect protein expression, since unprocessed transcripts are degraded or not exported to the cytoplasm. In addition, multiple polyadenylation sites allow the generation of different transcript isoforms of a single gene by alternative polyadenylation.

To characterize the catalytic core of the polyadenylation complex in *T. brucei*, we first identified the poly(A) polymerase [Tb927.7.3780] as the major functional, nuclear-localized enzyme in trypanosomes. In contrast, another poly(A) polymerase, encoded by an intron-containing gene [Tb927.3.3160], localizes mainly in the cytoplasm and appears not to be functional in general 3´ end processing of mRNAs. Based on tandem affinity purification with tagged CPSF160 and mass spectrometry, we identified ten associated components of the trypanosome polyadenylation complex, including homologues to all four CPSF subunits, Fip1, CstF50/64, and Symplekin, as well as two hypothetical proteins. RNAi-mediated knockdown revealed that most of these factors are essential for growth and required for both *in vivo* polyadenylation and *trans* splicing, arguing for a general coupling of these two mRNA-processing reactions.

By combining genome-wide analysis of expression (RNA-seq) and *in vivo* RNA binding (iCLIP), we identified for the first time a *trans*-acting RNA-binding protein, the trypanosomatid polypyrimidine tract binding protein (PTB/hnRNP I) homolog DRBD4, as a regulator of polyadenylation. Based on SELEX-seq and iCLIP, we delineated purine-rich sequences containing AUGA elements as DRBD4 RNA-binding motif and mapped *in vivo* binding sites mainly in untranslated regions (UTRs). Integrating RNA-seq and iCLIP datasets revealed that DRBD4 binds upstream of poly(A) sites and modulates both their activation and repression, thereby affecting general transcript and isoform expression levels.

2 Zusammenfassung

Alle proteinkodierenden Gene des Parasiten *Trypanosoma brucei*, der zu den Protozoen zählt, sind in tandemartigen Clustern angeordnet und werden polycistronisch transkribiert. Die Prozessierung dieser Primärtranskripte in einzelne mRNAs erfordert eine gekoppelte *trans*-Spleiß- und Polyadenylierungsreaktion. Trotz der Identifizierung zahlreicher Faktoren des Spleißosomes in der letzten Dekade, ist nur wenig über die Faktoren, Mechanismen und Dynamik der Polyadenylierungsreaktion in Trypanosomen bekannt. Außerdem verfügen die meisten Gene über ein bis drei *trans*-Spleißstellen und stark degenerierte Polyadenylierungsstellen, wodurch sich eine weitere Ebene der posttranskriptionalen Genregulation ergibt, die jedoch weitgehend unerforscht ist: Eine Veränderung der Polyadenylierungseffizienz bei einem Transkript, das nur über eine Polyadenylierungsstelle verfügt, hat direkte Auswirkungen auf die Proteinexpression, da nicht prozessierte Transkripte degradiert oder nicht in das Cytoplasma exportiert werden. Außerdem ermöglichen mehrere Polyadenylierungsstellen die Herstellung von verschiedenen Transkriptisoformen eines einzelnen Genes durch alternative Polyadenylierung.

Im Rahmen der Charakterisierung des *T. brucei* Polyadenylierungskomplexes haben wir zunächst die funktionelle, Zellkern-lokalisierte Poly(A) Polymerase [Tb927.7.3780] identifiziert. Die zweite Poly(A) Polymerase [Tb927.3.3160], die von einem Gen mit einem Intron kodiert wird, ist hingegen überwiegend cytoplasmatisch lokalisiert und nicht an der Polyadenylierung von mRNAs beteiligt. Mittels *tandem affinity purification* von Epitop-markiertem CPSF160 und einer anschließenden massenspektrometrischen Analyse konnten wir zehn Proteinfaktoren des Polyadenylierungskomplexes in *T. brucei* identifizieren: Homologe der vier CPSF Untereinheiten, Fip1, CstF50/64, Symplekin sowie zwei hypothetische Proteine. Des Weiteren konnten wir anhand eines RNAi-induzierten *knockdowns* der identifizierten Faktoren zeigen, dass die meisten sowohl für das Zellwachstum als auch für die *in vivo* Polyadenylierungs- und *trans*-Spleißreaktion essentiell sind.

Durch die Kombination von genomweiten Genexpressions- (RNA-seq) und *in vivo* RNA-Bindungsdaten (iCLIP) konnten wir das RNA-Bindeprotein DRBD4, ein Homolog des humanen *polypyrimidine tract binding proteins* (PTB/hnRNP I), als ersten *trans*-aktiven Polyadenylierungsregulator in Trypanosomen identifizieren. Mittels SELEX-seq wurden Purin-reiche Sequenzen, die AUGA Tetramere enthalten, als Bindemotiv charakterisiert, und mittels iCLIP wurde die überwiegende Zahl der DRBD4 Bindungsstellen in untranslatierten Bereichen (UTR) von mRNAs lokalisiert. Anhand der kombinatorischen Auswertung der RNA-seq und

iCLIP Datensätze konnten wir zeigen, dass DRBD4 *upstream* von Polyadenylierungsstellen bindet und sowohl für die Aktivierung als auch die Repression essenziell ist, wodurch generelle Transkript- und Isoformexpressionslevel reguliert werden.

3 Introduction

3.1 Gene expression in eukaryotes

The genetic information of eukaryotes is mostly stored as DNA in the nucleus. For the expression of genes, the DNA is first transcribed into RNA and in case of protein-coding genes, the mRNA is exported from the nucleus and translated into protein by the ribosome. Three major DNA-dependent RNA polymerases are involved in transcription of RNA: RNA polymerase I and III are responsible for the transcription of ribosomal RNAs (rRNA) and transfer RNAs (tRNA), whereas RNA polymerase II (Pol II) transcribes messenger RNAs (mRNA) of protein-coding genes. Moreover, Pol II transcribes non-coding RNAs and most small nuclear RNAs (snRNAs). The carboxy-terminal domain (CTD) of the largest PoI II subunit is involved in regulation of transcription by differential phosphorylation and couples transcription to important RNA processing reactions.

The first transcription-coupled processing step is capping of the 5´ end of the nascent mRNA with 7-methylguanosine, forming the m^7GpppN cap structure (Ghosh & Lima, 2010). This structure is required for mRNA stability, export, splicing and efficient translation initiation. After capping, the mRNA precursor undergoes *cis* splicing (see 3.2) since the genetic information of protein-coding genes is stored discontinuously in higher eukaryotes: The open reading frame (ORF) of a protein is encoded by exons (expressed regions), which are interspaced by non-coding introns (intervening regions) that are removed during co-transcriptional *cis* splicing. The splicing reaction is catalyzed by a macromolecular complex, the spliceosome, which assembles while transcription still takes place. During complex assembly, conserved sequences of the exon/intron borders, the splice sites, are recognized by the spliceosome and the exons are joined together, while the intron is removed. Finally, Pol II reads through the polyadenylation signal required for 3´ end maturation of the transcription (see 3.3 and 3.4): The polyadenylation complex assembles on the nascent transcript, which is then cleaved by CPSF73 and polyadenylated by the poly(A) polymerase (PAP). The added poly(A) tail has an approximate length of 250 nucleotides (nts) and is essential for RNA stability, export and translation. Afterwards transcription is terminated via the degradation of the 3´ cleavage product by exonucleases Xrn2 (Kuehner *et al.*, 2011). During all processing steps, a multitude of proteins bind to the RNA forming an mRNA-protein complex important for further downstream processes: RNA export (Kohler & Hurt, 2007), RNA surveillance and quality control (van Hoof & Wagner, 2011, Schweingruber *et al.*, 2013), translation into protein (Merrick, 2010), and degradation of the RNA (Houseley & Tollervey, 2009).

3.2 Pre-mRNA splicing in eukaryotes

The removal of intronic, non-coding sequences and the fusion of the coding exons is an essential step in pre-mRNA maturation (Sharp, 1994). Besides the above mentioned *cis* splicing (see 3.1), exons derived from two transcripts can be joined by *trans* splicing (Hastings, 2005). *Trans* splicing in trypanosomes (see 3.7) requires the spliced-leader (SL) donor RNA, from which a miniexon is transferred to the splice acceptor site (3´ splice site) of the pre-mRNA transcribed as a long polycistronic precursor.

The chemical basis of both *cis* and *trans* splicing is a two-step transesterification reaction (**Figure 3.1**): In the first reaction, the 2´ hydroxyl group of the branch point adenosine carries out a nucleophilic attack on the 5´ splice site phosphate, forming the lariat intron (*cis* splicing) or the Y structure (*trans* splicing) both characterized by the 2´-5´ phosphodiester bond at the branch point. In the second step, the phosphate group at the 3´ splice site is nucleophilically attacked by the 3´ hydroxyl group of the released exon/miniexon, resulting in the ligation of the exons and the release of the intron. Finally, the intron lariat or Y structure is degraded by the debranching enzyme and exonucleases.

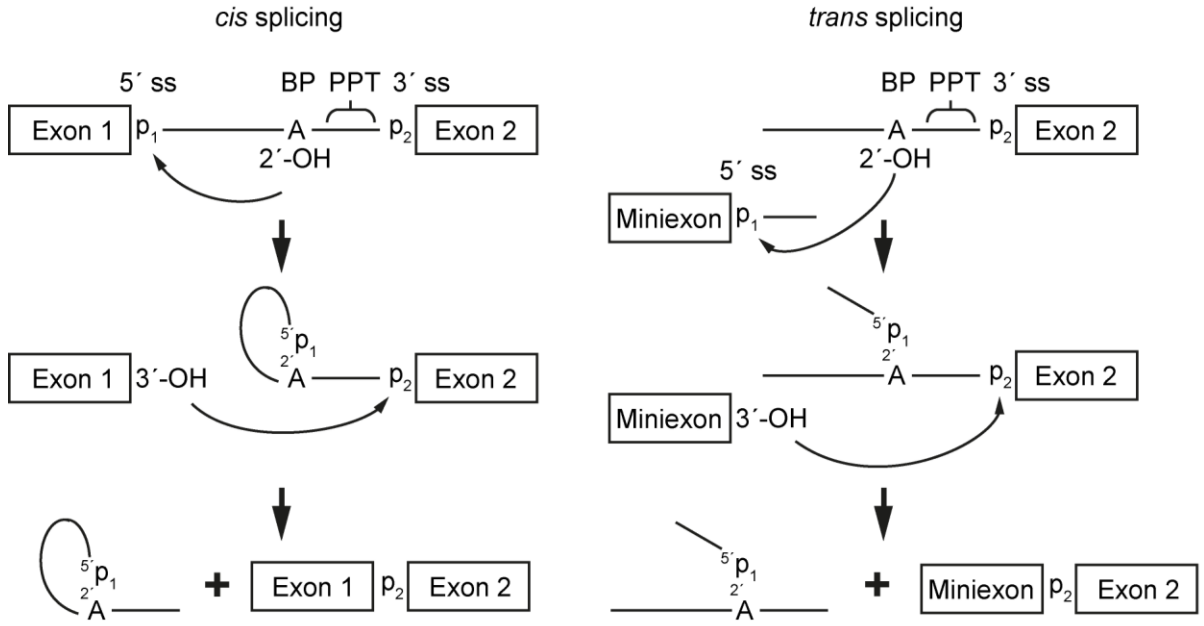

Figure 3.1 Schematic models of *cis* and *trans* splicing.

The model splice substrates consist of two exons (*cis* splicing; left) or one miniexon and a second exon (*trans* splicing; right) depicted as boxes. The introns are shown as solid lines. Both the 5´ and 3´ splice sites (5´ ss and 3´ ss) including the phosphate group (p), the branch point (BP) adenosine (A) and the polypyrimidine tract (PPT) are indicated. The splicing reaction is based on a two-step transesterification reaction: First, the 2´ hydroxyl group of the branch point adenosine carries out a nucleophilic attack on the 5´ splice site phosphate, forming the lariat intron (*cis* splicing) or the Y structure (*trans* splicing) each characterized by the 2´-5´ bond at the branch point. In the second step, the phosphate group at the 3´ splice site is nucleophilically attacked by the 3´ hydroxyl group of the released exon/miniexon, resulting in the ligation of the exons and the release of the intron.

For spliceosome assembly and efficient splicing conserved, *cis*-acting sequence motifs in the intron are required (**Figure 3.2**): The first two and the last two nucleotides in the intron at the 5´ donor (GT) and 3´ acceptor splice site (AG) define the exon/intron borders. The branch point adenosine carries out the nucleophilic attack on the 5´ splice site phosphate and the polypyrimidine tract serves as another essential sequence element (Patel & Steitz, 2003).

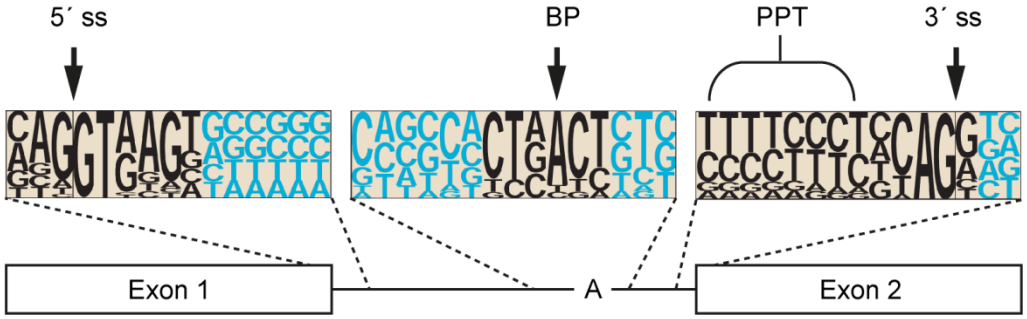

Figure 3.2 Consensus sequences of mammalian introns.
Consensus sequences of the 5´ and 3´ splice sites (5´ ss and 3´ss), the branch point (BP) adenosine (A) and the polypyrimidine tract (PPT). The letter heights at each position represent the frequency of occurrence of the corresponding nucleotides at that position. The positions that are involved in intron recognition are shown in black; other positions are shown in blue. Frequencies were derived from a set of mammalian introns. The exons 1 and 2 are shown as boxes and the intron as solid line. From Patel & Steitz, 2003; modified.

The splicing reaction is catalyzed by the macromolecular spliceosome, which is composed of five (U1, U2, U4, U5 and U6) small nuclear ribonucleoprotein particles (snRNPs) as well as a large set of proteins (Will & Lührmann, 2011, Matera & Wang, 2014). Each snRNP consists of a specific small, U-rich RNA, each containing the conserved Sm site (5´ AUUUGUG 3´), which is bound by seven common Sm-proteins (B/B′, D3, D2, D1, E, F, and G) forming a heptameric ring. In contrast, the U6 snRNA is bound by seven related LSm-proteins (Lsm2-8) that assemble to an analogous heptameric ring. In addition, each snRNP carries several specific proteins. It was recently shown that the U2, U5 and U6 snRNPs form the catalytic center making the spliceosome indeed a ribozyme (Hang *et al.*, 2015).

Spliceosome assembly is a highly ordered process involving the five snRNPs, the pre-mRNA and numerous splicing factors (Will & Lührmann, 2011). Moreover, the spliceosome undergoes major rearrangements during the splicing reaction.

Pre-mRNA splicing harbors an important regulatory potential, extending the complexity of the proteome by alternative *cis* splicing: 95% of all human genes undergo alternative *cis* splicing and approximately 100,000 of these events have been detected in major human tissues (Lee & Rio, 2015). Five variants of alternative *cis* splicing can be distinguished from constitutive splicing, when all exons of a single gene are included in the mature mRNA (**Figure 3.3**; page 13)

(Hui & Bindereif, 2005): The selection of alternative 5´ or 3´ splice sites results in different exon lengths. Furthermore, a whole exon can be skipped or included (cassette exon). The inclusion of a cassette exon can also lead to skipping of the adjacent exon and *vice versa*, making them mutually exclusive exons. In case of intron retention, an intron is not removed from the transcript. Functional consequences of alternative *cis* splicing are altered localization, activity or function of a protein, since single exons often encode for functional protein domains (Sharp, 1994).

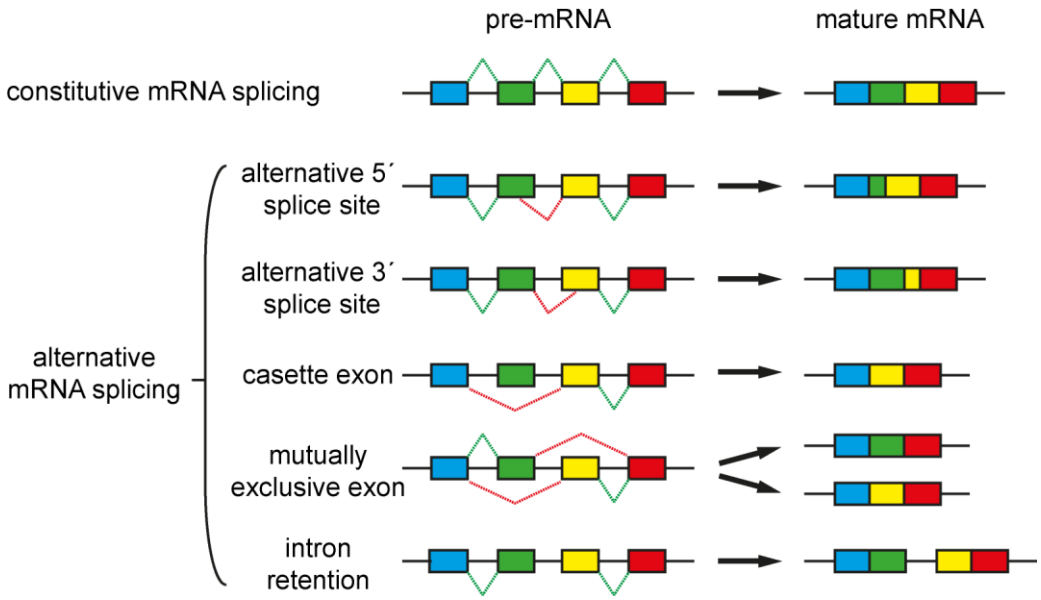

Figure 3.3 Alternative *cis* splicing patterns.
In constitutive splicing, a single mRNA is generated from the pre-mRNA. In contrast, alternative splicing produces many splice variants from a single pre-mRNA, using the following principles: Alternative 5´ or 3´ splice sites, cassette exons, mutually exclusive exons and intron retention. Exons are depicted as boxes and introns as solid lines. Constitutive and alternative splicing is indicated by green and red lines, respectively. From Hui & Bindereif, 2005; modified.

In general, alternative splicing is tissue-, development- and differentiation-specifically regulated, but it can be also activated by external stimuli like signal transduction cascades (Lee & Rio, 2015). Regulators of alternative splicing are in most cases *cis*-acting proteins belonging to the SR-protein and hnRNP-protein families, which specifically bind to exonic or intronic splicing enhancers and silencers. SR-proteins (e.g. SRSF1) bind predominantly to splicing enhancer elements and activate splicing (Shepard & Hertel, 2009). They display a characteristic domain structure with a C-terminal domain containing arginine-serine dipeptides (SR-domain; protein-protein interaction) and one or two N-terminal RNA recognition motifs (RRM) for RNA binding. In contrast, most hnRNP proteins (e.g. hnRNP I) bind splicing silencer elements and are involved in repression of splicing. Common domains of these proteins are RRMs that are often present in tandem (Han *et al.*, 2010). Both SR- and hnRNP proteins often regulate splicing by affecting

early spliceosome assembly but they can regulate splicing also by other mechanisms, e.g. looping out exons as described for hnRNP I (see 3.8).

3.3 The human polyadenylation complex and its function

Cleavage and polyadenylation of Pol II-transcribed nascent pre-mRNAs is an essential step in 3´ end maturation (Xiang *et al.*, 2014). The only exceptions are the canonical histone (H1, H2A, H2B, H3 and H4) pre-mRNAs, which are only cleaved and end with a highly conserved stem-loop (Marzluff *et al.*, 2008). The nascent pre-mRNA is during 3´ end maturation in most cases cut at a CA dinucleotide, and a poly(A) tail of approximately 250 nts is added, first in a distributive, and after binding of PABPN1 (nuclear poly(A)-binding protein 1) in a processive manner by the poly(A) polymerase (PAP) (Brawerman, 1981, Wahle, 1991a, Bienroth *et al.*, 1993, Wahle, 1995a, Wahle, 1995b). For the correct procession of the 3´ end, several *cis*-acting elements of the RNA (**Figure 3.4**) are required (Proudfoot, 2011): First, the highly conserved AAUAAA hexanucleotide polyadenylation signal (PAS) typically located 15 to 30 nts upstream of the cleavage site (Sheets *et al.*, 1990, Beaudoing *et al.*, 2000, Hu *et al.*, 2005). However, the PAS hexamer sequence can display microheterogeneity and an AUUAAA hexamer is common as well (Pauws *et al.*, 2001). The second element is the GU- (YGUGUUYY; Y=pyrimidine) or U-rich (UUUU) downstream sequence element (DSE) within 20 nts downstream of the cleavage site (Hart *et al.*, 1985, McLauchlan *et al.*, 1985, Gil & Proudfoot, 1987, MacDonald *et al.*, 1994, Hu *et al.*, 2005). Third, multiple UGUA upstream sequence elements (USE) are positioned 40 to 100 nts upstream of the cleavage site (Hu *et al.*, 2005). Mutations in these sequence elements, in particular the PAS, are associated with diseases like α- and β-thalassemia when the PAS is mutated to AAUAAG or AACAAA, respectively (Higgs *et al.*, 1983, Orkin *et al.*, 1985).

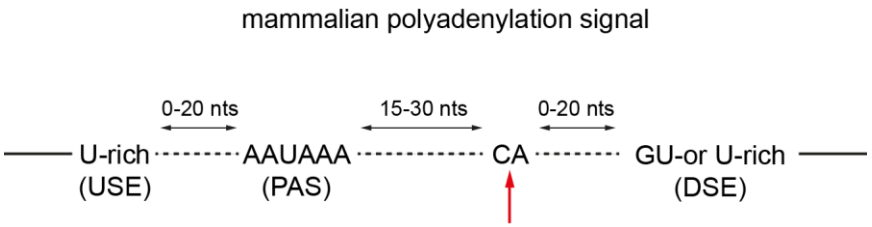

Figure 3.4 Consensus sequence elements of the polyadenylation signal.
The upstream sequence element (USE), the hexameric polyadenylation signal (PAS), the CA dinucleotide (cleavage site marked by a red arrow) and the downstream sequence element (DSE) are indicated. Moreover, the respective distances between the sequence elements are shown. From Proudfoot, 2011; modified.

Cleavage and polyadenylation is carried out by a large multiprotein complex composed of more than 85 associated proteins in humans (Shi *et al.*, 2009). The core factors of the complex are the cleavage and polyadenylation specificity factor (CPSF), the cleavage stimulation factor (CstF), cleavage factor I (CFI), cleavage factor II (CFII), Symplekin, nuclear poly(A)-binding protein 1 (PABPN1), the poly(A) polymerase and the CTD of Pol II (**Figure 3.5**). The above-mentioned *cis*-acting elements are essential for polyadenylation complex formation and directly bound by the CPSF (PAS binding), CstF (DSE binding) and CFI (USE binding).

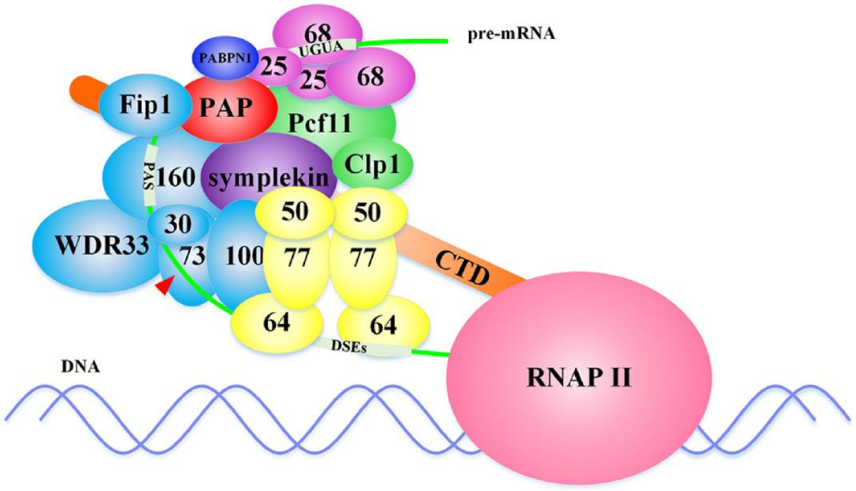

Figure 3.5 Simplified model of the human core cleavage and polyadenylation complex.
The cleavage and polyadenylation specificity factor (CPSF160/100/73/30, Fip1 and WDR33; light blue) binds the hexameric AAUAAA polyadenylation signal (PAS). However, note that the PAS is directly bound to CPSF30 and WDR33, but not to CPSF160. The red arrow indicates cleavage of the RNA substrate mediated by the endonuclease CPSF73. The cleavage stimulation factor (CstF77/64/50; yellow) binds the downstream GU-or U-rich sequence element (DSE) via CstF64, and the UGUA upstream sequence element (USE) is bound to cleavage factor I (CFIm 25/68; pink). In addition, the scaffold protein Symplekin (purple), the poly(A) polymerase (PAP; red), cleavage factor II (CFII; composed of PcfI I and Clp I; green) and the RNA polymerase II (RNAP II) including the C-terminal domain (CTD) are indicated. From Xiang *et al.*, 2014.

The CPSF subcomplex consists of six different proteins CPSF160, 100, 73 and 30 (according to their molecular mass in kDa), Fip1 and WDR33, which are required for efficient cleavage and polyadenylation, since the PAS is directly bound to CPSF and CPSF73 is the processive endonuclease (Gilmartin & Nevins, 1989, Takagaki *et al.*, 1989, Bienroth *et al.*, 1991, Murthy & Manley, 1992, Benz *et al.*, 2005, Mandel *et al.*, 2006, Shi *et al.*, 2009, Chan *et al.*, 2014, Schönemann *et al.*, 2014,). Moreover, the complex is recruited to the initiation complex and accompanies Pol II throughout transcription, coupling both transcription and 3´ end processing (Dantonel *et al.*, 1997).

The largest protein, CPSF160, is composed of tandem WD40 repeats that cluster into three major β-propellers, which generally serve as protein scaffold but can also bind nucleic acids (Neuwald & Poleksic, 2000, Scrima *et al.*, 2008, Stirnimann *et al.*, 2010). This is consistent with CPSF160 RNA and protein interactions (CPSF100, Fip1, CstF77 and PAP) (Murthy & Manley, 1992, Murthy & Manley, 1995).

Both CPSF100 and 73 belong to the metallo-β-lactamase superfamily, whose members are mostly hydrolases depending on metal ions (Jenny *et al.*, 1996, Callebaut *et al.*, 2002). CPSF100 and CPSF73 have a ß-lactamase domain with a ß-caspase domain (ß-casp) inserted like a cassette with the active site of the protein at the interface of these two domains. However, only CPSF73 harbors the conserved residues (mainly histidine) that coordinate two zinc atoms involved in RNA cleavage making it the processive endonuclease (Mandel *et al.*, 2006). Both proteins are tightly associated via their C-terminal domains, arguing for heterodimerization being required for cleavage, which is in line with homodimerization of other β-casp proteins (Dominski, 2007, Michalski & Steiniger, 2015).

CPSF30 consists of five C3H1 zinc fingers and a C-terminal C2HC zinc finger and binds in cooperation with WDR33 via zinc fingers two and three (minor contribution of the C-terminal zinc finger) directly to the PAS (Barabino *et al.*, 1997, Chan *et al.*, 2014, Schönemann *et al.*, 2014, Shimberg *et al.*, 2016). In addition, CPSF30 interacts with the Pol II body and likely participates in the association of CPSF and Pol II during transcription (Nag *et al.*, 2007).

Fip1 was discovered more than a decade later than the above mentioned proteins and interacts with the poly(A) polymerase, CPSF30, CPSF160 and CstF77 via the N-terminal region (Kaufmann *et al.*, 2004). Moreover, the C-terminal arginine-rich domain can bind RNA, in particular U-rich sequences.

The last CPSF subunit is WDR33 consisting of an N-terminal WD40 repeats, a middle collagen-like domain and a C-terminal glycine-proline-arginine domain (Ito *et al.*, 2001, Shi *et al.*, 2009). WDR33 is essential for RNA binding of the polyadenylation complex since it recognizes in cooperation with CPSF30 the hexameric PAS (Chan *et al.*, 2014, Schönemann *et al.*, 2014, Shimberg *et al.*, 2016).

The second subcomplex of the polyadenylation machinery is termed CstF and composed of CstF77, 64 and 55 with two copies of each subunit (Takagaki *et al.*, 1990, Gilmartin & Nevins, 1991). The complex couples transcription and polyadenylation via the association with Pol II and directly binds the *cis*-acting DSE on the RNA transcript (MacDonald *et al.*, 1994, McCracken *et al.*, 1997).

The largest factor, CstF77, harbors an N-terminal, half a TPR domain that is most likely involved in self-dimerization followed by a proline-rich segment, which binds the hinge domain of CstF64

and the WD40 repeats of CstF50 bridging them, since they do not make direct contact (Takagaki & Manley, 1994, Preker & Keller, 1998, Takagaki & Manley, 2000, Bai *et al.*, 2007, Hockert *et al.*, 2010). Additionally, the Pol II CTD is bound to CstF77 as well (McCracken *et al.*, 1997).

The second factor, CstF64, consists of an N-terminal RRM for DSE binding, a central hinge domain for CstF77 or Symplekin association, and a proline-glycine-rich region (Takagaki *et al.*, 1992, MacDonald *et al.*, 1994, Takagaki & Manley, 1997, Takagaki & Manley, 2000, Perez Canadillas & Varani, 2003, Ruepp *et al.*, 2011b). CstF64 as well as the isoform tauCstF64 are involved in the regulation of alternative polyadenylation (APA; see 3.4 and 3.5) and may have redundant functions (Wallace *et al.*, 1999, Li *et al.*, 2012, Shankarling & MacDonald, 2013, Yao *et al.*, 2013).

The last CstF subunit is CstF50 harboring an N-terminal self-dimerization domain and a C-terminal WD40 repeat domain which functions as a binding platform for CstF77 (Takagaki & Manley, 1992, Takagaki & Manley, 2000). Moreover, CstF50 binds the Pol II CTD with high affinity and couples in cooperation with CstF77 (see above) transcription and 3´ end processing (McCracken *et al.*, 1997).

CFI is composed of two CFIm25 proteins and two proteins of the paralogous genes CFIm59, CFIm68 or CFIm72, of which the latter one is a larger isoform of CFIm68 (Rüegsegger *et al.*, 1996, Rüegsegger *et al.*, 1998, Ruepp *et al.*, 2011a). CFI associates early with the transcription elongation complex, recognizes the USE to stabilize the CPSF complex and is involved in mRNA export and regulation of APA (Rüegsegger *et al.*, 1996, Venkataraman *et al.*, 2005, Ruepp *et al.*, 2009, Kim *et al.*, 2010, Ruepp *et al.*, 2011a, Gruber *et al.*, 2012, Martin *et al.*, 2012). Knockdown of both CFIm25 and CFIm68 leads to an increased usage of proximal poly(A) sites, resulting in shorter 3´ untranslated regions (UTR), whereas in the wildtype situation the use of distal poly(A) sites (long 3´ UTRs) is preferred.

The smallest protein of this complex, CFIm25, encompasses a central NUDIX domain without hydrolase activity serving as a binding platform for the USE (the CFIm25 dimer binds two USEs in an antiparallel fashion via CFIm68-mediated RNA looping), CFIm68, PABPN1 and the poly(A) polymerase (Dettwiler *et al.*, 2004, Coseno *et al.*, 2008, Tresaugues *et al.*, 2008, Yang *et al.*, 2010, Li *et al.*, 2011, Yang *et al.*, 2011).

In contrast to CFIm59 and 72, is CFIm68 the most common second subunit of the CFI complex. It is composed of an N-terminal RRM, a middle proline-rich region and a C-terminal RS domain resembling the domain organization of the previously mentioned SR proteins (see 3.2) (Rüegsegger *et al.*, 1998). CFIm68 is involved in USE binding (see above) and interacts with the nuclear export machinery through the Thoc5 protein (TREX complex) and the export receptor NXF1/TAP (Gooding *et al.*, 1998, Ruepp *et al.*, 2009, Li *et al.*, 2011, Yang *et al.*, 2011).

CFII is the least-well characterized subcomplex of the polyadenylation machinery, since the factors with the exception of Clp I and PcfI I remain poorly defined and were mostly studied in yeast (de Vries *et al.*, 2000). Knockdown of PcfI I impairs RNA cleavage and transcription termination, and Clp I was shown to interact with CPSF as well as CFI and likely tethers them to CFIIm (de Vries *et al.*, 2000, West & Proudfoot, 2008).

Symplekin is an essential scaffold protein of the polyadenylation complex and contains seven pairs of antiparallel α-helices (ARM repeat) at the N-terminus that are often involved in protein-protein interactions (Takagaki & Manley, 2000, Andrade *et al.*, 2001, Kennedy *et al.*, 2009, Xiang *et al.*, 2010). The central domain binds the hinge domain of CstF64 and, in addition, Symplekin associates with both CPSF73 and CPSF100 forming a stable complex required for RNA cleavage (Takagaki & Manley, 2000, Hofmann *et al.*, 2002, Sullivan *et al.*, 2009, Ruepp *et al.*, 2011b).

The canonical, nuclear localized poly(A) polymerase of the polyadenylation core complex, which adds the poly(A) tail to the pre-mRNA, is encoded by the human *PAPOLA* gene and belongs to the nucleotidyltransferase superfamily of DNA polymerase β (Edmonds, 1990, Raabe *et al.*, 1991, Wahle, 1991a, Wahle, 1991b, Colgan & Manley, 1997). At the N-terminus of the protein, the catalytic nucleotidyltransferase domain is inserted like a cassette in the PAP central domain (Raabe *et al.*, 1994, Zhelkovsky *et al.*, 1995, Martin & Keller, 1996, Martin *et al.*, 1999, Martin *et al.*, 2000). The catalytic domain contains the conserved aspartate triad that coordinates the magnesium ions that are essential for catalysis and ATP binding. Following the PAP central domain, a RNA-binding region and a C-terminal nuclear localization signal (NLS) are located. The general processivity of the poly(A) polymerase is regulated by the PABPN1 protein and the poly(A) tail is first synthesized in a distributive, and after binding of PABPN1 to the poly(A) tail, in a processive manner (Wahle, 1991a, Bienroth *et al.*, 1993, Wahle, 1995b).

As discussed above, PABPN1 stimulates the catalytic activity of the poly(A) polymerase to ensure a proper length of the poly(A) tail (see above) and may also regulate APA (see 3.4 and 3.5) (Jenal *et al.*, 2012). The middle coiled-coiled domain directly stimulates the poly(A) polymerase and the following RRM and C-terminal region are required for RNA binding, allowing PABPN1 to coat the newly synthesized poly(A) tail (Nemeth *et al.*, 1995, Keller *et al.*, 2000, Kerwitz *et al.*, 2003). It was proposed that this structure restricts the CPSF complex to the PAS, to facilitate the interaction between CPSF and the poly(A) polymerase until the correct length of the poly(A) tail is reached (Kuhn *et al.*, 2009).

The last core subunit of the polyadenylation complex is the Pol II CTD that links both transcription and polyadenylation and is directly required for the latter one (McCracken *et al.*,

1997, Hirose & Manley, 1998). However, the precise mechanism is not yet understood but a platform role was proposed, since several proteins (e.g. CstF77 and CstF50) bind to the CTD.

Recent data from two studies suggested a new model for the previously introduced CPSF complex, dividing it into a RNA-binding module composed of CPSF160, CPSF30, Fip1 as well as WDR33 and a RNA-cleavage module built by CPSF100, CPSF73 and Symplekin (Chan *et al.*, 2014, Schönemann *et al.*, 2014, Shimberg *et al.*, 2016). The hexameric PAS is directly bound to CPSF30 (zinc fingers two and three) and WDR33, whereas Fip1 binds U-rich sequences upstream and downstream of it. Moreover, CPSF160 binds RNA upstream of the cleavage site over a brought region (**Figure 3.6**). RNA cleavage is catalyzed by the endonuclease CPSF73 (see above) of the cleavage module, which is only essential for cleavage but not for PAS binding and polyadenylation.

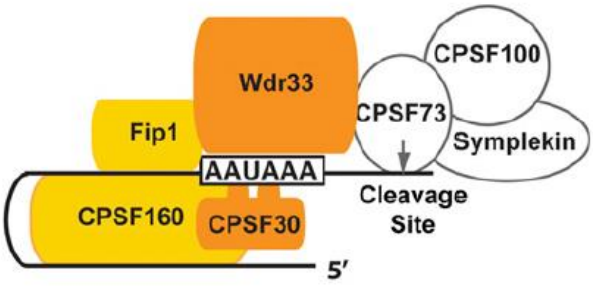

Figure 3.6 A new model for CPSF-RNA interaction.
Multiple proteins mediate CPSF-RNA interactions: CPSF30 and Wdr33 directly interact with the hexameric AAUAAA polyadenylation signal (PAS), and CPSF30 binds to the AAUAAA motif via its zinc fingers two and three (shown as two fingers). Fip1 binds the U-rich auxiliary sequence upstream and downstream of the AAUAAA motif (shown only upstream of the AAUAAA). CPSF160 binds to RNA over a broad region upstream of the cleavage site. CPSF73, CPSF100 and Symplekin do not participate in AAUAAA binding, but function as the RNA cleavage module mediated by the endonuclease CPSF73. From Chan *et al.*, 2014.

3.4 Alternative polyadenylation (APA) and its biological importance

Recent discoveries showed that most human genes contain more than one polyadenylation site, suggesting that APA is a widespread phenomenon generating RNA transcripts with different 3´ ends (Millevoi & Vagner, 2010, Shi, 2012, Elkon *et al.*, 2013). Four classes of APA events can be distinguished (**Figure 3.7**; page 20): Tandem 3´ UTR APA and alternative-terminal-exon APA are the most frequent, the less frequent intonic APA and the last frequent internal-exon APA type.

In tandem 3´ UTR APA, alternative poly(A) sites are located in the last exon of the transcript, allowing the generation of mRNAs with different 3´ UTR lengths via the usage of proximal or distal poly(A) sites without any effect on the encoded protein. In contrast, the other three APA

types can directly affect the coding potential of the mRNA. Alternative splicing (see 3.2) can generate transcripts with alternative-terminal-exons causing the second APA type. An intronic, cryptic poly(A) site is activated during intronic APA resulting in the extension of an internal-exon making it the terminal one. Finally, in internal-exon APA, a poly(A) site in an internal exon is used for premature cleavage and polyadenylation in the coding region of the mRNA.

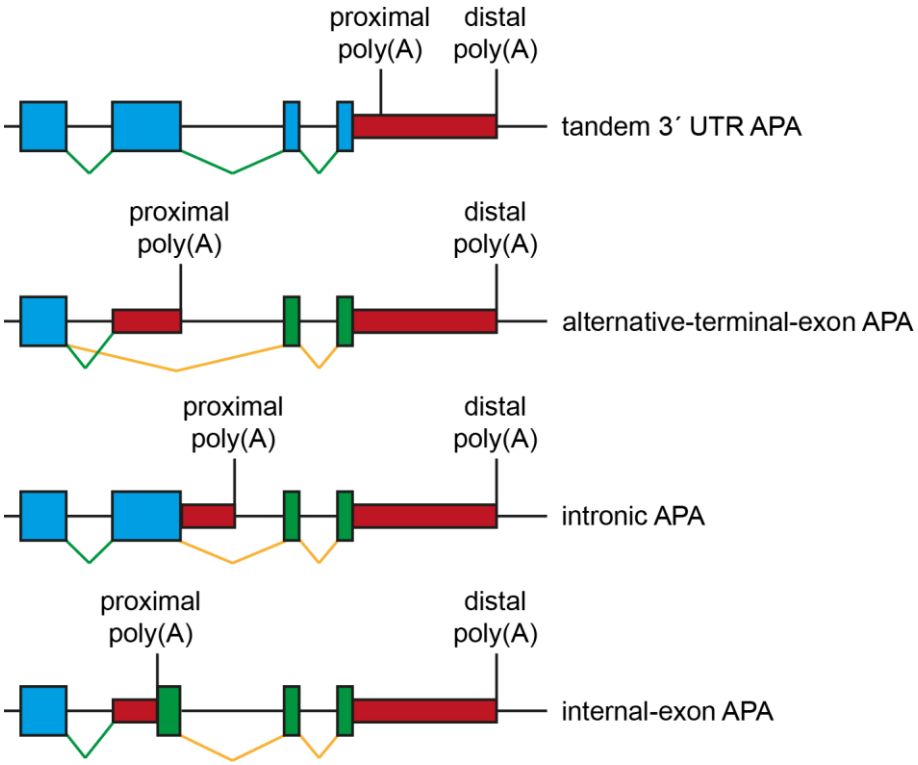

Figure 3.7 The four different APA types.
Tandem 3´ UTR APA involves alternative poly(A) sites within the same terminal-exon and hence generates multiple isoforms that differ in their 3´ UTR length, without affecting the protein encoded. The three other APA types potentially affect the coding sequence in addition to the 3´ UTR. In alternative-terminal-exon APA, alternative splicing generates isoforms that differ in their last exon. Intronic APA involves cleavage at a cryptic, intronic poly(A) site extending an internal-exon making it the terminal one. Internal-exon APA involves premature cleavage and polyadenylation within an internal-exon of the coding region. Internal-exons are depicted as large boxes, 3´ UTRs as small red boxes and introns as solid black lines. Constitutive spliced (green lines) exons are shown in blue and alternatively spliced (orange lines) exons in green. From Elkon *et al*., 2013; modified.

APA increases like alternative splicing (see 3.2) the complexity of the transcriptome by generating mRNA isoforms that differ either in their coding sequence or in their 3´ UTR, affecting protein function, mRNA stability or translation efficiency (Andreassi & Riccio, 2009, Fabian *et al.*, 2010). In particular, the 3´ UTR is very important since it functions as a binding platform for miRNAs that mainly regulate translation efficiency and for *trans*-acting proteins that influence mRNA stability.

Diverse biological processes are linked to APA: Many tissue-specific polyadenylation events and global trends in poly(A) site selection (brain and nervous system: distal poly(A) site; placenta, ovaries and blood: proximal poly(A) site) argue for a general role in development and cellular differentiation (Zhang *et al.*, 2005). Perhaps the most profound association of APA was found with cellular proliferation (Sandberg *et al.*, 2008, Elkon *et al.*, 2012): The activation of T cell proliferation is linked to a usage of proximal poly(A) sites, and a general shortening of 3´ UTRs was also observed in cancer cells (Mayr & Bartel, 2009, Lin *et al.*, 2012, Morris *et al.*, 2012). This can most likely be explained by binding sites for miRNAs or *trans*-acting proteins in the 3´ UTR that can negatively affect mRNA stability or translation efficiency. In addition, APA is involved in neuronal activation upon external stimuli (Timmusk *et al.*, 1993, An *et al.*, 2008, Lau *et al.*, 2010). The brain-derived neurotrophic factor gene contains two poly(A) sites, allowing the generation of two isoforms with either a short 3´ UTR, which is translated into protein at basal levels, or a long 3´ UTR only translated after external stimulation. Such a regulation is most likely mediated by a *trans*-acting factor like an RNA-binding protein or a miRNA, but remains elusive.

3.5 Regulation of polyadenylation

The above described APA (see 3.4) requires precise regulation, since it is involved in diverse biological processes, and dysregulation can result in non-functional proteins and is generally associated with cancer (Millevoi & Vagner, 2010, Shi, 2012, Elkon *et al.*, 2013). Differential regulation of the polyadenylation efficiency of a transcript containing a single poly(A) site directly affects protein expression, since unprocessed transcripts are degraded or not exported to the cytoplasm (Millevoi & Vagner, 2010). Three simplified models for the regulation of polyadenylation have been proposed: “First come, first serve”, “Survival of the fittest” and “Agonist/Antagonist” (Davis & Shi, 2014).

The “First come, first serve” model describes the predominant usage of the proximal poly(A) site since it is transcribed earlier, reflecting a direct linkage to transcription. This has been observed for both slow Pol II mutants in *Drosophila melanogaster* and drugs that reduce the transcription elongation rate (Pinto *et al.*, 2011, Yu & Volkert, 2013). Further studies also suggested a direct influence of the chromatin structure because it often influences the elongation rate under physiological conditions (Brown *et al.*, 2012). The promoter of the retrogene Mcts2 is located within an intron of the mouse H13 gene, which is due to CpG methylation imprinted and only expressed from the paternal allele (Wood *et al.*, 2008, Cowley *et al.*, 2012). Depending on the Mcts2 expression status, either the proximal (Mcts2 expressed) or the distal (Mcts2 not expressed) H13 poly(A) site is used, indicating that the expression of the retrogene reduces the transcription rate favoring the usage of the proximal H13 poly(A) site.

The “Survival of the fittest model” is based on the observation that distal poly(A) sites are often stronger than proximal ones because their PAS and DSE better resemble the conserved canonical sequences (Martin *et al.*, 2012, Smibert *et al.*, 2012, Tian & Graber, 2012, Yao *et al.*, 2012, Lackford *et al.*, 2014). However, poly(A) sites are regulated by additional factors including the concentration of various core polyadenylation complex constituents (Takagaki *et al.*, 1996, Takagaki & Manley, 1998). For example, Immunglobulin M (IgM) is subjected to intronic APA that produces an mRNA encoding a secreted protein, whereas polyadenylation at the distal site generates a membrane-bound IgM. This process is directly controlled by the up-regulation of CstF64 levels during B cell activation: In contrast to low CstF64 levels, where the strong, distal poly(A) site is used, high CstF64 levels favor the weak proximal poly(A) site. This is in line with an increased usage of distal poly(A) sites upon co-depletion of CstF64 and tauCstF64, indicating that both factors are essential for proximal poly(A) site activation (Yao *et al.*, 2012). Depletion of CFIm25 or CFIm68 has the opposite effect, the activation of proximal poly(A) sites, suggesting the requirement of both factors for the maintenance of long 3´ UTRs (Gruber *et al.*, 2012, Martin *et al.*, 2012).

The last model “Agonist/Antagonist” is based on individual positive or negative effects on poly(A) site choice by *trans*-acting factors such as RNA-binding proteins (Shi, 2012). The polypyrimidine tract binding protein (PTB/hnRNP I) represses poly(A) sites via competing with CstF64 for the downstream GU/U-rich sequence element, resulting in an inhibition of mRNA 3´ end cleavage and an accumulation of unprocessed pre-mRNAs (Castelo-Branco *et al.*, 2004). In addition, PTB can activate polyadenylation by, first, promoting RNA binding of hnRNP H close to the polyadenylation site, which in turn facilitates the recruitment of CstF or the poly(A) polymerase, and, second, by increasing the processivity of the poly(A) polymerase (Millevoi et al. 2009). Finally, general splicing factors can also participate in the regulation of polyadenylation. The U1 snRNP is essential for *cis* splicing and binds to nascent pre-mRNAs repressing cryptic poly(A) sites, often located in introns preventing premature cleavage and polyadenylation (Kaida *et al.*, 2010, Berg *et al.*, 2012).

3.6 The African trypanosomes: *Trypanosoma brucei*

Trypanosoma brucei is a protozoan parasite belonging to the order of Kinetoplastida and the name of the order is derived from the kinetoplast, the DNA-containing compartment in their single mitochondrion (Achcar *et al.*, 2014). The parasite undergoes a complex life-cycle in an insect vector, the tsetse fly (*Glossina spp.*) and a vertebrate host. *Trypanosoma brucei* can be divided in three subspecies causing different forms of trypanosomiasis, a lethal tropical disease common in Africa (Malvy & Chappuis, 2011, Migchelsen *et al.*, 2011, Lejon *et al.*, 2013): *T.*

brucei gambiense is most prevalent in central and western Africa and causes chronic human trypanosomiasis, leading to death of the untreated patient within three years. In contrast, *T. brucei rhodesiense* causes acute human trypanosomiasis, which is deadly within six months and is most common in southern and eastern Africa. The last subspecies is *T. brucei brucei* that is non-infective for humans but causes the Nagana cattle disease (also caused by several other *Trypanosoma* species). About 10,000 people get infected every year by human trypanosomiasis, which in over 96% is caused by *T. brucei gambiense*, and 70 million people in Africa live in the risk of being infected. Moreover, T*rypanosoma brucei* became due to some special biochemical and cellular characteristics an important model organism: The expression of variant surface glycoproteins allowing the evasion of the hosts immune response, and RNA editing of mitochondrial mRNAs (deletion or insertion of uridine nucleotides) by guide RNAs and the editosome. The special characteristics in gene expression, namely spliced-leader *trans* splicing and the polycistronic organization of protein-coding genes, which will be discussed in the following (see 3.7).

3.7 Expression of protein-coding genes in trypanosomes

In trypanosomes all protein-coding genes are arranged in long, polycistronic transcription units (PTU) with up to 100 functionally unrelated genes, which are transcribed by Pol II (**Figure 3.8**; page 24) (Johnson *et al.*, 1987, Berriman *et al.*, 2005). Genes within a PTU are transcribed from the same strand, whereas neighboring PTUs are transcribed from the opposite strand separated by a strand switch region (SSR). Transcription of neighboring PTUs is either divergent or convergent and the SSR functions as transcription start site (TSS) or transcription termination site (TTS), respectively (Martinez-Calvillo *et al.*, 2003, El-Sayed *et al.*, 2005). Surprisingly, no Pol II promoter sequence has been identified in trypanosomes with the exception of the SL RNA gene (see below and 3.2), suggesting that transcription of protein-coding genes is not regulated and proceeds roughly at the same rate (Luo *et al.*, 1999, Ruan *et al.*, 2004, Das *et al.*, 2005, Schimanski *et al.*, 2005a, Palenchar & Bellofatto, 2006, Schimanski *et al.*, 2006, Lee *et al.*, 2007, Lee *et al.*, 2009). An enrichment of specific histone modifications and variants at both TSS and TTS argues for an epigenetic mechanism of transcription initiation and termination: The histone modifications H4K10ac and H3K4me^3, histone variants H2A.Z and H2B.Z and the bromodomain factor 3 protein (Bdf3), which binds acetylated lysine, are enriched at convergent SSRs functioning as transcription start sites (Hassan *et al.*, 2002, Siegel *et al.*, 2009, Wright *et al.*, 2010). Nucleosomes containing H2A.Z are less stable, suggesting less condensed chromatin-favoring transcription (Jin & Felsenfeld, 2007, Siegel *et al.*, 2009). In contrast, transcription terminates at convergent SSRs, which display an enrichment of H3K76m$^{1/2}$, H3.V,

H4.V and base J, suggesting that they serve as marks for transcription termination, and two recent studies showed indeed that H3.V and base J are required for transcription termination (Siegel *et al.*, 2009, Gassen *et al.*, 2012, van Luenen *et al.*, 2012, Reynolds *et al.*, 2016, Schulz *et al.*, 2016). Moreover, Pol I transcribed tRNA genes are often located at TTS and may contribute to termination of Pol II transcription (Hull *et al.*, 1994).

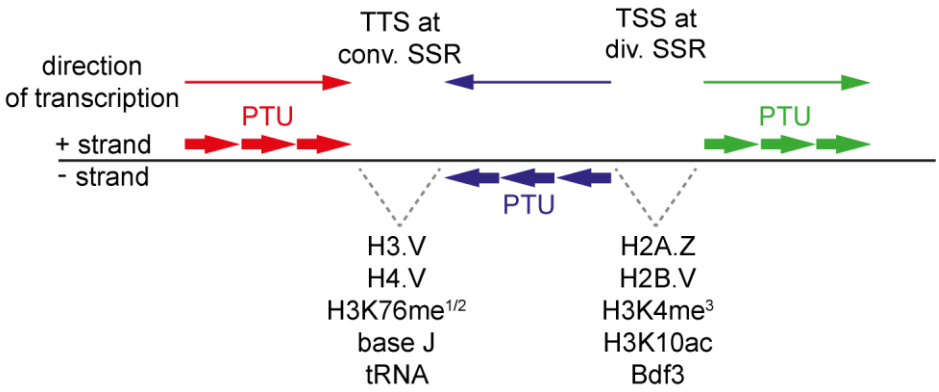

Figure 3.8 Organization of polycistronic transcription units in trypanosomes.
Transcription of polycistronic transcription units (PTU; indicated as colored bold arrow) starts at (transcription start site, TSS) divergent (div.) strand switch regions (SSR) and terminates (transcription termination site, TTS) at convergent (conv.) SSRs. Genes within a PTU are transcribed from the same strand, whereas neighboring PTUs are transcribed from opposing strands separated by a SSR. At TSS H4K10ac and H3K4me^3, H2A.Z, H2B.Z and bromodomain factor 3 protein (Bdf3) are enriched, whereas at TTS H3K76m$^{1/2}$, H3.V, H4.V, base J and tRNA genes are enriched. From Siegel *et al.*, 2011; modified.

After transcription of polycistronic transcription units, single mRNAs need to be processed by two coupled mechanisms, namely *trans* splicing and polyadenylation (**Figure 3.9**; page 25) (Boothroyd & Cross, 1982, Agabian, 1990, Huang & van der Ploeg, 1991a, Huang & Van der Ploeg, 1991b, LeBowitz *et al.*, 1993, Ullu *et al.*, 1993, Matthews *et al.*, 1994, Benz *et al.*, 2005, Günzl, 2010, Preußer *et al.*, 2012, Preußer *et al.*, 2012). Both processes are regulated by the polypyrimidine tract upstream of a *trans* splice site, which affects polyadenylation of the upstream gene and *trans* splicing of the downstream gene. During *trans* splicing a 39 nts long miniexon derived from the SL RNA, which already contains a highly modified m^{7}G cap structure termed cap4, is added to the 5´ end of all mRNAs (Bangs *et al.*, 1992). The *trans* splicing reaction is catalyzed by the spliceosome (see 3.2) and it is assumed that the SL RNP replaces the U1 snRNP. However, two genes, the putative poly(A) polymerase Tb927.3.3160 and an ATP-dependent DEAD box helicase Tb927.8.1510, contain an intron with a conserved sequence and require additional U1 snRNP-dependent *cis* splicing (see 3.2) (Tschudi & Ullu, 1990, Mair *et al.*, 2000, Liang *et al.*, 2003, Berriman *et al.*, 2005, Kolev *et al.*, 2010, Siegel *et al.*, 2010, Tkacz *et al.*, 2010).

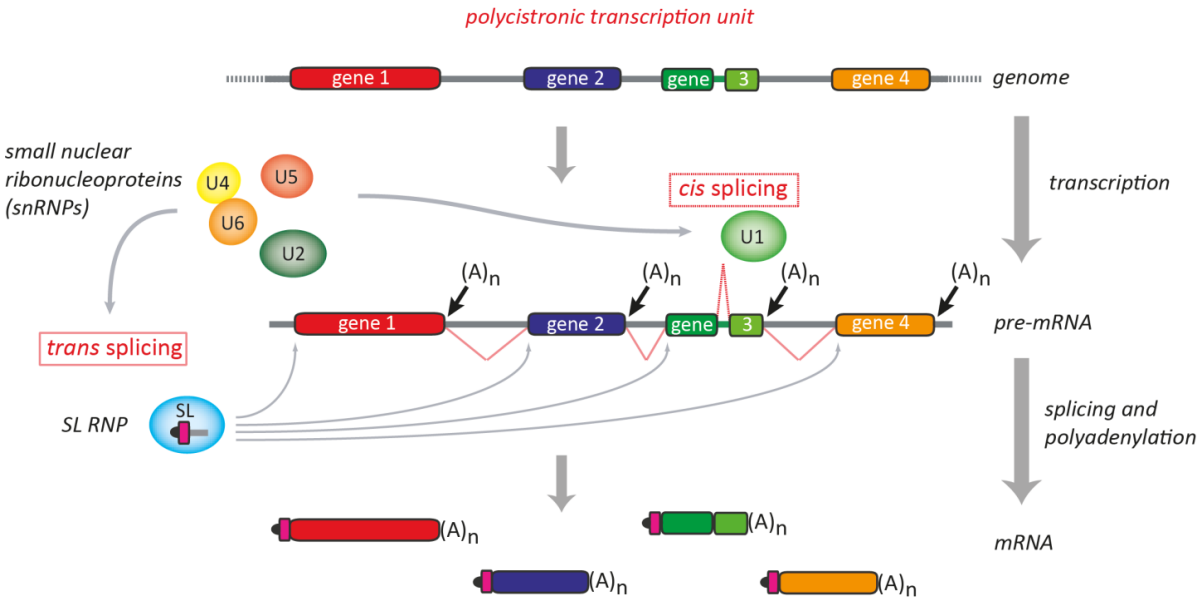

Figure 3.9 mRNA processing in trypanosomatids.
Schematic representation of the major mRNA processing steps in trypanosomatids. After transcription of polycistronic transcription units (colored boxes), which are separated by strand switch regions (SSR), the pre-mRNAs undergo *trans* splicing and polyadenylation [$(A)_n$]. Each of the protein-coding genes (shown in different colors) is processed through *trans* splicing, whereby the SL RNA with its cap 4 structure provides the 5´ exon (miniexon, in magenta); in addition, very few genes require *cis* splicing of an internal intron (see green boxes). Both *cis* and *trans* splicing proceed through two transesterification steps and require the U2, U4/U6, and U5 small nuclear ribonucleoproteins (snRNPs) as well as many additional protein factors. Moreover, *cis* splicing requires the U1 snRNP, *trans* splicing the SL RNP as specific factors. From Preußer *et al.*, 2012.

The 3´ end of each mRNA is processed by cleavage and polyadenylation (see 3.3 and 3.4), which is catalyzed in other eukaryotes by the polyadenylation complex. However, in trypanosomes most constituents of the polyadenylation machinery remain still elusive. So far only three subunits of the CPSF complex -CPSF30, CPSF73, and Fip1- have been identified as orthologues of their mammalian counterparts (see 3.3) and were biochemically characterized to some extent. *T. brucei* CPSF30 has a conserved domain structure similar to its human counterpart, harboring five C3H1 zinc fingers and a C-terminal C2HC zinc finger. CPSF30 is essential for cell viability and processing of polycistronic pre-mRNAs, since its depletion results in an accumulation of dicistonic α/β-tubulin pre-mRNA (Hendriks *et al.*, 2003). Fip1 is mainly localized in the nucleus, essential for cell viability and contains the conserved Fip1 domain, which is required for interaction with CPSF30 (zinc fingers four and five) in trypanosomes (Bercovich *et al.*, 2009). Moreover, the protein harbors an C3H1 zinc finger and a histidine- (H-

rich) and a proline-rich (P-rich) region. CPSF73 was recently co-purified with the spliceosomal U1 snRNP protein U1A, arguing for a coupling of both pre-mRNA processing reactions (Tkacz *et al.*, 2010). However, even for the poly(A) polymerase, in other eukaryotes probably the best delineated component, a definitive identification and biochemical characterization have not been accomplished in trypanosomes. At least two genes code for putative poly(A) polymerases [Tb927.3.3160 and Tb927.7.3780], the first of which is peculiar in that it represents one of the two genes in trypanosomes that require *cis* splicing (see above). In addition, the polyadenylation signal itself is poorly defined, since the two canonical *cis*-acting elements, the AAUAAA motif (PAS) and the GU/U-rich sequence (DSE), are not conserved in trypanosomes. The only known *cis*-acting element required for polyadenylation is the above mentioned polypyrimidine tract.

Genome-wide data showed that most genes contain one to three *trans* splice- and even more dispersed polyadenylation sites, allowing both alternative *trans* splicing and polyadenylation (Kolev *et al.*, 2010, Nilsson *et al.*, 2010, Siegel *et al.*, 2010, Veitch *et al.*, 2010, Siegel *et al.*, 2011). For alternative *trans* splicing four biological roles have been discussed (**Figure 3.10 A**; page 28) (Preußer *et al.*, 2012): (1) Skipping of the canonical AUG start codon; (2) in- or exclusion of targeting signals; (3) in- or exclusion of regulatory elements (e.g. upstream open reading frames); (4) usage of an alternative ORF. However, only for the in- or exclusion of targeting signals a specific example has been described so far (Rettig *et al.*, 2012). Alternative *trans* splicing creates a long and a short isoform of the isoleucyl-tRNA synthetase mRNA. The long isoform encodes for a protein, which is due to an additional N-terminal signal sequence imported into the mitochondrion, whereas the second protein isoform, encoded by the short mRNA, remains in the cytoplasm. This indicates an important role of alternative *trans* splicing in post-transcriptional gene regulation in trypanosomes. However, *trans*-acting factors, which contribute to the regulation of alternative splicing still remain elusive. So far only a few splicing repressors, such as the trypanosomatid orthologue of hnRNP F/H, and splicing activators, like the *T. brucei* PTB homologs DRBD3/4 (see 3.8), have been identified (Stern *et al.*, 2009, Gupta *et al.*, 2013). With to alternative polyadenylation, which may affect mature transcript levels by altering the length of the 3´ UTR and also 5´ UTR of the downstream gene, so far neither any regulatory elements nor *trans*-acting factors have been identified (**Figure 3.10 B**; page 28). Variations in the length of the 3´ UTR and 5´ UTR possibly alter the inclusion of important regulatory elements in the mature mRNA. These RNA elements, located mainly in the 3´ UTR, are of special interest in trypanosomes, since gene expression is regulated mostly on the post-transcriptional level with effects on either mRNA stability or translation efficiency (Clayton & Shapira, 2007, Haile & Papadopoulou, 2007, Kramer & Carrington, 2011, Kramer, 2012, Clayton, 2013, Clayton, 2014, Kolev *et al.*, 2014). Key players in the regulation of mRNA stability

are *trans*-acting RNA-binding proteins: As an example, the RRM-containing proteins DRBD3 and DRBD4 are involved in positive and negative regulation of mRNA stability, and in case of DRBD3 it was shown that the regulatory sequence elements are located in the mRNA 3´ UTR (Estevez, 2008, Stern *et al.*, 2009). The best understood example is the stabilization of chaperone mRNAs during heat shock of bloodstream form trypanosomes by the ZC3H11 zinc finger protein (Delhi *et al.*, 2011, Droll *et al.*, 2013, Singh *et al.*, 2014). The N-terminal zinc finger binds to UAU repeats in the mRNA 3´ UTR, while the C-terminal domain is required for stabilization. ZC3H11 interacts with MKT1 and PBP1, which in turn interacts with PABP that is known to increase mRNA stability when recruited to the 3´ UTR. RNA degradation in trypanosomes is in general similar to other eukaryotes. First, the RNA is deadenylated by the CAF1-NOT complex (CAF1 is the processive deadenylase) and afterwards decapped at the 5´ end by an enzyme still not identified (Milone *et al.*, 2002, Schwede *et al.*, 2008, Schwede *et al.*, 2009, Farber *et al.*, 2013, Erben *et al.*, 2014). Finally, the mRNA is either degraded from the 5´ end by the exonuclease Xrna or from the 3´ end by the exosome (Clayton & Estevez, 2011, Manful *et al.*, 2011).

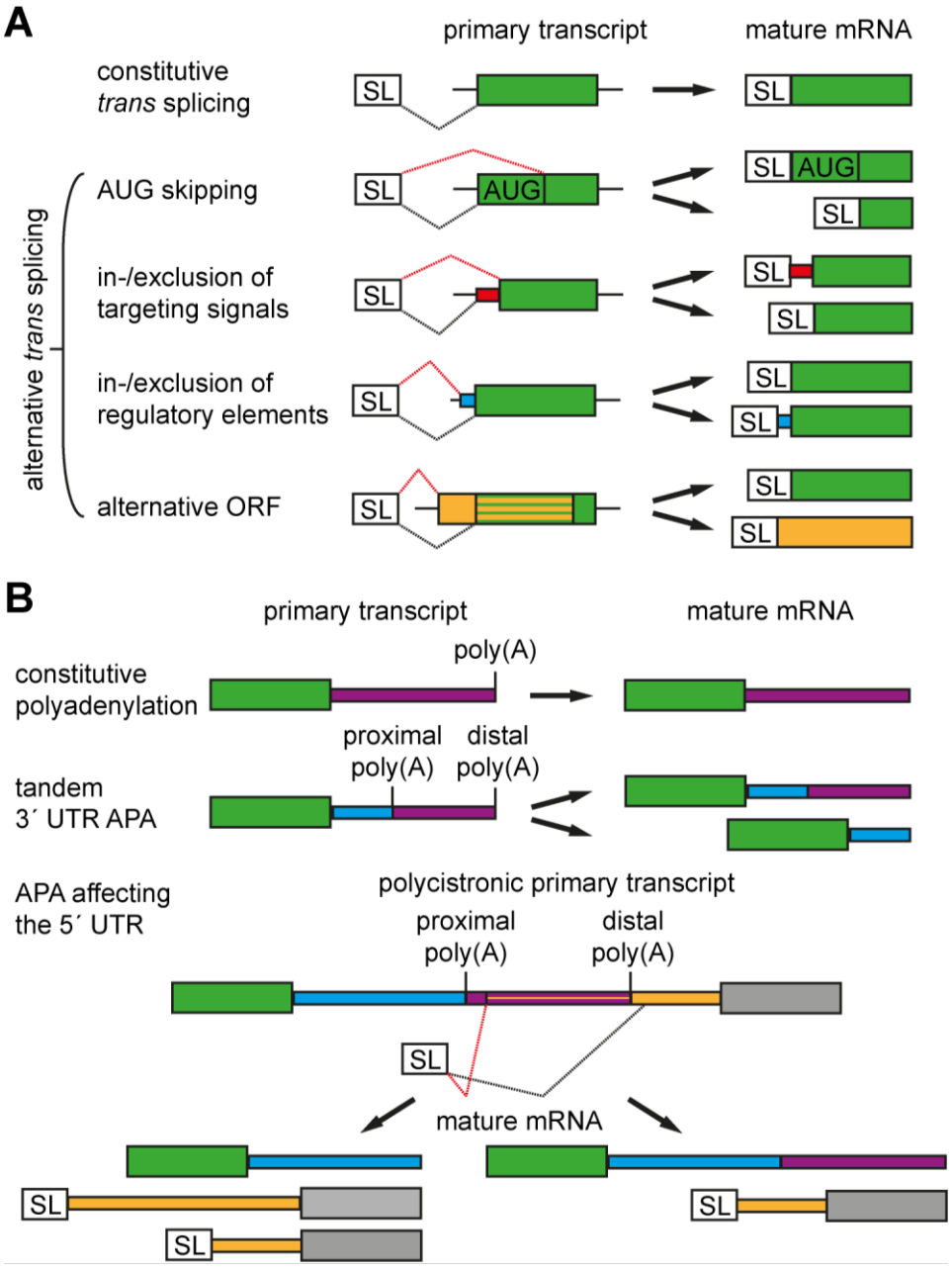

Figure 3.10 Biological functions of alternative *trans* splicing and polyadenylation.
Alternative *trans* splicing **(A)** and polyadenylation **(B)** patterns of pre-mRNAs and the different resulting mature mRNAs are schematically shown. **(A)** Protein-coding exons (green or yellow) and the SL RNA-derived miniexon (SL) are represented as large boxes, targeting signals and regulatory elements as small boxes (red or blue) and intergenic regions as black lines. Four potential biological roles of alternative *trans* splicing have been reported in trypanosomes, including skipping of the AUG start codon, in- or exclusion of targeting signals, in- or exclusion of regulatory elements, and the usage of an alternative open reading frame (orange box). **(B)** Protein-coding genes (green or gray) and the SL RNA-derived miniexon (SL) are represented as large boxes. The intergenic region forming alternative 5´ and 3´ UTRs between two genes is indicated by small colored boxes (blue, purple and yellow). Alternative polyadenylation affects the 3´ UTR (tandem 3´ UTR APA) and can, due to the polycistronic gene organization, also affect the 5´ UTR of the downstream gene by altering *trans* splice site choice (APA affecting the 5´ UTR). From Preußer *et al.*, (2012); modified.

3.8 The trypanosomatid PTB/hnRNP I homologs DRBD3 and DRBD4

The *Trypanosoma brucei* homologs of vertebrate PTB are DRBD3 and DRBD4 (De Gaudenzi *et al.*, 2005, Stern *et al.*, 2009). Vertebrate PTB belongs to the hnRNP protein family (see 3.2) and is a classical repressor of alternative splicing (Romanelli *et al.*, 2013). PTB is a shuttling protein mainly localized in the nucleus that binds via its four RRMs 15-25 nts long polypyrimidine tracts containing UCUUC and CUCUCU elements (Perez *et al.*, 1997, Oberstrass *et al.*, 2005, Ray *et al.*, 2009, Reid *et al.*, 2009, Lamichhane *et al.*, 2010, Maynard & Hall, 2010). The RRMs one and two are connected by a flexible linker allowing independent RNA binding, whereas the RRMs three and four interact, resulting in an antiparallel orientation of their bound RNA. Moreover, the polypyrimidine motifs bound to the RRMs three and four are separated by a minimum of 15 nts, allowing RNA looping. The expression of PTB and the neuronal-specific paralog nPTB is auto- and cross-regulated by alternative splicing (Markovtsov *et al.*, 2000, Rahman *et al.*, 2002, Wollerton *et al.*, 2004). PTB represses splicing of its own exon 11, causing nonsense-mediated decay (NMD) and promotes skipping of nPTB exon 10, causing NMD as well. However, in neuronal cells nPTB autoregulates exon 10 inclusion, resulting in higher nPTB protein levels (Ni *et al.*, 2007).

Several PTB-mediated mechanisms for repression of exon inclusion during *cis* splicing have been characterized: PTB binding sites within the polypyrimidine tract overlap with U2AF and U2 snRNP binding sites, arguing for a competition of these factors for their respective binding sites resulting in regulation of splicing. Based on the RNA-binding properties of PTB (see above) it can also loop out the branch point adenosine or a whole exon leading to exon skipping (Liu *et al.*, 2002, Oberstrass *et al.*, 2005, Spellman *et al.*, 2005, Auweter & Allain, 2008, Lamichhane *et al.*, 2010, Maynard & Hall, 2010).

Additionally, PTB can also promote exon inclusion and two different models have been proposed. First, via PTB binding to a polypyrimidine stretch positioned exclusively downstream of the respective regulated exon (Izquierdo *et al.*, 2005). Second, by binding near the splice sites of the exon antagonizing the action of different splicing repressors (Xue *et al.*, 2009).

In addition to splicing, PTB also increases the stability of various mRNAs e.g. pre-proinsulin, prohormone convertase 1/3 and 2 (Knoch *et al.*, 2004, Fred & Welsh, 2009).

Moreover, PTB can both stimulate and repress polyadenylation: PTB activates polyadenylation by, first, promoting RNA binding of hnRNP H close to the polyadenylation site, which in turn facilitates the recruitment of CstF or the poly(A) polymerase, and, second, by increasing the processivity of the poly(A) polymerase (Millevoi et al. 2009). In contrast, PTB represses polyadenylation by competing with CstF64 for the downstream GU/U-rich sequence element,

resulting in an inhibition of 3´ end cleavage and an accumulation of unprocessed pre-mRNAs (Castelo-Branco *et al.*, 2004).

The trypanosomatid homologs DRBD3 and DRBD4 are required for cell viability and contain two and four RRM domains, respectively (De Gaudenzi *et al.*, 2005, Stern *et al.*, 2009). In contrast to DRDB4, which is predominantly nuclear, DRBD3 can be detected in both cytoplasm and nucleus (Stern *et al.*, 2009, Fernandez-Moya *et al.*, 2012). Both proteins are no general splicing factors but are required for efficient *trans* splicing of genes having a C-rich polypyrimidine tract and moreover, DRBD3 is needed for *cis* splicing. In addition, DRBD3 and 4 regulate the stability of different subsets of mRNAs either in a positive or negative manner (Estevez, 2008, Stern *et al.*, 2009). DRBD3 was shown to have a polypyrimidine-rich binding motif and to bind mRNAs preferentially in their 3´ UTR (Das *et al.*, 2015). Moreover, DRBD3 is involved in the intracellular trafficking of bound mRNAs in form of ribonucleoprotein complexes, in response to stress conditions such as heat shock and starvation (Fernandez-Moya *et al.*, 2012).

3.9 Aims of this work

The expression of polycistronic protein-coding genes in the protozoan parasite *Trypanosoma brucei* requires coupling of the two major mRNA processing steps, *trans* splicing and polyadenylation, to produce mature mRNAs (see 3.7). The protein components, the mechanisms and dynamics of both processes and in particular their mechanistic linkage are still not well characterized. Although studies in the last decade have identified numerous spliceosomal components, we still know very little about the composition and functioning of the polyadenylation machinery in trypanosomes: Only CPSF73, CPSF30 and Fip1 had previously been identified and to some extent functionally described.

The first aim of this work was the initial characterization of the polyadenylation complex in *T. brucei*, including the identification of both the functional poly(A) polymerase and the other constituents of the polyadenylation machinery. Afterwards the proteins should be further investigated with regard to their role in *trans* splicing and polyadenylation, since these processes are coupled *in vivo*.

The second aim was to analyze the regulation of polyadenylation in trypanosomes. This was based on the exemplary DRBD4 protein, which is a homolog of human PTB that is known to regulate both splicing and polyadenylation *in vivo*. As a starting point for our functional analysis, we planned to determine both the DRBD4 RNA-binding motif and genome-wide binding sites. Afterwards DRBD4-dependent poly(A) sites should be identified and analyzed for DRBD4 binding, with the aim to characterize poly(A) sites directly regulated by DRBD4 *in vivo*.

4 Material and Methods

4.1 Material

4.1.1 Chemicals and reagents

2 (β)-mercaptoethanol	Roth
4´,6-diamidino-2-phenylindole (DAPI)	Roth
Acetic acid	Roth
Agarose ultra pure	Roth
Amberlite® MB-1 hydrogen and hydroxide form	Sigma-Aldrich
Ammonium persulfate (APS)	Bio-Rad
Ampicillin	Roth
Antibiotic-antimycotic (100×)	ThermoFischer Scientific
Anti-protein C affinity matrix	Roche Applied Science
Blasticidin	Sigma-Aldrich
Boric acid	Roth
Bovine serum albumin (20 mg/ml) (BSA)	Roche Applied Science
Bromphenol blue	Merck
Calcium chloride ($CaCl_2$)	Merck
Cellfectin® II reagent	ThermoFischer Scientific
Chloroform	Roth
Ciprofloxacin	AppliChem
Cold-water fish gelatin	Sigma-Aldrich
Dimethyl pyrocarbonate (DMPC)	Sigma-Aldrich
Dimethyl sulfoxide (DMSO)	Sigma-Aldrich
Dipotassium phosphate (K_2HPO_4)	Roth
Disodium hydrogen phosphate ($Na_2HPO_4 \times 2H_2O$)	Roth
Dithiothreitol (DTT)	Roth
DNAzol®	ThermoFischer Scientific
Doxycyclin (Dox)	Sigma-Aldrich
Ethanol (≥ 99,8%)	Roth
Ethidium bromide	Roth
Ethylenediaminetetraacetic acid (EDTA)	Roth
Ethyleneglycoltetraacetic acid (EGTA)	Sigma-Aldrich

Fetal bovine serum (FBS)	ThermoFischer Scientific
Ficoll® PM 400	Sigma-Aldrich
Formamide	Roth
Geniticin	ThermoFischer Scientific
Glucose	Sigma-Aldrich
Glutamin	Sigma-Aldrich
Glutathione sepharose 4B beads	GE Healthcare
Glycerol	Roth
Glycine	Roth
GlycoBlue (15 mg/ml)	ThermoFischer Scientific
Glycogen (20 mg/ml)	PeqLab
Glyoxal solution ~40% in H_2O (~8.8 M)	Sigma-Aldrich
Hemin	Sigma-Aldrich
Heparin sodium salt	Sigma-Aldrich
Hygromycin	ThermoFischer Scientific
Hypoxanthine	Sigma-Aldrich
IgG sepharose™ 6 fast flow	GE Healthcare
Immu-Mount™	ThermoFischer Scientific
InstantBlue-protein stain	Expedeon
Isopropanol	Roth
Isopropyl-β-D-thiogalactopyranosid (IPTG)	Roth
LB-agar (Luria/Miller)	Roth
LDS loading-buffer (4×)	ThermoFischer Scientific
L-proline	Sigma-Aldrich
L-threonine	Sigma-Aldrich
Magnesium chloride ($MgCl_2$)	Merck
Mangan chloride ($MnCl_2$)	Merck
Methanol	Roth
Milk-powder (fat-free)	Roth
Monopotassium phosphate (KH_2PO_4)	Roth
N-2-hydroxyethylpiperazine (HEPES)	Roth
N,N,N´,N´-tetramethylenediamine (TEMED)	Bio-Rad
Nonidet P-40 (NP-40)	Sigma-Aldrich
PageBlue™ protein staining solution	ThermoFischer Scientific
Penicillin G	Serva

Phleomycin	Sigma-Aldrich
Phosphate-buffered saline (PBS; 10×)	ThermoFischer Scientific
Polyoxyethylene (20) sorbitan monolaurate (Tween 20)	Sigma-Aldrich
Polyvinyl alcohol (PVA)	Sigma-Aldrich
Polyvinylpyrrolidone	Sigma-Aldrich
Potassium chloride (KCl)	Roth
Potassium phosphate (KH_2PO_4)	Roth
Puromycin	Sigma-Aldrich
Reducing agent (10×)	ThermoFischer Scientific
Roti-phenol (Phenol/Chloroform/Isoamylalcohol 25:24:1)	Roth
Rotiphorese gel 30 (30% Acrylamide/bisacrylamide 37.5:1)	Roth
Rotiphorese gel 40 (40% Acrylamide/bisacrylamide 19:1)	Roth
SDM-79 CGGGPPTA	PAA
Sf-900™ II SFM	ThermoFischer Scientific
Sodium acetate	Merck
Sodium azide (NaN_3)	Merck
Sodium chloride (NaCl)	Roth
Sodium citrate	Roth
Sodium dodecyl sulfate (SDS)	Roth
Sodium pyrophosphate tetrabasic ($Na_4P_2O_7$)	Sigma-Aldrich
Sodium pyruvate	Sigma-Aldrich
StrataClean resin	Agilent Technologies
Tris-hydroxymethylaminomethane (Tris)	Roth
Triton X-100	Merck
TRIzol® reagent	ThermoFischer Scientific
tRNA from yeast	Roche Applied Science
Trypton	Roth
Urea	Roth
Xylene cyanole	Fluka
Yeast extract	Roth

4.1.2 Commercial Kits

Bac-to-Bac® baculovirus expression system	ThermoFischer Scientific
Bio-Rad silver stain	Bio-Rad
High sensitivity DNA analysis kit	Agilent Technologies
HiScribe™ T7 high yield RNA synthesis kit	New England Biolabs
LabChip XT DNA 750 assay kit	PerkinElmer
Lumi-Light western blotting substrate	Roche Applied Science
PerfeCTa® SYBR® green FastMix®	Quanta Biosciences
Prime-It® RmT random primer labeling kit	Agilent Technologies
Qiagen® plasmid plus maxi kit	QIAGEN
QIAprep spin miniprep kit	QIAGEN
QIAquick gel extraction kit	QIAGEN
QIAquick PCR purification kit	QIAGEN
qScript™ cDNA synthesis kit	Quanta Biosciences
qScript™ flex cDNA kit	Quanta Biosciences
Qubit® dsDNA HS assay kit	ThermoFischer Scientific
RNeasy mini kit	QIAGEN

4.1.3 Enzymes and enzyme inhibitors

Accuprime supermix 1	ThermoFischer Scientific
AcTEV protease (10 U/µl)	ThermoFischer Scientific
Circligase II (100 U/µl)	Epicentre
cOmplete™ EDTA-free protease inhibitor	Roche Applied Science
Fast digest *Bam*HI	ThermoFischer Scientific
Phusion® high-fidelity DNA polymerase	New England Biolabs
Proteinase K (PK; 20 mg/ml)	Roth
Restriction endonucleases	New England Biolabs
RNase I (100 U/µl)	ThermoFischer Scientific
RNase A/T1 Mix (2 mg/ml; 5000 U/ml)	ThermoFischer Scientific
RNaseOUT RNase inhibitor (40 U/µl)	ThermoFischer Scientific
RQ1-DNase (1 U/µl)	Promega
Shrimp alkaline phosphatase (SAP; 1 U/µl)	ThermoFischer Scientific
Superscript III reverse transcriptase (200 U/µl)	ThermoFischer Scientific
T4 DNA ligase (400 U/µl)	New England Biolabs
T4 polynucleotide kinase (PNK; 10 U/µl)	New England Biolabs

T4 RNA ligase (10 U/µl)	ThermoFischer Scientific
T7 RNA polymerase (20 U/µl)	ThermoFischer Scientific
Taq DNA polymerase	expressed and purified by Silke Schreiner
TURBO DNase (2 U/µl)	ThermoFischer Scientific
USB® sequenase™ version 2.0 DNA polymerase	Affymetrix

4.1.4 Nucleotides

Deoxynucleoside triphosphate mix (dNTPs, 100 mM)	Peqlab
Ribonucleoside triphosphates (100 mM)	Roche Applied Science
[α-^{32}P]-ATP (3000 Ci/mmol; SCP-207)	Hartmann Analytic
[α-^{32}P]-CTP (3000 Ci/mmol; SCP-209)	Hartmann Analytic
[α-^{32}P]-dCTP (3000 Ci/mmol; SCP-205)	Hartmann Analytic
[γ-^{32}P]-ATP (800 Ci/mmol; SCP-801)	Hartmann Analytic

4.1.5 Markers

DIG-labeled DNA molecular weight marker VII	Roche Applied Science
Gene ruler DNA ladder mix	ThermoFischer Scientific
Gene ruler low range DNA ladder mix	ThermoFischer Scientific
pBR322 (Bolivar *et al.*, 1977); *Hpa*II digested	kindly provided by Michael R. Green (University of Massachusetts Medical School, Worcester, USA)
pcDNA3.1(+); *Hpa*II digested	ThermoFischer Scientific
peqGOLD protein-marker IV	Peqlab

4.1.6 Antibodies

Anti-GFP antibody	Roche Applied Science
Anti-protein A antibody produced in rabbit	Sigma-Aldrich
Anti-protein C antibody ab18591 (rabbit)	Abcam
Anti-rabbit IgG; peroxidase antibody (goat)	Sigma-Aldrich
Goat anti-rabbit IgG; secondary antibody; Alexa fluor® 488 conjugate	ThermoFischer Scientific
Goat anti-rabbit IgG; secondary antibody; Alexa fluor® 594 conjugate	ThermoFischer Scientific

4.1.7 Plasmids

pBR322 (Bolivar *et al.*, 1977)	kindly provided by Michael R. Green (University of Massachusetts Medical School, Worcester, USA)
pcDNA3.1(+)	ThermoFischer Scientific
pC-PTP-NEO (Schimanski *et al.*, 2005b)	kindly provided by Arthur Günzl (University of Connecticut Health Center, Connecticut, USA)
pFastBac^{TM}HT B	ThermoFischer Scientific
pGEX-6P-2	GE Healthcare
pLEW100 (Shi *et al.*, 2000)	kindly provided by Arthur Günzl (University of Connecticut Health Center, Connecticut, USA)
pJM326 (Schrader *et al.*, 1998)	kindly provided by Arthur Günzl (University of Connecticut Health Center, Connecticut, USA)

4.1.8 Bacterial and eukaryotic cells

DRBD4-PTP/YFP	all DRBD4 cell lines were kindly provided by Mark Carrington (University of Cambridge, Department of Biochemistry, Cambridge, UK)
DRBD4-RNAi (Tb427/pSPR2/p3217/p4379)	
DRBD4-RNAi (Tb427/p4106/p3217/p4379)	
MAX efficiency® DH10Bac™ competent cells	ThermoFischer Scientific
One shot® BL21 Star™ (DE3) chemically competent *E. coli*	ThermoFischer Scientific
Sf9 insect cells in Sf-900™ II SFM	ThermoFischer Scientific
Single step (KRX) competent cells	Promega
Tb427 29.13 (Wirtz *et al.*, 1999)	kindly provided by Ulrich Göringer (TU Darmstadt, Molecular Genetics, Darmstadt, GER)

4.1.9 *T. brucei* SDM-79 medium

Ciprofloxacin	1.5 mg/l
Fetal bovine serum (FBS)	10%
Glucose	1 g/l
Hemin (2.5 mg/ml in 0.05 M NaOH)	5 mg/l
L-proline	600 mg/l
L-threonine	350 mg/l
Penicillin G	60 mg/l
SDM-79 CGGGPPTA	One pack for 5 l medium
Sodium pyruvate	100 mg/l

The pH is adjusted with NaOH to 7.4 and the medium is filter sterilized with a Sartolab-P20 plus 0.20 µm filter (Sartorius).

4.1.10 Laboratory equipment

ÄKTA purifier 10	GE Healthcare
Agilent 2100 Bioanalyzer	Agilent Technologies
Axioskop 20 fluorescence microscope	Zeiss
BioPhotometer	Eppendorf
BLX-254 UV-Crosslinker	Bio-Link
Cooling-Thermomixer MKR 13	HLC
Curix60	AGFA
Electro cell manipulator 600	BTX
Foto/PrepI	Fotodyne
G:BOX gel documentation system	Syngene
GeneAmp PCR system 9700	Applied Biosystems
LabChip XT/XTe	PerkinElmer
Mastercycler ep realplex² S	Eppendorf
Mini-PROTEAN tetra electrophoresis system	Bio-Rad
NanoDrop 1000 spectrophotometer	ThermoFischer Scientific
NuPAGE electrophoresis and blotting system	ThermoFischer Scientific
PerfectBlue gelsystem mini M	Peqlab
Qubit® 2.0 fluorometer	ThermoFischer Scientific
Safety stand 630 A	BTX
Slab gel dryer SE1160	Hoefer Scientific Instruments
SpeedVac® plus SC100A	Savant

Sub-Cell GT agarose gel system	Bio-Rad
SureCycler 8000	Agilent Technologies
Trans-Blot® turbo™ transfer system	Bio-Rad
Tri-Carb 1600TR	PACKARD
Typhoon™ FLA 9500	GE Healthcare
Veriti thermal cycler	Applied Biosystems
Wide mini sub cell 41E/1261	Bio-Rad

4.1.11 DNA and RNA oligonucleotides (in 5´ to 3´direction)

Cloning of *T. brucei* pC-PTP-NEO constructs (Sigma-Aldrich)

PAP-PTP Tb927.3.3160 fw.	ATAAGGGCCCGGTTTGTCAGGTGCTTCCAT
PAP-PTP Tb927.3.3160 rv.	ATAAGCGGCCGCGCCTTCAGGTCTTGTAACAGGTG
PAP-PTP Tb927.7.3780 fw.	GATTA GGGCCCCGTACCAAGGCTACGTGGAT
PAP-PTP Tb927.7.3780 rv.	GATTAGCGGCCGCGCAAAACCGAGTCCCAGCGCTT
CPSF160-PTP fw.	GATTAGGGCCCCGAAGCGGTCTGAAATTTGT
CPSF160-PTP rv.	GATTAGCGGCCGCGC CTGCCTTCCCGTTGCATCAC
CPSF30-PTP fw.	GATTAGGGGCCCCGAAGCGGTCTGAAATTTGT
CPSF30-PTP rv.	GATTAGCGGCCGCGCCTGCCTTCCCGTTGCATCAC

Cloning of *T. brucei* pLEW100 RNAi constructs (Sigma-Aldrich)

PAP Tb927.3.3160 RNAi fw.	GCATAAAGCTTACGCGTTCAGGTGCTTCCATCTTCTC
PAP Tb927.3.3160 RNAi rv.	GCATATCTAGA GCCACATAGGAACTCCACAC
PAP Tb927.7.3780 RNAi fw.	CATAAAGCTTACGCGTGGTTGACCTTGCTCCCAGTA
PAP Tb927.7.3780 RNAi rv.	GCATATCTAGATGGCCAGTTGAATTATCACG
CPSF160 RNAi fw.	CATAAAGCTTACGCGTGCGGGTACCTTTGACAGAAA
CPSF160 RNAi rv.	CATATCTAGA AACCTCGTTGCGTACATTCC
CPSF100 RNAi fw.	ATATAAGCTTACGCGTAGCCCTCGTACGCACTTAAT
CPSF100 RNAi rv.	ATATTCTAGATTGGTCCCGCTACACTCATT
CPSF73 RNAi fw.	ATATAAGCTTACGCGTCTTCGCGCAGAGTCAAATGT
CPSF73 RNAi rv.	ATATTCTAGAATCCTCTAACTCCACGGTGC
CPSF30 RNAi fw.	ATATAAGCTTACGCGTGCCTTTTATCAGCGTCTCGG
CPSF30 RNAi rv.	ATATTCTAGAGACCTCATGCCCCTCTTCTC
Fip1 RNAi fw.	ATATAAGCTTACGCGTCGGTTTCAACGAGAGCAGTT
Fip1 RNAi rv.	ATATTCTAGATGCTGGTGTATTCGGATCCA
CstF50 RNAi fw.	ATATAAGCTTACGCGTGGACTGGCACCCTTATCACT
CstF50 RNAi rv.	ATATTCTAGAAATGGCATTGATCGGGTTGG
CstF64 RNAi fw.	ATATAAGCTTACGCGTTACTTCGAAGAGGAAGAGAATAATG
CstF64 RNAi rv.	ATATTCTAGATACCCAACTGCTATACCCCGT
Symplekin RNAi fw.	ATATAAGCTTACGCGTCACGTGGCATTCTCAGTTCC
Symplekin RNAi rv.	ATATTCTAGAGATGAGGACCTGATCTGGCA
CFIm25 RNAi fw.	ATATAAGCTTACGCGTTACCTGCGACGAACACAAAC

CFIm25 RNAi rv.	ATATTCTAGAGAGATCGAACAATGGAGCGG
CFIIm RNAi fw.	ATATAAGCTTACGCGTGGTAACTGACATGGGGCTTG
CFIIm RNAi rv.	ATATTCTAGACCGGGGAGAGAAACGAAAAG
Tb927.11.13860 RNAi fw.	ATATAAGCTTACGCGTCCAACATACTTGCCGTGGTC
Tb927.11.13860 RNAi rv.	ATATTCTAGACAACGATGACCAGCAACACA
Tb927.8.4480 RNAi fw.	ATATAAGCTTACGCGTACTTCTGCTAGCTGGGGAAG
Tb927.8.4480 RNAi rv.	ATATTCTAGATAATCCATGCCTCTTCGCCA

Cloning of baculovirus pFastBac^{TM}HT B expression constructs (Sigma-Aldrich)

PAP Tb927.3.3160 fw.	CATAGGATCCGAGTGGATGTATGGCCCAAC
PAP Tb927.3.3160 rv.	CATATCTAGATTACTTCAGGTCTTGTAACAGGT
PAP Tb927.7.3780 fw.	CATAGGATCCTCACGAACAGACAAGTCGTTC
PAP Tb927.7.3780 rv.	CATATCTAGATCAAAAACCGAGTCCCAGCGC

Cloning of bacterial pGEX-6P-2 expression constructs (Sigma-Aldrich)

GST-CPSF30 fw.	CCTGGGATCCTTTACTGACAACGCTGCCCACA
GST-CPSF30 rv.	CCGGGAATTCTTACTGCCTTCCCGTTGCATC
GST-DRBD4 fw.	ATATGTCGACTCAAACCTGTCTTTTGAGTAACATTC
GST-DRBD4 rv.	ATATGCGGCCGCTCACTCATTCTGTTCGTCCTGTG

Sequencing primer (Sigma-Aldrich)

pc-PTP-NEO seq rv.	AATTCTCGCTAGCAGTAGTTGG
pGEX-6P-2 seq fw.	AAGCCACGTTTGGTGGTG
pGEX-6P-2 seq rv.	CCGGGAGCTGCATGTGTCAGAGG
pFastBac^{TM}HT B seq.	AAATGATAACCATCTCGC

mRNA detection primer (Sigma-Aldrich)

mRNA CPSF160 fw.	AAGTCCTCGAGTCGGTTCTC
mRNA CPSF160 rv.	AAACATGCGTGGTGTCAGTC
mRNA CPSF100 fw.	GTTGGTTGGGTGGAAGGTTC
mRNA CPSF100 rv.	CACGCAACTTATGGAGGTCG
mRNA CPSF73 fw.	GAGCACGAGATCTCAGACGA
mRNA CPSF73 rv.	ATCCTCTAACTCCACGGTGC
mRNA CPSF30 fw.	CCCACCGTGTGTCTTTTACC
mRNA CPSF30 rv.	CACTTTGCATACCCGGACAG
mRNA Fip1 fw.	CTGTCAGCGTTTCTTGGAGG
mRNA Fip1 rv.	GTTGTTGTTGTGGTGGTGGT
mRNA CstF50 fw.	GGACTGGCACCCTTATCACT
mRNA CstF50 rv.	CTCCACTCGTTCCACTGACT
mRNA CstF64 fw.	AACACCACCAGCCGATGTAT
mRNA CstF64 rv.	TTCAGGAAGGGGCACAATCT
mRNA Symplekin fw.	CCGGATATGCAGAGTTCGCT

mRNA Symplekin rv.	TCGAGAAGCAACACTGGCAT
mRNA CFIm25 fw.	GAAGTGGTGGTTGATGTCGG
mRNA CFIm25 rv.	GAGATCGAACAATGGAGCGG
mRNA CFIIm fw.	CGTTCACTTCATCCACGCTT
mRNA CFIIm rv.	AAGGTGGCACTTTATCCCGT
mRNA Tb927.11.13860 fw.	ACAACTTAGTGGGCTCGTCA
mRNA Tb927.11.13860 rv.	CAACGATGACCAGCAACACA
mRNA Tb927.8.4480 fw.	CTGCAGATGTGGCCAGTTTT
mRNA Tb927.8.4480 rv.	TAATCCATGCCTCTTCGCCA

Polyadenylation assay (Sigma-Aldrich)

Poly(T) with G	CGGGGGTTTTTTTTTTTTTTTTTTT

Trans splicing assay (Sigma-Aldrich)

PPIase exon rv.	CGTTGCGACCACTTCTGCA
PRP8 exon rv.	GATGACCACTTCTCAGTGAC
SL RNA 6-28 fw.	ACGCTATTATTAGAACAGTTTCT
SL RNA rv.	CAGGAACCAACAGCACAATG

PCR primer for loading controls (Sigma-Aldrich)

7SL RNA fw.	GTTGCGTTGACTTGGTGTTC
7SL RNA rv.	TCGGTGTGCTTCTGCAAC
U3 RNA fw.	CCGTACTCTGAACAGAATCGTTTT
U3 RNA rv.	CCGTTCATCGAACAGCTCTC'

SELEX annealing oligonucleotides (Sigma-Aldrich); N: random nucleotide

SLX-N20	GCGTCTCGAGCGTAGTTANNNNNNNNNNNNNNNNNNAG TCGGCATCTTGGTACCCTATAGTGAGTCGTATTA
T7 fw.	TAATACGACTCACTATAGGG

SELEX RT-PCR primer (Sigma-Aldrich)

SLX-RT	GCGTCTCGAGCGTAGTTA
SLX-T7 fw.	TAATACGACTCACTATAGGGTACCAAGATGCCGACT

SELEX RT barcoding primer (Sigma-Aldrich); N: random nucleotide; experimental barcode

SLX_R1	CAAGCAGAAGACGGCATACGAGATCGGTCTCGGCATTCCTGN NCCAANNNGCGTCTCGAGCGTAGTTA
SLX_R2	CAAGCAGAAGACGGCATACGAGATCGGTCTCGGCATTCCTGN NCACCNNNGCGTCTCGAGCGTAGTTA
SLX_R3	CAAGCAGAAGACGGCATACGAGATCGGTCTCGGCATTCCTGN NGTTCNNNGCGTCTCGAGCGTAGTTA

SLX_R4	CAAGCAGAAGACGGCATACGAGATCGGTCTCGGCATTCCTGNNGGCTNNNGCGTCTCGAGCGTAGTTA
SLX_R5	CAAGCAGAAGACGGCATACGAGATCGGTCTCGGCATTCCTGNNTGCANNNGCGTCTCGAGCGTAGTTA
SLX_R6	CAAGCAGAAGACGGCATACGAGATCGGTCTCGGCATTCCTGNNAGCTNNNGCGTCTCGAGCGTAGTTA
SLX_R7	CAAGCAGAAGACGGCATACGAGATCGGTCTCGGCATTCCTGNNCGTCNNNGCGTCTCGAGCGTAGTTA
SLX_R8	CAAGCAGAAGACGGCATACGAGATCGGTCTCGGCATTCCTGNNATACNNNGCGTCTCGAGCGTAGTTA
SLX_R9	CAAGCAGAAGACGGCATACGAGATCGGTCTCGGCATTCCTGNNCTTGNNNGCGTCTCGAGCGTAGTTA
SLX_R10	CAAGCAGAAGACGGCATACGAGATCGGTCTCGGCATTCCTGNNTAACNNNGCGTCTCGAGCGTAGTTA
SLX_R11	CAAGCAGAAGACGGCATACGAGATCGGTCTCGGCATTCCTGNNTTCTNNNGCGTCTCGAGCGTAGTTA
SLX_R12	CAAGCAGAAGACGGCATACGAGATCGGTCTCGGCATTCCTGNNACTCNNNGCGTCTCGAGCGTAGTTA

SELEX library amplification primer (Sigma-Aldrich); N: random nucleotide

SLX-Sol-5×N fw.	AATGATACGGCGACGTCCGAGATCTACACTCTTTCCCTACACGACGCTCTTCCGATCTNNNNNGGGTACCAAGATGCCGACT
SLX_Sol rv.	CAAGCAGAAGACGGCATACG

Oligonucleotides for T7 *in vitro* transcription (Sigma-Aldrich)

DRBD4 motif_1_s (T7 fw.)	TAATACGACTCACTATAGGG
DRBD4 motif_1_as	TTGGGTTCATTGGGTTGGGTTCATTGGGTTCCCTATAGTGAGTCGTATTA
DRBD4 motif_2_s	TAATACGACTCACTATAGGGAAATGAATGACGTCGAG
DRBD4 motif_2_as	CTCGACGTCATTCATTTCCCTATAGTGAGTCGTATTA
DRBD4 motif_3_s	TAATACGACTCACTATAGGGAAGAAATGAACGTCGAG
DRBD4 motif_3_as	CTCGACGTTCATTTCTTCCCTATAGTGAGTCGTATTA
DRBD4 motif_4_s	TAATACGACTCACTATAGGGAAATGAATGAATGA CGTCGAG
DRBD4 motif_4_as	CTCGACGTCATTCATTCATTTCCCTATAGTGAGTCGTATTA
DRBD4 motif_5_s	TAATACGACTCACTATAGGGAAAAGAATGAAGAACGTCGAG
DRBD4 motif_5_as	CTCGACGTTCTTCATTCTTTTCCCTATAGTGAGTCGTATTA
DRBD4 motif_6_s	TAATACGACTCACTATAGGGAAATGAAAATGACGTCGAG
DRBD4 motif_6_as	CTCGACGTCATTTTCATTTCCCTATAGTGAGTCGTATTA
DRBD4 motif_7_s	TAATACGACTCACTATAGGGAAATGAAAAAATGACGTCGAG
DRBD4 motif_7_as	CTCGACGTCATTTTTTCATTTCCCTATAGTGAGTCGTATTA
DRBD4 motif_8_s	TAATACGACTCACTATAGGGAAATGAAAAAAAAAATGACGTCGAG
DRBD4 motif_8_as	CTCGACGTCATTTTTTTTTTCATTTCCCTATAGTGAGTCGTATTA

DRBD4 motif_9_s	TAATACGACTCACTATAGGGAAAAAAAAAAAAACGTCGAG
DRBD4 motif_9_as	CTCGACGTTTTTTTTTTTTTTCCCTATAGTGAGTCGTATTA
DRBD4 motif_10_s	TAATACGACTCACTATAGGGAAATTAATTAATTA CGTCGAG
DRBD4 motif_10_as	CTCGACGTAATTAATTAATTTCCCTATAGTGAGTCGTATTA
Tb927.1.2340_PPT_s	TAATACGACTCACTATAGGGTTCTCCTCTCCTCACCCCCTC
Tb927.1.2340_PPT_as	GAGGGGGTGAGGAGAGGAGAACCCTATAGTGAGTCGTATTA
Tb927.11.3630_PPT_s_1	TAATACGACTCACTATAGGGTTTCCTTCTCTTTCTCCTTTTCTT TCCTTTCTT
Tb927.11.3630_PPT_as_1	AAGAAAGGAAAGAAAAGGAGAAAGAGAAGGAAACCCTATAG TGAGTCGTATTA
Tb927.11.3630_PPT_s_2	TAATACGACTCACTATAGGGCTTCCCTCCTTTCTCTTTCTTTTT
Tb927.11.3630_PPT_as_2	AAAAAGAAAGAGAAAGGAGGGAAGCCCTATAGTGAGTCGTAT TA
Tb927.6.510_PPT_s (T7 fw.)	TAATACGACTCACTATAGGG
Tb927.6.510_PPT_as	GAAAAAAATGGGGAAAAGGAAAAAAAAGCCCTATAGTGAGTC GTATTA

iCLIP RNA oligonucleotide (Dharmacon); P: phosphate

3´-linker	P-UGAGAUCGGAAGAGCGGUUCAG-Puromycin

iCLIP RT-primer (Sigma-Aldrich); P: phosphate; N: random nucleotide; experimental barcode

iCLIP-RT4	P- NNAGGTNNNAGATCGGAAGAGCGTCGTGGATCCTGAACC GC
iCLIP-RT8	P-NNCATTNNNAGATCGGAAGAGCGTCGTGGATCCTGAACC GC
iCLIP-RT9	P-NNGCCANNNAGATCGGAAGAGCGTCGTGGATCCTGAACC GC
iCLIP-RT10	P-NNGACCNNNAGATCGGAAGAGCGTCGTGGATCCTGAACC GC

iCLIP oligonucleotide for linearization of circular ssDNA (MWG Eurofins)

Cut_oligo	GTTCAGGATCCACGACGCTCTTCAAAA

iCLIP PCR-primer compatible with high-throughput sequencing (MWG Eurofins)

Solexa P5	AATGATACGGCGACCACCGAGATCTACACTCTTTCCCTACAC GACGCTCTTCCGATCT
Solexa P3	CAAGCAGAAGACGGCATACGAGATCGGTCTCGGCATTCCTGC TGAACCGCTCTTCCGATCT

PCR-primer for Northern blot probes (Sigma-Aldrich)

Probe Tb927.8.760 fw.	CCGAAGATACCCGAAGACCA
Probe Tb927.8.760 rv.	AACATCCGAACATGAGGGGA

Probe Tb927.8.770 fw.	GATAACGTGTCGCTGACCAC
Probe Tb927.8.770 rv.	TGCCTCCTCGTCAAAGTGAT
Probe Tb927.11.5440 fw.	TGTTTCAAAGGTGGGGCTTG
Probe Tb927.11.5440 rv.	CGTGAGAAGTTTGGCTACCG
Probe Tb927.6.1470 fw.	CAAGGTGGAGTGAGGAAGGA
Probe Tb927.6.1470 rv.	TGCGCCTTTTGTCTACCATG
Probe Tb927.2.6000 fw.	CCAGTTCTCCCCGTGTTTTG
Probe Tb927.2.6000 rv.	CCAAATCACGCGTCATGAGT
Probe 18S rRNA fw.	CAGCGGATCACGCGCTTACA
Probe 18S rRNA rv.	CTGTGCAATTATACATGCA

4.2 General techniques

4.2.1 Guideline

All methods were adapted from laboratory protocols or the cited literature. Enzymes, reagents and kits were, if not otherwise stated, used according to the manufactures instructions. If not otherwise mentioned, all reactions and incubation steps were performed at room temperature.

4.2.2 Working with RNA

All steps were performed with certified RNase-free material and all buffers were prepared with RNase-free water. This was prepared by addition of 1:1,000 volumes of dimethyl pyrocarbonate (DMPC) to deionized water, stirring for 1 h and two times autoclaving (120°C, 20 min, 2 bar). In the following, RNase-free water is termed “DMPC-water”. If not otherwise mentioned, samples where always kept on ice.

4.2.3 Isolation of nucleic acids from *T. brucei* cells

For the isolation of genomic DNA or total RNA from procyclic *T. brucei* cells, the DNAzol® or TRIzol® reagent (both ThermoFischer Scientific) was used, respectively. If high-quality RNA was required, e.g. for RT-PCR, the RNA precipitation step was skipped, the RNA solution was mixed 1:1 with 70% ethanol and further purified using RNeasy columns (QIAGEN).

4.2.4 Purification of nucleic acids

Phenol/chlorofrom extraction was used to purify nucleic acids form enzymatic reactions. The nucleic acid/protein solution was dissolved with DMPC-water >300 µl and an equal volume of RNA-grade phenol/chloroform/isoamylacohol (25:24:1) was added. The mixture was vigorously mixed for 30 sec and centrifuged (4°C, 5 min, 25,000 × g) for phase separation. The upper, aqueous phase was transferred in a new reaction tube and nucleic acids were precipitated (see 4.2.5). If the yield was critical, PhaseLock heavy gel tubes (5 Prime) were used.

4.2.5 Precipitation of nucleic acids

To concentrate or desalt nucleic acids, ethanol or isopropanol precipitation was used. The nucleic acid solution was mixed with 1:10 volumes of 3M sodium-acetate (pH 5.2) and 10-20 µg glycogen (PeqLab) or 7.5-15 µg GlycoBlue (ThermoFischer Scientific). To precipitate nucleic acids, 2.5 volumes of 100% ethanol or 0.7-0.8 volumes of isopropanol were added, followed by incubation (4°C, -20°C or -80°C for 30 min to 16h) and centrifugation (4°C, 30 min, 25,000 × g). The pellet was washed with 70% ethanol and centrifuged for 5 min using the same conditions.

Precipitated nucleic acids were dissolved in deionized water or in case of RNA in DMPC-water. RNA-pellets were for subsequent denaturing polyacrylamide/urea gel electrophoresis directly dissolved in 1× formamide loading buffer (0.5× TBE, 45% formamide, 0.025% bromphenol blue, 0.025% xylene cyanol).

4.2.6 Photometric determination of nucleic acid concentration

To determine the nucleic acid concentration, the NanoDrop 1000 spectrophotometer (ThermoFischer Scientific) or BioPhotometer (Eppendorf) was used. In case of iCLIP and SELEX-seq libraries, the nucleic acid concentration was measured using the Qubit® 2.0 fluorometer (ThermoFischer Scientific) and the Qubit® dsDNA HS assay kit (ThermoFischer Scientific).

4.2.7 Databases, web-based bioinformatics and programs

As a general database for *T. brucei* specific genome-data "TriTrypDB" was used (Aslett *et al.*, 2010). Pairwise nucleotide and protein sequence alignments were performed by the "EMBOSS Needle" and multiple sequence alignments by the "Clustal Omega" program. Pattern and profile search were done by "InterProScan" (Jones *et al.*, 2014). Protein structure prediction was carried out via the "GeneSilico metaserver" (Kurowski & Bujnicki, 2003). PCR primer were designed using "Primer3" (Rozen & Skaletsky, 2000) and melting temperatures were calculated by "Oligo Calc" (Kibbe, 2007). In addition, useful tools like "Reverse complement" from "The sequence manipulation suite" (Stothard, 2000), "NEBcutter V2.0" as well as "Double digest finder" provided by New England Biolabs, "LIGATION CALCULATOR" and "BLAST®" (Altschul *et al.*, 1990) were used. For planning of molecular cloning strategies "Vector NTI 10.3.1" (ThermoFischer Scientific) and for analysis of genome-wide data the "Integrative genomics viewer" were utilized (Robinson *et al.*, 2011, Thorvaldsdottir *et al.*, 2013). Mass spectrometry data were evaluated with "Scaffold version 4.0.4" (Proteome Software) and relative band intensities were measured using "ImageJ" (Schneider *et al.*, 2012). Literature search was performed using "PubMed".

BLAST®	http://blast.ncbi.nlm.nih.gov/Blast.cgi
Clustal Omega	http://www.ebi.ac.uk/Tools/msa/clustalo/
Double digest finder	https://www.neb.com/tools-and-resources/interactive-tools/double-digest-finder
EMBOSS Needle	http://www.ebi.ac.uk/Tools/psa/emboss_needle/
GeneSilico metaserver	https://www.genesilico.pl/meta2/

InterProScan	http://www.ebi.ac.uk/interpro/search/sequence-search
LIGATION CALCULATOR	http://www.insilico.uni-duesseldorf.de/Lig_Input.html
NEBcutter V2.0	http://nc2.neb.com/NEBcutter2/
Oligo Calc	http://biotools.nubic.northwestern.edu/OligoCalc.html
Primer3	http://primer3.ut.ee/
PubMed	http://www.ncbi.nlm.nih.gov/pubmed
Reverse complement	http://www.bioinformatics.org/sms/rev_comp.html
The sequence manipulation suite	http://www.bioinformatics.org/sms/index.html
TriTrypDB	http://tritrypdb.org/tritrypdb/

4.3 Cell culture of procyclic *T. brucei*

4.3.1 Cultivation of procyclic *T. brucei* cells

Cell culture of eukaryotic cells was carried out under sterile conditions, using a clean bench in a designated cell culture laboratory. Commercially available flasks and pipettes were used. Procyclic *T. brucei* cells were grown for two to three days at 28°C in SDM-79 medium (see 4.1.9) after dilution to 2×10^6 cells/ml. Glycerol stocks were prepared in SDM-79 (containing 10% glycerol) and stored at -80°C or in liquid nitrogen. According to the type of cell line antibiotics were added to the media (**Table 4.1**).

Table 4.1 Antibiotics for *T. brucei* cell culture.

Cell line	Antibiotic
PTP/YFP-tag	Geniticin [40 µg/ml]
Tb427 29.13	Geniticin [15 µg/ml]
	Hygromycin [50 µg/ml]
Tb427 29.13 + pLEW100	Geniticin [15 µg/ml]
	Hygromycin [50 µg/ml]
	Phleomycin [2.5 µg/ml]
DRBD4-RNAi (pSPR2/p3217/p4379)	Blasticidin [10 µg/ml]
	Geniticin [15 µg/ml]
	Puromycin [1 µg/ml]
DRBD4-RNAi (p4106/p3217/p4379)	Blasticidin [10 µg/ml]
	Geniticin [15 µg/ml]
	Puromycin [1 µg/ml]

4.3.2 Transfection of procyclic *T. brucei* cells

Procyclic *T. brucei* cells (see 4.3.1) were transfected with 10 µg linearized plasmid (in 20 µl sterile water) by electroporation. The cells (8×10^7 to 1×10^8) were suspended in 380 µl Cytomix pH 7.6 (120 mM KCl, 0.15 mM $CaCl_2$, 10 mM K_2HPO_4/KH_2PO_4 pH 7.6, 25 mM HEPES pH 7.6, 5 mM $MgCl_2$, 2 mM EGTA pH 7.6, 0.5% glucose, 100 µg/ml BSA, 1 mM hypoxanthine), mixed with the plasmid, transferred in a Gene pulser®/MicroPulser™ electroporation cuvette 0.2 cm (Bio-Rad) and electroporated (1500 V, 25 µF, 24 Ω) using a Electro cell manipulator 600 (BTX). Afterwards 10 ml fresh SDM-79 medium was added and the cells were grown for 8 h before the selective antibiotic was added (see 4.3.1). Finally, the cells were spread (200 µl each) in 96-well plates for growing to obtain clonal cell lines.

4.3.3 Generation of clonal cell lines

To generate a stable RNAi cell line, the linearized pLEW100 construct (see 4.9.1) was transfected into Tb427 29.13 cells and integrated into an rDNA spacer. The plasmid (10 µg) was linearized using *Sac*II (see 4.6.2), isopropanol precipitated (see 4.2.5, no addition of glycogen or sodium-acetate) and transfected (see 4.3.2). To generate a C-terminal PTP-tagged cell line, the pC-PTP-NEO construct (see 4.9.2) was transfected (see 4.3.2) in *T. brucei* 427 (WT) cells and integrated in the endogenous locus. The constructs were linearized in the insert using *Xho*I (Tb927.7.3780, Tb927.3.3160, CPSF160) or *Bsm*I (CPSF30), precipitated and transfected as described above.

4.3.4 Reverse knockdown using procyclic *T. brucei* RNAi cell lines

For a specific, RNAi-mediated knockdown of a single gene (see 4.3.3), 2×10^6 cells/ml were treated for 24 h with 1 mg/ml doxycyclin (Sigma-Aldrich, in 70% ethanol). Afterwards the cells were counted, diluted to 2×10^6 cells/ml and treated again with doxycyclin. As control 70% ethanol was used. The cells were harvested for a large, preparative knockdown after day one, two and three after RNAi induction. The knockdown was extended for up to five days for growth curve experiments. RNAi for RNA-seq was induced in the cell line Tb427/pSPR2/p3217/p4379 by the addition of 0.2 mg/ml doxycycline and cells were diluted every day to 2×10^4 cell/ml. For Northern blotting (cell line: Tb427/p4106/p3217/p4379) RNAi was induced by the addition of 0.2 mg/ml doxycycline at a cell density of 2×10^4/ml or 1 mg/ml doxycycline at a cell density of 2×10^6/ml.

4.4 Reverse transcription (RT) and polymerase chain reaction (PCR)

4.4.1 Reverse transcription (RT)

RNA was reverse transcribed for PCR-based analysis using the qScript™cDNA synthesis kit (Quanta Biosciences) containing oligo(dT) and random hexamer primer. For specific RT the Superscript III reverse transcriptase (ThermoFischer Scientific) or the qScript™ flex cDNA kit (Quanta Biosciences) was used. Total RNA was isolated as described in 4.2.3.

4.4.2 Polymerase chain reaction (PCR)

Taq polymerase and a 10× *Taq* PCR buffer (100 mM Tris-Cl pH 9.0, 500 mM NaCl, 15 mM $MgCl_2$, 1% Triton X-100) were used for standard PCR. Preparative PCR for cloning of protein-coding genes was performed using Phusion® high-fidelity DNA polymerase (New England Biolabs). As template either cDNA (see 4.4.1) or genomic DNA (see 4.2.3) was used.

Standard 25 µl PCR and temperature profile

Volume	Component	Concentration
2.5 µl	10× *Taq* PCR buffer	1× (1.5 mM $MgCl_2$)
0.5 µl	*Taq* DNA polymerase	-
1.0 µl	$MgCl_2$ (25 mM)	1.0 mM
1.0 µl	dNTPs (10 mM each)	0.4 mM
1.0 µl	forward primer (10 µM)	0.4 µM
1.0 µl	reverse primer (10 µM)	0.4 µM
1.0 µl	DNA template	-
17.0 µl	deionized water	
25.0 µl		

initial denaturation	94°C	2 min	
denaturation	94°C	10 sec	25-35 cycles
annealing	52-62°C	20 sec	
elongation	72°C	30-120 sec	
final elongation	72°C	7 min	
storage	4°C	hold	

If required, the PCR reaction was scaled up to 2× (50 µl) or 4× (100 µl) and the magnesium chloride concentration was altered for optimization. The annealing temperature of each primer pair was empirically determined or by using “Oligo Calc” (see 4.2.7). For primer design “Primer3” (see 4.2.7) was used (with the exception of open reading frame primer for protein expression constructs). The elongation time was set depending on the length of the PCR product by

assuming an average elongation of 1 kb per min. The cycle number was determined empirically. PCR reactions were analyzed by gel electrophoresis and ethidium bromide staining (see 4.5.1). Preparative PCR products were gel purified (see 4.5.2). Primer sequences are summarized in 4.1.11.

4.4.3 Quantitative RT-PCR (RT-qPCR)

Since PCR described in 4.4.2 allows only semiquantitative measurements, quantitative RT-PCR (RT-qPCR) was used to determine RNA levels precisely. Total RNA was isolated (see 4.2.3) and converted into cDNA according to 4.4.1. All experiments were performed as biological replicates and technical triplicates. The Quanta PerfeCTa® SYBR® green FastMix® (Quanta Biosciences) and Mastercycler ep realplex² S (Eppendorf) were used. qPCR data was analyzed using the provided software and quantified according to an established strategy (Pfaffl, 2001). Primer amplification efficiencies were determined by a dilution series of cDNA (see 4.4.1) from *T. brucei* 427 (WT) cells. C_T values were plotted against the logarithm of the dilution factor to obtain the slope. Finally, the amplification efficiency was calculated according to the formula: $E = 10^{(-1/slope)}$. Relative expression levels were calculated using the following formula:

$$relative\ expression = \frac{(E_{target\ RNA})^{\Delta C_{T\ target\ RNA}(control-knockdown)}}{(E_{reference\ RNA})^{\Delta C_{T\ reference\ RNA}(control-knockdown)}}$$

E is the amplification efficiency and ΔC_T is the difference between the control and knockdown sample.

4.5 Gel electrophoresis-based analysis and detection methods

For gel electrophoresis of nucleic acids the Tris-Borate-EDTA (TBE) buffer system was used. The 10× TBE buffer stock solution (890 mM Tris-Cl pH 8.0, 890 mM boric acid, 20 mM EDTA) was diluted as indicated.

4.5.1 Gel electrophoresis of DNA

Agarose gel electrophoresis was used as standard method for the analysis of DNA. The agarose concentration was chosen depending on the fragment length to obtain optimal resolution (**Table 4.2**).

Table 4.2 Agarose concentration in DNA gels.
DNA fragment-dependent agarose concentration used for gel electrophoresis including running behavior of tracking dyes

Fragment size	Agarose concentration (w/v)	Bromphenol blue	Xylen cyanol
0.5-7 kb	1.0	300 bp	3.0 kb
0.4-6 kb	1.2	200 bp	1.5 kb
0.2-3 kb	1.5	120 bp	1.0 kb
0.1-2 kb	2.0	<100 bp	0.8 kb

Agarose was dissolved in 0.5× TBE by boiling in a microwave, supplemented with ethidium bromide (final concentration 0.5 µg/ml) and stored at 50°C. Gels were poured and run in horizontal gel systems (PerfectBlue gelsystem mini M [Peqlab] or Sub-Cell GT [Bio-Rad]). DNA samples were diluted 1:6 with a 6× DNA loading dye (1× TBE, 20% glycerol, 0,025% xylen cyanol, 0,025% bromphenol blue) and run for 30-60 min at 120 V in 0.5× TBE. Gels were analyzed and documented under UV-irradiation using the G:BOX gel documentation system (Syngene). Gene ruler DNA ladder mix or Gene ruler low range DNA ladder mix (both ThermoFischer Scientific) was used as marker.

Polyacrylamide gel electrophoresis (Mini-PROTEAN tetra electrophoresis system [Bio-Rad]) was used for high resolution analysis of very short DNA fragments (<200 bp, e.g. iCLIP library preparation PCR). A 6% solution of acrylamide/bisacrylamide (19:1) was prepared in 1× TBE, and polymerization was initiated by adding 1:125 volumes of 10% APS and 1:1,250 volumes of TEMED. Gels were run for 25 min at 200 V (1× TBE), stained for 10 min with ethidium bromide (5 µg/ml in 1× TBE) and destained for 2 min in deionized water. Analysis was carried out as

described above. As marker, Gene ruler low range DNA ladder (ThermoFischer Scientific) was used.

4.5.2 Extraction of DNA from agarose gels

Gel purification was used for the isolation of a single DNA species from a complex mixture. Agarose gel electrophoresis was performed with an agarose concentration <2% according to 4.5.1, followed by purification using the QIAquick gel extraction kit (QIAGEN).

4.5.3 Denaturing polyacrylamide/urea gel electrophoresis of RNA

For the analysis of RNA, the samples were diluted 1:2 in 2× formamide loading buffer (1× TBE, 90% formamide, 0.05% bromphenol blue, 0.05% xylene cyanol) or as pellets directly dissolved in 1× formamide loading buffer after precipitation (see 4.2.5). RNA was denatured for 5 min at 95°C and put on ice for additional 3 min. The samples were loaded onto denaturing TBE polyacrylamide/urea gels for electrophoresis, using either the Mini-PROTEAN tetra electrophoresis system (Bio-Rad) or a custom gel system (21 cm × 18 cm × 0.5 mm). The gel was prepared using a 10 to 15% solution of acrylamide/bisacrylamide (19:1) in 1× TBE containing 50% urea. Polymerization was initiated by the addition of 1:125 volumes of 10% APS and 1:1,250 volumes of TEMED. The gels were run for 20 min at 23 W prior loading of the sample. Samples were loaded and separated for 40 to 110 min at 23W (0.5× TBE). For unspecific detection of RNA Bio-Rad silver stain (Bio-Rad) was used. As a marker, DIG-labeled DNA molecular weight marker VII (Roche Applied Science) was used.

Radioactive labeled samples were detected by autoradiography (see 4.5.4). As marker, pcDNA3.1(+) or pBR322 were *Hpa*II digested, fragments were SAP (ThermoFischer Scientific) treated and radioactive labeled at their 5´ end using T4 PNK (New England Biolabs) and [γ-^{32}P]-ATP (800 Ci/mmol; SCP-801 [Hartmann Analytic]).

4.5.4 Autoradiography

After separation of radioactively labeled RNA samples by gel electrophoresis (see 4.5.3), autoradiography was performed for detection. One glass plate was removed and the gel was covered with plastic wrap. An X-ray film (-80°C) or phosphorimaging screen (room temperature) was exposed in a film cassette for up to several days depending on the signal strength. Phosphorimaging screens were scanned using a Typhoon FLA 9500 (GE Healthcare) and quantified using the provided “ImageQuant TL” program.

4.5.5 Glyoxal RNA gel and Northern blotting

Five µg of total RNA form *T. brucei* (see 4.2.3) was denatured for 40 min at 50°C (in 50% DMSO, 4% glyoxal, 10 mM sodium phosphate, pH 6.9) and separated on a 1.2 % agarose gel (10 mM sodium phosphate, pH 6.9). In the following, RNA was capillary blotted overnight on an Amersham Hybond-N membrane (GE Healthcare) using 20× SSC (150 mM NaCl, 15 mM sodium citrate), crosslinked at 254 nM (120 mJ/cm^2), incubated at 80°C for 60 min and pre-hybridized (5× SSC, 5× Denhardt's solution, 10% SDS, 0.1% $Na_4P_2O_7$, 0.1 % heparin sodium salt) for 1 h at 65°C. Following overnight (65°C) hybridization with ^{32}P-dCTP-labeled PCR probes (3000 Ci/mmol; SCP-205 [Hartmann Analytic]) complementary to the ORF of the target gene (Prime-It® RmT random primer labeling kit [Agilent Technologies]), the membrane was wash twice (0.1× SSC, 0.1% SDS) for 30 min at 60°C and quantified by autoradiography using the Typhoon FLA 9500 (GE Healthcare) imaging system and X-ray films (see 4.5.4).

4.5.6 Denaturing polyacrylamide/SDS gel electrophoresis of proteins

For gel electrophoresis of proteins, the discontinuous Laemmli gel/buffer system and Mini-PROTEAN tetra electrophoresis system (Bio-Rad) were used (Laemmli, 1970). A 10-15% acrylamide/bisacrylamide (37.5:1) solution was prepared in separating gel buffer (375 mM Tris-Cl pH 8.8, 0.1% SDS) depending on the protein to be analyzed. Polymerization was initiated by adding 1:125 volumes of 10% APS and 1:1,250 volumes of TEMED. Stacking gels were poured after polymerization of the separating gel, using a 5% acrylamide/bisacrylamide (37.5:1) solution in stacking gel buffer (62.5 mM Tris-Cl pH 6.8, 0.05% SDS). Polymerization was initiated by adding the same ratios of TEMED and APS. Protein samples were mixed 1:1 with 2× SDS sample buffer (125 mM Tris-Cl pH 6.8, 20% glycerol, 4% SDS, 5% ß-mercaptoethanol, 0.025 mg/ml bromphenol blue) and boiled for 10 min in a water bath. Electrophoresis was performed for 45-90 min in SDS running buffer (25 mM Tris-Cl, 192 mM glycine, 0.1% SDS) with a current limit of 15 mA in stacking- and 35 mA in separating gels. For unspecific detection of proteins, the PageBlue™ protein staining solution (ThermoFischer Scientific) or InstantBlue-protein stain (Expedeon) was used. After destaining with water, the gels were dried on a Slab gel dryer SE1160 (Hoefer Scientific Instruments). As marker, peqGOLD protein marker IV (Peqlab) was used.

4.5.7 Western blotting

Western blotting was performed for specific detection of proteins in cellular lysates. After gel electrophoresis, (see 4.5.6) the gel, the PVDF western blotting membrane (Roche Applied Science) and the blotting paper (Bio-Rad) were soaked in blotting buffer (25 mM Tris, 190 mM

glycine, 0.025% SDS). The blotting sandwich was assembled from the bottom as following: blotting paper, PVDF membrane, gel, blotting paper. Transfer was performed using the Trans-Blot® turbo™ transfer system (Bio-Rad) and the standard SD (semi-dry) program. The membrane was blocked (5% milk powder in 1× PBS, 0.1% Tween 20) for 1 h or overnight at 4°C. The primary antibody (**Table 4.3**) was added for 1 h in blocking buffer and after binding, the membrane was washed (1× PBS, 0.1% Tween 20) three times for 10 min. The secondary antibody (**Table 4.3**) was bound for 1 h in blocking buffer and the membrane was washed as described above. Finally, the membrane was dried and Lumi-Light western blotting substrate (Roche Applied Science) was added for detection using X-ray films (GE Healthcare).

Table 4.3 Primary and secondary antibodies used for Western blotting.

Antibody	Dilution
Anti-protein A antibody produced in rabbit	1:5,000
Anti-protein C antibody ab18591 (rabbit)	1:400
Anti-rabbit IgG; peroxidase antibody (goat)	1:10,000

4.6 Cloning of DNA fragments in *E. coli*

4.6.1 Cultivation of *E. coli*

Bacterial cells were cultured under sterile conditions. All used consumables were certified sterile, autoclaved (120°C, 20 min, 2 bar) or heated (180°C, 2 h). LB-medium (10 g/l NaCl, 10 g/ml trypton, 5 g/ml yeast extract) or LB-agar (Roth) for cultivation was dissolved in deionized water, autoclaved and handled using a Bunsen burner. For selective growing according to the resistance of the transformed plasmid, the following antibiotics were added to the media: Ampicillin [100 µg/ml], Gentamicin [7 µg/ml], Kanamycin [50 µg/ml] and Tetracyclin [10 µg/ml].

4.6.2 Digestion of DNA fragments

PCR products were amplified (see 4.4.2) using primer with 5´ overhangs containing restriction sites. Plasmid DNA and PCR products were digested with New England Biolabs restriction enzymes. For simultaneous double digestion, the optimal buffer conditions were selected using the “Double digest finder” on the New England Biolabs webpage (see 4.2.7).

4.6.3 Ligation of DNA fragments

For cloning of DNA fragments, both the plasmid and insert were digested according to 4.6.2. Linearized plasmid and insert were gel purified (see 4.5.2) and molar ratios were determined by agarose gel electrophoresis (see 4.5.1). A five to seven fold molar excess of the insert was mixed with the plasmid (calculated using the “LIGATION CALCULATOR“; see 4.2.7) and incubated for 1 h or overnight at 16°C for ligation, using the T4 DNA ligase (New England Biolabs).

4.6.4 Transformation of *E. coli* cells

One vial of Single step (KRX) competent cells (Promega) was thawed on ice, mixed with 5 µl ligation reaction or 20 ng plasmid and incubated for 5 min on ice. For One shot® BL21 (DE3) chemically competent *E. coli* cells (ThermoFischer Scientific), the incubation time was prolonged to 20-30 min. Cells were incubated for 2 min on ice after head shock (42°C, 30 sec), mixed with 450 µl LB medium and shacked for 1 h at 37°C. Cells were plated on LB-agar plates, supplemented with antibiotics according to 4.6.1 and grown overnight at 37°C.

4.6.5 Identification and analysis of bacterial clones

Colony PCR was used for screening of bacterial clones. A single colony was picked using a pipet tip and stirred in a 1× PCR reaction (see 4.4.2) with insert specific primer. To ensure

efficient cell lysis, the initial denaturation step in the temperature profile was extended to 5 min. LB-medium (5 ml) containing antibiotics (see 4.6.1) was inoculated with selected clones and incubated overnight at 37°C while shaking. Plasmid DNA was isolated using the QIAprep spin miniprep kit (QIAGEN). Plasmids were analyzed by restriction digestion (see 4.6.2) and gel electrophoresis (see 4.5.1). Plasmids containing an insert with the expected length were sequenced by SeqLab (Sequence Laboratories Göttingen). For large scale-preparation of plasmid DNA, the Qiagen® plasmid plus maxi kit (QIAGEN) was used.

4.7 Protein expression and purification

4.7.1 Expression of GST-fusion proteins in *E. coli*

For the expression of N-terminal GST-fusion proteins in *E. coli*, the recombinant (see 4.9.3) pGEX-6-P2 vector (GE Healthcare) was transformed in One shot® BL21 (DE3) chemically competent *E. coli* cells (ThermoFischer Scientific) according to 4.6.4. The expression culture was inoculated 1:1000 and overexpression (16 °C, shaking, overnight) was induced with 0.1 mM IPTG when OD_{600} 0.4-0.6 was reached. The cells were harvested by centrifugation (4°C, 5 min, 5,000 × g) and stored at -80°C after washing with 1× PBS.

4.7.2 Purification of GST-fusion proteins from *E. coli*

The cell pellet (see 4.7.1) was thawed on ice and resuspended in GST-lysis buffer (10 mM Tris-Cl pH 7.5, 100 mM KCl, 2.5 mM $MgCl_2$, 0.1 mM DTT, cOmplete™ EDTA-free protease inhibitor [Roche Applied Science]) and incubated for 30 min at 4°C on wheel. Afterwards, the cells were sonicated (3×10) on ice and the lysate was supplemented with 0.01% NP-40. Cell debris was removed by two times centrifugation (4°C, 20 min, 20,000 × g) and the cell lysate was finally cleared using a syringe with a 0.45 µm filter (Rotilabo® syringe filter CME [Roth]). Prior addition of cell lysate and protein binding for 30 min on wheel, 80 µl (packed bead volume) pre-blocked (1× PBS, 0.2 mg/ml glycogen, 0.1 mg/ml BSA, 10 mM DTT, 0.05% Tween 20) glutathione sepharose 4B beads (GE Healthcare) were washed 3× with GST-binding buffer (10 mM Tris-Cl pH 7.5, 100 mM KCl, 2.5 mM $MgCl_2$, 0.1 mM DTT, 0.01% NP-40). Beads were washed with 5 ml GST-binding buffer, twice with 5 ml GST-binding buffer 600 (10 mM Tris-Cl pH 7.5, 600 mM KCl, 2.5 mM $MgCl_2$, 0.1 mM DTT, 0.01% NP-40), transferred in a 1.5 ml tube and washed again (3× GST-binding 600 and twice GST-binding buffer). Proteins bound to beads were stored in GST-lysis buffer at 4°C for up to 4 weeks. An aliquot of the slurry was analyzed by SDS-PAGE (see 4.5.6), including a BSA standard to determine the protein concentration and purity of the sample.

4.7.3 Cultivation of Sf9 insect cells

Cell culture of Sf9 insect cells (ThermoFischer Scientific) was carried out under sterile conditions using a clean bench in a designated cell culture laboratory. Commercially available flasks and pipettes were used. The adherent growing Sf9 insect cells were cultured at 28°C in Sf-900™ II SFM medium (supplemented with 10% FBS and 0.5× Antibiotic-antimycotic, all ThermoFischer Scientific). The cells were resuspended in fresh medium and split in a 1:5 or 1:10 dilution after three to four days, when a high confluency was reached.

4.7.4 Expression of recombinant proteins in Sf9 insect cells

Recombinant pFastBac^{TM}HT B (ThermoFischer Scientific) vector was cloned according to 4.9.3 and baculovirus for protein expression in Sf9 insect cells was obtained, using the Bac-to-Bac® baculovirus expression system (ThermoFischer Scientific).

4.7.5 Purification of baculovirus-expressed proteins

Sf9 insect cells (see 4.7.4) were harvested by centrifugation (4°C, 5 min, 1,000 × g), washed with 1× PBS and resuspended in a fourfold packed cell volume of lysis buffer (50 mM NaH_2PO_4, 300 mM NaCl, 10 mM imidazole, 1% NP-40, cOmplete™ EDTA-free protease inhibitor [Roche Applied Science], pH 8.0 using NaOH). The cells were lysed for 10 min on ice and cell debris was removed by centrifugation (4°C, 20 min, 20,000 × g). Recombinant proteins were affinity-purified, using an ÄKTA purifier 10 and 1ml HisTrap FF Crude columns (both GE Healthcare). The column was washed (50 mM NaH_2PO_4, 300 mM NaCl, 10 mM imidazole, pH 8.0 using NaOH) with a tenfold column volume, using a flow rate of 1 ml/min and a maximal pressure of 0,5 MPa. The protein was eluted (50 mM NaH_2PO_4, 300 mM NaCl, 100 mM imidazole, pH 8.0 using NaOH) and further gel-purified on an ÄKTA purifier 10 and a Superdex 200 16/60 column (both GE Healthcare) using storage buffer (20 mM Tris-Cl, pH 8.0, 200 mM NaCl, 10% glycerol, 5 mM β-mercaptoethanol) and a flow rate of 1 ml/min and a maximal pressure of 0,3 MPa. For storage of purified protein, the samples were frozen in liquid nitrogen.

4.8 Special techniques

4.8.1 Indirect Immunofluorescence

T. brucei cells (2×10^7 to 4×10^7) expressing PTP-tagged proteins were harvested, washed with 1× PBS and resuspended in 1× PBS. 20 µl of the cell suspension were fixed for 30 min at 4°C with 4% paraformaldehyde in 1× PBS on a coverslip. The cells were washed (1× PBS), permeabilized for 5 min (1% TritonX-100 in 1× PBS), washed again (1× PBS) and blocked (1× PBS, 0.05% Tween 20, 0.02% NaN_3, 1% cold-water fish gelatin [Sigma Aldirch]). Afterwards the cells were incubated for 1 h with a 1:40,000 dilution of anti-protein A antibody (Sigma-Aldrich) in blocking solution. After washing (1× PBS, 0.05% Tween 20), goat anti-rabbit Alexa fluor® 488/594 secondary antibodies (1:400 dilution [ThermoFischer Scientific]) were added for 1 h in blocking solution (including 1 µg/ml DAPI). Finally, cells were washed (1× PBS, 0.05% Tween 20) and coverslips were mounted in Immu-Mount™ (ThermoFischer Scientific). For imaging, an Axioskop 20 fluorescence microscope (Zeiss) and the provided Axio Vision software were used.

4.8.2 DNA oligonucleotide annealing

400 pmol of complementary DNA oligonucleotides (see 4.1.11) were annealed in 25 µl annealing buffer (10 mM Tris-Cl pH 7.5, 50 mM NaCl, 1 mM EDTA) as follows:

94°C	1°C in 45 sec
4°C	
4°C	hold

4.8.3 *In vitro* transcription

In vitro transcription was performed from annealed DNA oligonucleotides (see 4.8.1) or a linearized plasmid that contained the 3´ UTR of the *T. brucei* α-Tubulin gene (provided by Christian Preußer), using T7 RNA polymerase (ThermoFischer Scientific). The reaction was incubated for 3 h at 37°C and set up as follows:

Volume	Component
5.00 µl	5× transcription buffer
2.50 µl	DTT (100 mM)
6.75 µl	DMPC-H_2O
2.50 µl	ATP or CTP (2mM; depending on labeling)
1.25 µl	UTP (10 mM)
1.25 µl	GTP (10 mM)
1.25 µl	ATP or CTP (10 mM; depending on labeling)

1.00 µl	DNA template (0.1-0.2 µg oligonucleotide or 1 µg plasmid)
0.50 µl	RNaseOUT
1.00 µl	T7 RNA polymerase
2.00 µl	[α^{32}P]-ATP or CTP (10µCi/µl; SCP-207 or SCP-209)
25.00 µl	

The DNA template was digested by the addition of 3 µl RQ1 DNase (1 U/µl) and incubation for 30 min at 37°C. Prior RNA purification using Mini quick spin RNA columns (Roche Applied Science), a 1 µl aliquot was taken for scintillation (Tri-Carb 1600TR [PACKARD]). Afterwards the transcripts were ethanol precipitated (see 4.2.5), separated on a 15% denaturing polyacrylamide/urea gel (see 4.5.3), detected by autoradiography (see 4.5.4) and excised from the gel. To isolate RNA, the gel piece was crushed and rotated overnight in 400 µl 1× PK buffer (100 mM Tris-Cl pH 8.0, 12.5 mM EDTA, 150 mM NaCl, 1% SDS). The liquid portion was transferred, the RNA was ethanol precipitated (see 4.2.5), subjected to scintillation (Tri-Carb 1600TR [PACKARD]) and resuspended in DMPC-H_2O after calculating the yield according to the following formula:

$$RNA[ng] = NTP_{total\ unlabeled}\ [\mu M] \times reaction\ volume\ [\mu l] \times \frac{RNA\ activity}{activity\ reaction} \times 1.32$$

4.8.4 *In vitro* polyadenylation assay

For standard *in vitro* polyadenylation assays, 4 nM *in vitro* transcribed ^{32}P-labeled RNA (see 4.8.3), derived from the 3´ end of *T. brucei α*-tubulin mRNA, was assembled with poly(A) buffer (25 mM Tris-Cl pH 7.4, 50 mM KCl, 1.5 mM $MgCl_2$, 1.5 mM $MnCl_2$, 0.05 mM EDTA, 0.5 mM DTT, 10% glycerol, 2.6% polyvinyl alcohol [PVA]). 32 nM recombinant purified poly(A) polymerase (see 4.7.5) was added on ice. The reaction was started by the addition of 1 mM ATP and incubation at 37°C. RNAs were ethanol precipitated (see 4.2.5) and analyzed by denaturing polyacrylamide/urea gel electrophoresis (see 4.5.3) in combination with autoradiography (see 4.5.4).

4.8.5 Tandem affinity purification (TAP) and mass spectrometry

Tandem affinity purification of PTP-tagged proteins was done as described by Schimanski *et al*., 2005, with minor modifications: Briefly, *T. brucei* cells were collected from 3-liter cultures (corresponding to ~4 ml packed cell volume) and lysed in 7 ml extraction buffer (150 mM KCl, 20 mM Tris-Cl pH 7.7, 3 mM $MgCl_2$, 0.5 mM DTT, cOmplete™ EDTA-free protease inhibitor [Roche Applied Science]). For IgG affinity chromatography, 300 µl of IgG sepharose 6 fast flow beads (packed bead volume [GE Healthcare]) were incubated with extract for two hours at 4°C. Beads

were washed extensively with PA-150 buffer (150 mM KCl, 20 mM Tris-Cl pH 7.7, 3 mM $MgCl_2$, 0.5 mM DTT, 0.1% Tween 20), followed by TEV protease buffer (150 mM KCl, 20 mM Tris-Cl pH 7.7, 3 mM $MgCl_2$, 0.5 mM EDTA, 0.5 mM DTT, 0.1% Tween 20). Tagged proteins were eluted in 2 ml of TEV protease buffer containing 250 units of AcTEV protease (ThermoFischer Scientific). For anti-protein C affinity purification, $CaCl_2$ was added to the eluate to a final concentration of 2 mM. The eluate was incubated for 2 hours at 4°C with 300 µl of anti-protein C affinity matrix (packed bead volume [Roche Applied Science]). The beads were washed with PC-150 buffer (150 mM KCl, 20 mM Tris-Cl pH 7.7, 3 mM $MgCl_2$,1 mM $CaCl_2$, 0.1% Tween 20), and the protein C-tagged proteins were eluted with 0.5 ml EGTA elution buffer (5 mM Tris-Cl pH 7.7, 10 mM EGTA, 5 mM EDTA). Eluted proteins were concentrated, using a SpeedVac® plus SC100A (Savant) vacuum concentrator and StrataClean resins (Stratagene), analyzed on 4-12% NuPAGE gels (ThermoFischer Scientific), and stained with InstantBlue-protein stain (Expedeon) (see 4.5.6) Proteins were in-gel digested with endoproteinase trypsin and analyzed by LC-MS/MS under standard conditions. Data were searched against a *T. brucei* protein sequence database (NCBInr v.11.09.2013, 38,057 entries). Data were evaluated with "Scaffold version 4.0.4" (Proteome Software), and proteins were ranked by their unique peptide counts in LC-MS/MS analysis, using a peptide and protein threshold of 95.0% and a minimum of three peptides.

4.8.6 *In vivo* polyadenylation assay

To determine the general polyadenylation status of mRNAs, we measured the length of the poly(A) tails by splint labeling according to Tkacz *et al*., 2010. Briefly: Two to five µg of total RNA (see 4.2.3) was mixed with 200 pmol oligo(dG)-oligo(dT) primer in 1× sequinase buffer, heated to 85°C and quenched on ice for 30 min. Prior heating, 1 µl of the reaction was analyzed by RT-PCR (see 4.4.1 and 4.4.2) using U3 or 7SL RNA specific primer, serving as loading control for normalization. Afterwards 0.1 nmol DTT, 4.8 U USB® sequenase™ version 2.0 DNA polymerase (Affymetrix) and 10 pmol dCTP including 2.5 µCi [α-^{32}P]-dCTP (3000 Ci/mmol; SCP-205 [Hartmann Analytic]) were added. The reaction was incubated for 30 min, ethanol precipitated (see 4.2.5) and resuspended in 50 µl RNase A/T1 mix (2 µg RNase A / 5U RNase T1 mix [ThermoFischer Scientific], 20 µg yeast tRNA [Roche Applied Science], 300 mM NaCl, 10 mM Tris-Cl pH 7.5, 5 mM EDTA) to digest (37°C, 30 min) the RNA leaving intact only the radioactively labeled poly(A) tails. The poly(A) tails were purified by phenol/chloroform extraction (see 4.2.4) and ethanol precipitation (see 4.2.5), separated on a denaturing 15% polyacrylamide/urea gel (see 4.5.3) and detected by autoradiography (see 4.5.4). Quantitation was performed by measuring the relative intensities of ^{32}P-labeled product bands, using

"ImageJ". Fold changes were obtained by calculating the middle "Riemann sum", which can be understood as a weighted average of the polyadenylation efficiency:

$$S = \sum_{i=1}^{n} f(1 + \frac{i}{2}) * \frac{1}{2}$$

in which *S* is the "Riemann sum" of the function *f(x)* over the total measured intensities (*n*) divided into separate sections (*i*).

4.8.7 Individual-nucleotide resolution UV cross-linking and immunoprecipitation (iCLIP)

Three biological replicates of iCLIP experiments using a stable PTP-tagged DRBD4 cell line and wildtype *T. brucei* 427 (WT) cells as negative control were performed according to an established strategy with minimal changes (Preußer *et al.*, 2014). In brief: After UV-C cross-linking, cell lysates were prepared in 1.2 ml extraction buffer (150 mM KCl, 20 mM Tris-Cl pH 7.7, 3 mM $MgCl_2$, 0.5 mM DTT, cOmplete™ EDTA-free protease inhibitor [Roche Applied Science]) using a Dounce homogenizer (25 strokes with a type B pestle) followed by sonication. The RNP-complexes were purified after DNase (Promega) and limited RNase I (final concentration 1 U/ml [ThermosFischer Scientific]) treatment by applying the first step of tandem affinity purification (IgG sepharose 6 fast flow beads [GE Healthcare]). After SAP (ThermoFischer Scientific) treatment, 3´ RNA-linker ligation (T4 RNA ligase [ThermoFischer Scientific]), AcTEV protease (ThermoFischer Scientific) cleavage, the second affinity step (anti-protein C affinity matrix [Roche Applied Science]) and 5´ terminal ^{32}P-labeling (T4 PNK [New England Biolabs]) the RNP-complexes were gel separated under denaturing conditions (NuPAGE electrophoresis and blotting system; NuPAGE™ Novex™ 4-12% Bis-Tris protein gels 1.0 mm 12-wells [both ThermoFischer Scientific]. Afterwards the complexes were electroblotted onto a nitrocellulose membrane (0.45 µm [Bio-Rad]) and bound RNA was recovered by PK (Roth) treatment and precipitation (see 4.2.5). RNA was reverse transcribed (Superscript III reverse transcriptase [ThermoFischer Scientific]), using oligonucleotides which introduce a 5´ barcode as well as a *Bam*HI restriction site. The cDNAs were size-fractionated by denaturing polyacrylamide gel electrophoresis (Novex® TBE-Urea gels 6% 10-wells [ThermoFischer Scientific]), circularized (Circligase II [Epicentre]) and after annealing of a complementary oligonucleotide, linearized between the two adapter regions by *Bam*HI (ThermoFischer Scientific) digestion. The cDNA was PCR amplified (30-32 cycles; Accuprime supermix 1 [ThermoFischer Scientific]) and the library was purified using QIAquick PCR purification kit (QIAGEN) and Caliper (XT DNA 750 assay kit [Perkin-Elmer]). After quality control using an Agilent 2100 Bioanalyzer and High sensitivity DNA analysis kit (both Agilent Technologies), the

library was subjected to high-throughput sequencing on an Illumina MiSeq instrument (single-read; 100 bp for DRBD4_1/2 and WT; 75 bp for DRBD4_3).

The YFP-based iCLIP protocol was adapted from the protocol described above with minimal changes, including skipping of AcTEV protease cleavage and the second affinity step: 2 µg anti-GFP antibody (Roche Applied Science) in TBS-T (50 mM Tris-Cl pH 7.5, 150 mM NaCl, 0.05% Tween20) was bound for 2 h (4°C) to Dynabeads protein G (ThermoFischer Scientific). The beads were washed with TBS-T and cell lysate was applied for 2 h at 4°C after DNase and RNase (final concentration 10 U/ml) treatment. Afterwards the beads were extensively washed using TBS-T1000 (50 mM Tris-Cl pH 7.4, 1 M NaCl, 0.05% Tween 20), followed by SAP treatment. The library was PCR amplified (27 cycles), purified and subjected to high-throughput sequencing on an Illumina MiSeq instrument (single-read; 75 bp).

Sequence reads were aligned to *T. brucei* 927 genome assembly (TriTrypDB; http://tritrypdb.org; release 6: TriTrypDB-6.0_TbruceiTREU927) to determine the crosslink sites and their corresponding crosslink-tag counts. For details of sequencing data analysis, see Preußer *et al*., 2014 and references therein. The *T. brucei* 927 genome was used for mapping because of its more comprehensive genome assembly and gene annotation in comparison with *T. brucei* 427.

4.8.8 Systematic evolution of ligands by exponential enrichment-sequencing (SELEX-seq)

An RNA pool with a degenerated sequence of 20 nts was prepared by T7 *in vitro* transcription (HiScribe™ T7 high yield RNA synthesis kit [New England Biolabs]), using a DNA oligonucleotide containing the random sequence annealed to a T7 promoter complementary DNA oligonucleotide. Selection was performed in a total volume of 200 µl (10 mM Tris-HCl pH 7.5, 100 mM KCl, 2.5 mM $MgCl_2$, 0.1% Triton X-100) with 40 pmol GST-DRBD4/GST-CPSF30 or GST (as negative control) bound (see 4.7.2) to pre-blocked glutathione sepharose 4B beads (GE Healthcare) and 4 nmol transcript. After a 20 min incubation at room temperature, the samples were washed three times with 1 ml of washing buffer (10 mM Tris-HCl pH 7.5, 100/300/600 mM KCl, 2.5 mM $MgCl_2$, 0.1% Triton X-100), treated with PK (Roth), phenol/chloroform extracted (see 4.2.4), and ethanol precipitated (see 4.2.5). The stringency of washing steps was increased for each round of selection. Selected RNAs were reverse-transcribed (qScript™ flex cDNA kit [Quanta Biosciences]) and PCR amplified (see 4.4.1 and 4.4.2). Transcripts for the next round of selection were generated by *in vitro* transcription as described above. After five rounds of selection, RNA aliquots from each round and from the fifth round of GST selection were used for barcoding (barcodes 1-5: GST-DRBD4 and 6: GST or barcodes 7-11: GST-CPSF30 and 12: GST) by reverse transcription (qScript™ flex cDNA kit

[Quanta Biosciences]). cDNA libraries were amplified by PCR (see 4.4.2), pooled in equal amounts and purified by QIAquick PCR purification kit (Qiagen) and Caliper (XT DNA 750 assay kit [Perkin-Elmer]). After quality control using an Agilent 2100 Bioanalyzer and High sensitivity DNA analysis kit (both Agilent Technologies), the library was subjected to high-throughput sequencing on a MiSeq instrument (single-read 100 bp [Illumina]). Sequence reads were first sample-barcode sorted, trimmed by PCR primer sequences on both ends, and further random-barcode filtered to obtain 20 nts sequence tags of the enriched RNA pools. The numbers of filtered sequence tags (from each SELEX round) containing either one of the 256 or 4,096 possible tetramer or hexamer motifs, respectively, was summarized, and the z-score values were calculated for enrichment of each motif. Moreover, the top eight tetramers from the final selection round were combined, allowing up to two nucleotides spacing between them, and ranked according to their frequency in the SELEX-sequence tags

4.8.9 GST pulldown assay

For assaying protein-RNA interactions, 10 pmol of GST-DRBD4 (or GST as negative control) was immobilized (see 4.7.2) on glutathione sepharose 4B beads (GE Healthcare) and incubated with 500 fmol denatured, *in vitro* transcribed, ^{32}P-labeled RNAs (see 4.8.3) in a final volume of 200 µl binding buffer (10 mM Tris-Cl pH 7.5, 100 mM KCl, 2.5 mM $MgCl_2$, 0.1 mM DTT, 0.01% NP-40). After binding at room temperature for 30 min, beads were washed four times with 1 ml binding buffer. Bound RNA was recovered by the addition of 400 µl PK buffer (100 mM Tris-Cl pH 7.5, 12.5 mM EDTA, 150 mM NaCl, 1% SDS) and 10 min incubation at 80°C. Afterwards the RNA was extracted with phenol/chloroform (see 4.2.4), ethanol precipitated (see 4.2.5), analyzed on a 15% denaturing polyacrylamide/urea gel (see 4.5.3) and detected by autoradiography (see 4.5.4). For quantification of pulldown efficiencies the Typhoon FLA 9500 (Ge Healthcare) imaging system was used (see 4.5.4).

4.8.10 RNA-seq and identification of polyadenylation sites

RNA-seq libraries for the determination of polyadenylation sites were made and sequenced at the Beijing Genomics Institute (Shenzhen, China). Poly(A)$^+$ RNA was purified from total RNA, converted to cDNA using a 5´-T15VN-3´ oligonucleotide (V=A, G or C; N=T, A, G or C), sheared, and size-selected for fragments ~200 bp in length, using the Illumina TruSeq RNA sample preparation kit v2 (Illumnia). Sequencing was performed on an Illumina Hiseq 2000 (Illumina) platform yielding 90 bp paired-end reads. Polyadenylation sites were identified by the SLaP mapper tool (Fiebig *et al.*, 2014), using the *T. brucei* 927 genome assembly.

4.8.11 Correlation between DRBD4 iCLIP binding and polyadenylation site choice

The poly(A) sites identified in uninduced control cells by RNA-Seq were clustered with a maximal spacing of 20 nucleotides. The poly(A) site reads from the control and the DRBD4-knockdown cells in each of the 8,962 clusters were summarized. The Bioconductor package DESeq (Anders & Huber, 2010) was applied to determine the differential expression of poly(A) site clusters. As a result, 234 down- and 248 up-regulated clusters with a minimum of 10 poly(A) site reads in control cells (14 in knockdown cells) were selected for further analysis, using as a criterion an absolute fold change greater than 0.75 in $\log_2$ value. Poly(A) site clusters with p-values greater than 0.75 (expression not affected by DRBD4 knockdown) were selected for background group selection. For each regulated cluster, four clusters with similar expression levels (in the range of 0.9 to 1.1) were randomly picked as background clusters. The position 0 of the poly(A) site cluster was defined as the nucleotide with the highest poly(A) read count within the cluster. The iCLIP crosslink-tag counts in the region between -200 nts and +200 nts of the regulated and background clusters were summarized. For the distribution of iCLIP crosslink tags, fitted values with 21-nts windows were used for smooth-line presentation, with iCLIP tag counts plotted on the Y-axis and positions relative to the defined position 0 on the X-axis.

4.8.12 Flow cytometry

Mid-log phase density cells (5×10^6 cells/ml) were analyzed with and without doxycycline induction, using a BD FACScan (BD Biosciences).

4.9 Constructs

4.9.1 Generation of pLew100 RNAi constructs

For a specific RNAi-mediated knockdown of a single gene (**Table 4.4**), 300-500 bp of the 3´ UTR were cloned (see 4.6) as a stem loop construct in the pLEW100 vector, allowing the expression of a double stranded RNA (Wang *et al.*, 2000). The target gene insert was amplified by PCR (see 4.4.2) using a forward primer containing a *Hin*dIII and *Mlu*I restriction site and a reverse primer containing a *Xba*I restriction site. The “sense insert” was first cloned in pJM325, using *Hin*dIII and *Xba*I restriction sites. The “antisense insert” was directly cloned into pLew100, using *Mlu*I and *Xba*I restriction sites. Afterwards the “sense insert” and a ~530 bp long stuffer derived from pJM325 were cloned into pLEW100, using *Hin*dIII and *Xba*I restriction sites.

Table 4.4 Generation of pLEW100 RNAi constructs.

Protein	TriTrypDB annotation	cloned nucleotides of the gene
PAP	Tb927.7.3780	1527-1997
PAP	Tb927. 3.3160	944-1440
CPSF160	Tb927.11.14650	3243-3720
CPSF100	Tb927.11.230	584-997
CPSF73	Tb927.4.1340	1683-2106
CPSF30	Tb927.11.12750	271-759
Fip1	Tb927.5.4320	285-765
Symplekin	Tb927.8.7490	3754-4235
CstF64	Tb927.8.8210	4-396
CstF50	Tb927.6.1830	744-1191
CFIm25	Tb927.7.1620	392-819
CFIIm	Tb927.6.3690	729-1183
hyp. Protein	Tb927.11.13860	234-710
hyp. Protein	Tb927.8.4480	264-724

4.9.2 Generation of PTP-tag fusion protein constructs

For the expression of C-terminal PTP-tagged proteins from the endogenous locus, the pC-PTP-NEO vector was used (Schimanski *et al.*, 2005b).

The ORFs of Tb927.3.3160 (nts 672-1461), Tb927.7.3780 (nts 1172-2061), CPSF160 (nts 3601-4356) and CPSF30 (nts 74-831), were PCR-amplified (see 4.4.2) and inserted in-frame (see 4.6)

into the pC-PTP-NEO vector upstream of the PTP tag sequence, using the *Apa*I and *Not*I restriction sites.

4.9.3 Generation of protein overexpression constructs

For overexpression of recombinant proteins in Sf9 insect or One shot® BL21 (DE3) chemically competent *E. coli* cells, the pFastBac^{TM}HT B (ThermoFischer Scientific) and pGEX-6P-2 (GE Healthcare) vectors were used, respectively. The ORFs of PAP Tb927.3.3160 (nts 3-1464) and PAP Tb927.7.3780 (nts 3-2064) were PCR amplified (see 4.4.2) and cloned (see 4.6) into the pFastBac^{TM}HT B vector, using the *Bam*HI and *Eco*RI restriction sites. The ORFs of Tb927.11.12750 (nts 3-834; CPSF30) and Tb927.11.14100 (nts 3-1518; DRBD4) were PCR amplified (see 4.4.2) and cloned (see 4.6) into the pGEX-6P-2 vector, using the *Bam*HI and *Eco*RI or *Sal*I and *Not*I restriction sites, respectively.

5 Results

5.1 The trypanosomatid polyadenylation complex

5.1.1 The trypanosomatid poly(A) polymerases

To identify the major functional poly(A) polymerase in *T. brucei*, we focus here on two putative poly(A) polymerases [Tb927.3.3160 and Tb927.7.3780] and initially compared the sequences with their human homolog, PAPOLA (**Figure 5.1** and **Supplementary Figure 8.1**; page 128-129). Based on the Needleman-Wunsch alignment algorithm, the human PAPOLA protein shows 17.4% and 24% identity with the trypanosomatid Tb927.3.3160 and Tb927.7.3780 proteins from *T. brucei*, respectively. Although there are regions of low sequence similarity, structure predictions of these two *T. brucei* poly(A) polymerases suggest a strong structure conservation of the two proteins. Moreover, by domain structure prediction of these two *T. brucei* poly(A) polymerases, the highly conserved domains of the poly(A) polymerase described in higher eukaryotes, such as the central domain harboring the nucleotidyltransferase activity including the three catalytic aspartic acid residues, are present in both trypanosomatid proteins (Zhelkovsky *et al.*, 1995, Martin & Keller, 1996, Martin *et al.*, 1999). Following the central domain, an RNA-binding domain was predicted for all three proteins. However, both trypanosomatid proteins lack a recognizable, classical nuclear localization signal at their C-terminus.

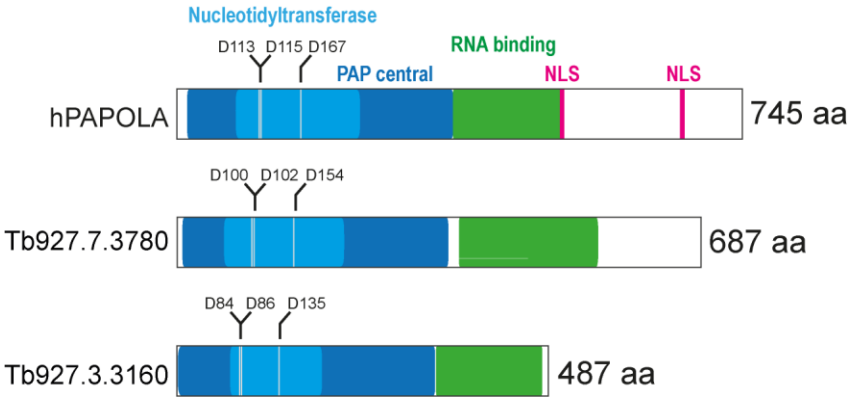

Figure 5.1 Domain structure of trypanosomatid poly(A) polymerases.
Domain organization of the PAPs, comparing the human poly(A) polymerase alpha (hPAPOLA) and two putative trypanosomatid PAPs [Tb927.7.3780 and Tb927.3.3160]. The PAP central domain, harboring the nucleotidyltransferase domain and the conserved catalytic aspartic acid residues (in blue), the RNA-binding domain (in green), and the known nuclear localization signals (NLS; in magenta) are illustrated.

To compare the two putative enzymes, we next generated two clonal procyclic cell lines, which stably express either Tb927.3.3160 or Tb927.7.3780, each with a C-terminal PTP-tag (protein C epitope / TEV cleavage site / 2× protein A epitope). Expression of both proteins was monitored by Western blot analysis (**Figure 5.2 A**) and in addition, the subcellular distribution of both proteins was visualized by indirect immunofluorescence (**Figure 5.2 C** and **D**). Interestingly, the PTP-tagged version of the Tb927.7.3780 predominantly localizes to the nucleus, whereas the putative poly(A) polymerase Tb927.3.3160 clearly localizes mainly in distinct cytoplasmic spots, suggesting differential functions. However, one has to consider that the large C-terminal tag may influence the localization within the cell.

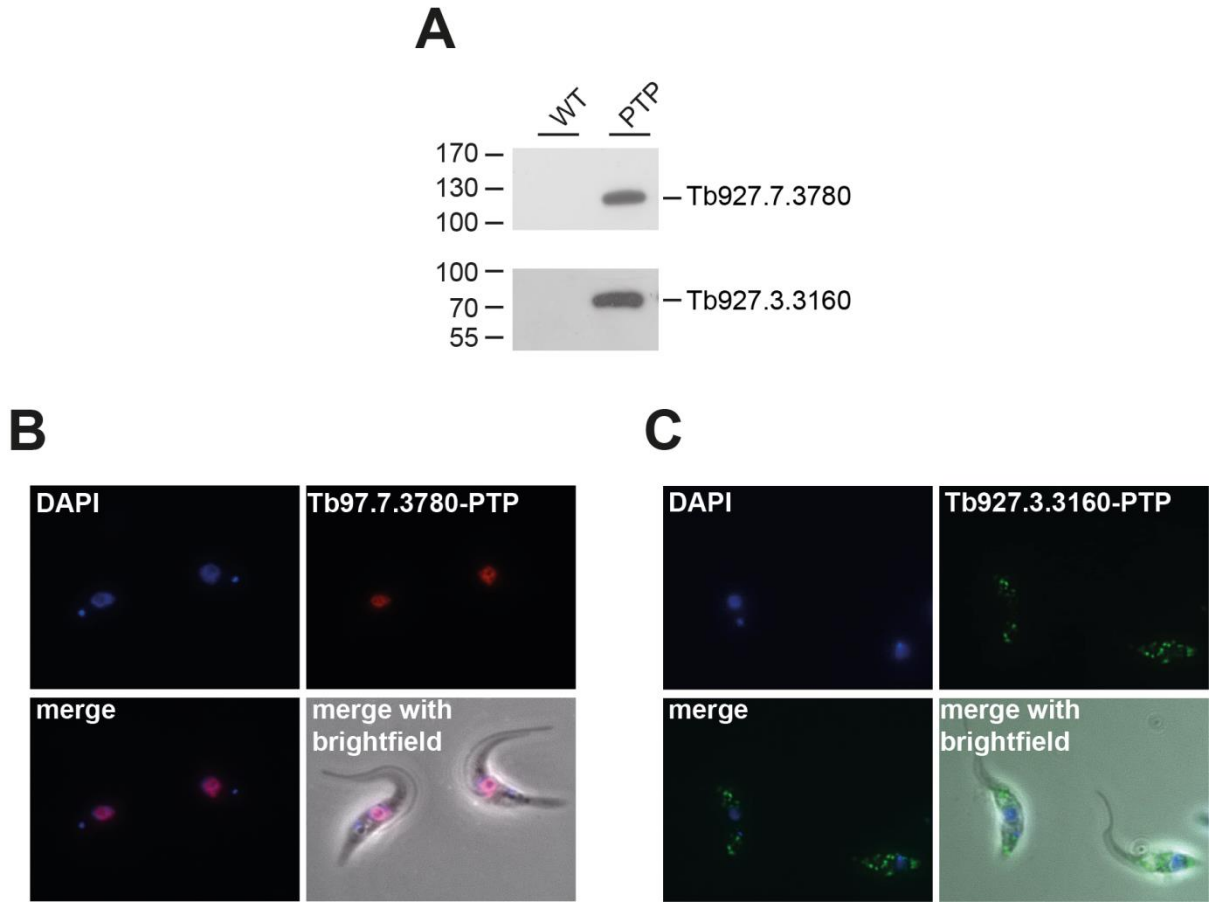

Figure 5.2 Expression and cellular localization of two poly(A) polymerases in *T. brucei*.
(A) The expression of PTP-tagged putative poly(A) polymerase [Tb927.7.3780] and [Tb927.3.3160] in *T. brucei* cells was detected by Western blotting, using polyclonal anti-protein A antibodies (lane PTP). As control, *T. brucei* 427 wildtype (lane WT) cells were included. Protein size markers in kDa.
(B and C) Cell lines stably expressing PTP-tagged versions of the two poly(A) polymerases were fixed and stained with DAPI. The localization of tagged proteins was assessed by indirect immunofluorescence, using anti-protein A antibodies followed by Alexa-594 and Alexa-488-coupled secondary antibodies for Tb927.7.3780 and Tb927.3.3160, respectively. Superimpositions of DAPI and PTP-tagged proteins (merge) as well as with brightfield are shown (merge with brightfield).

5.1.2 Only the putative poly(A) polymerase Tb927.7.3780 shows *in vitro* activity

To assess and compare the enzymatic activity of both proteins, we expressed His-tagged versions of the two poly(A) polymerases in Sf9 insect cells, using the Bac-to-Bac® baculovirus expression system followed by HPLC purification (**Figure 5.3**).

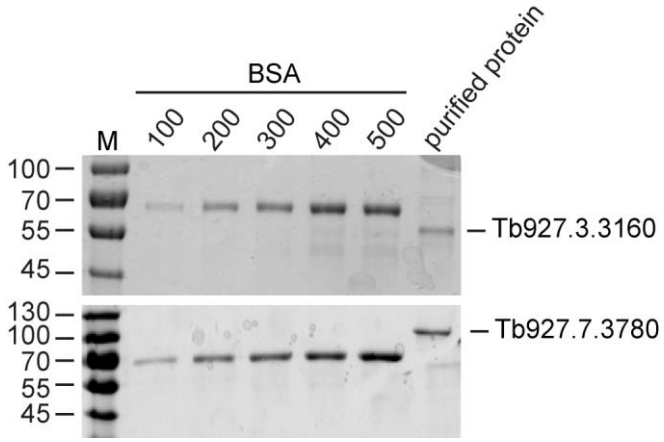

Figure 5.3 Recombinant expression of trypanosomatid poly(A) polymerases in Sf9 cells.
Recombinant proteins were expressed in baculovirus-infected Sf9 cells, HPLC-purified, and analyzed by SDS-PAGE and Coomassie staining. BSA standards (100-500 ng) were used for quantification. Protein size markers (M) in kDa.

The purified recombinant proteins were assayed for unspecific polyadenylation activity, using an RNA substrate derived from the 3´ end of the *T. brucei* α-tubulin mRNA. Interestingly, only the Tb927.7.3780 protein showed *in vitro* activity under these conditions, in contrast to the Tb927.3.3160 protein (**Figure 5.4**; page 71). The RNA substrate was efficiently elongated by Tb927.7.3780 (approximately 150 nts within 10 min), suggesting a high processivity of the enzyme. As previously shown for the human poly(A) polymerase, non-specific activity is very inefficient in the absence of specificity factors, such as CPSF or CFI; however, if Mg^{2+} is replaced by Mn^{2+}, the unspecific activity is strongly enhanced (Christofori & Keller, 1988, Wahle *et al.*, 1991). This is also the case for the poly(A) polymerase Tb927.7.3780 in trypanosomes (**Figure 5.4**; page 71).

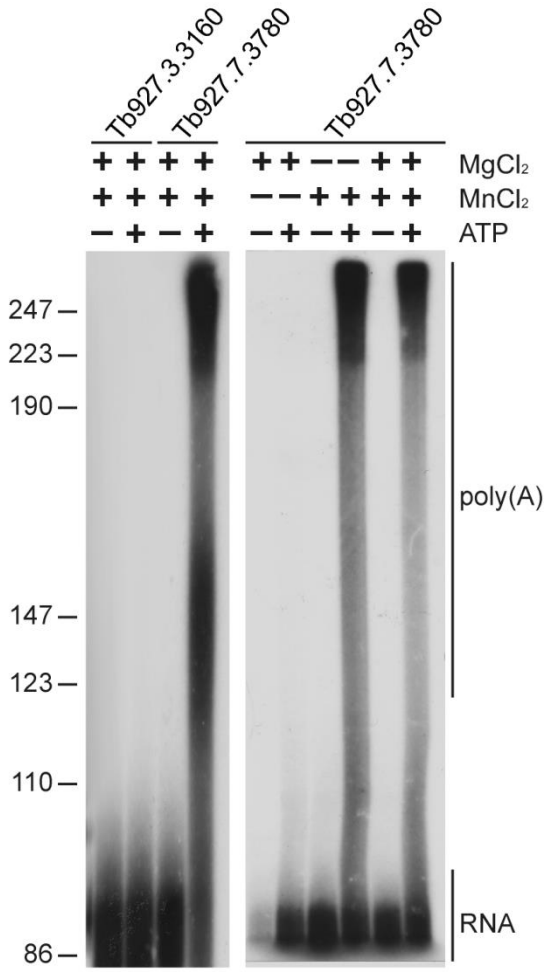

Figure 5.4 Recombinant putative poly(A) polymerase Tb927.7.3780 polyadenylates *in vitro*.
Only the putative poly(A) polymerase Tb927.7.3780 shows *in vitro* activity and requires manganese as a cofactor for unspecific polyadenylation. *In vitro* transcribed ^{32}P-labeled RNA (derived from the *T. brucei* α-tubulin 3´ UTR) was incubated at 37°C with baculovirus-expressed and purified putative poly(A) polymerase [Tb927.3.3160 or Tb927.7.3780]. Reactions were performed in the presence of $MnCl_2$ or $MgCl_2$ or a mixture of both (1.5 mM), and either in presence (+) or absence (-) of ATP. Reactions were analyzed after 30 minutes on a denaturing 12.5% polyacrylamide/urea gel. Marker sizes in nucleotides.

5.1.3 *In vivo* activity of the putative poly(A) polymerases

To compare the activities of the two trypanosomatid poly(A) polymerases *in vivo*, we silenced them individually in procyclic *T. brucei* by doxycycline-inducible RNAi. The knockdown efficiency was confirmed by RT-qPCR, using primer detecting the respective Tb927.3.3160 and Tb927.7.3780 mRNAs (**Figure 5.5 A**; left side; page 72). After three days of RNAi induction, we observed a knockdown efficiency of approximately 80% and 70%, respectively. In addition, we performed semiquantitative RT-PCR using the same primer pairs, confirming the knockdown (**Figure 5.5 A**; right side; page 72). When we monitored the cell viability upon knockdown, only

after silencing Tb927.7.3780 expression, cell growth was rapidly affected; in contrast, knockdown of Tb927.3.3160 did not result in a phenotypic growth defect (**Figure 5.5 B**).

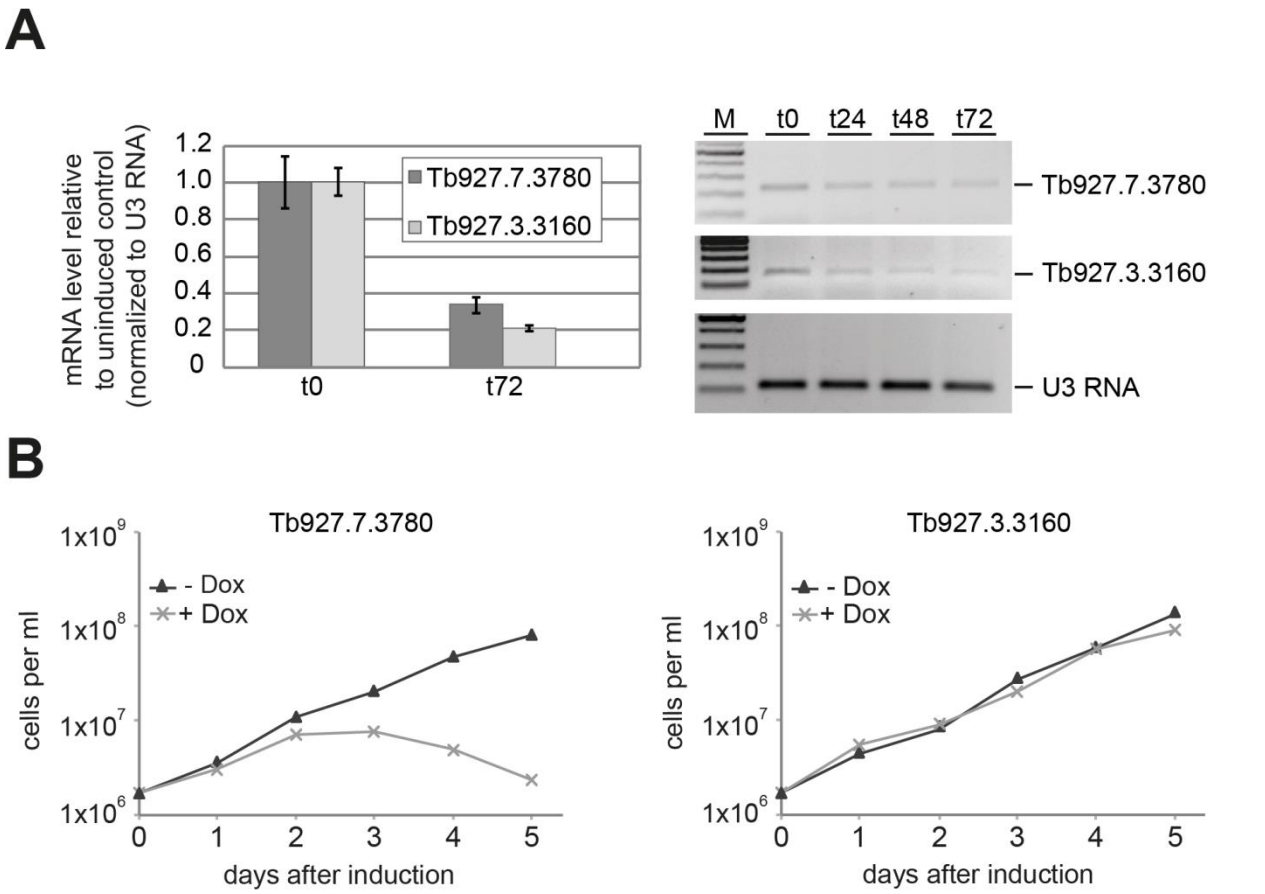

Figure 5.5 Only the putative poly(A) polymerase Tb927.7.3780 is required for cell viability.
(A) The mRNA levels were analyzed by real-time RT-PCR (left) or semiquantitative RT-PCR (right) from uninduced cells (t0) and after 1, 2, and 3 days of RNAi induction (t24-t72, as indicated). U3 RNA served for normalization and as control. M, markers (100, 200, 300, 400, and 500 bp).
(B) Growth curves of representative cell lines, in which RNAi was induced by doxycycline, (+ Dox, lines with asterisks) and respective uninduced controls (-Dox, lines with triangles).

To investigate whether individual knockdown of the two poly(A) polymerases affects the global mRNA polyadenylation status *in vivo*, total RNA was analyzed after three days, and the poly(A) tail length was examined according to Tkcaz *et al*., 2010. In brief, poly(A) tails were labeled at their 3´ end by splint ligation, using an oligo(dG)-oligo(dT) primer to allow subsequent fill-in with ^{32}P-dCTP. Total RNA was then treated with RNase A and T1, leaving intact poly(A) tails, which were analyzed by gel electrophoresis. The relative band intensities of the poly(A) tails were measured by ImageJ and normalized against signals of U3 RNA (**Figure 5.6**; page 73). The results clearly indicate that Tb927.7.3780 depletion severely reduced relative amounts and lengths of the poly(A) tails, unlike Tb927.3.3160 depletion, where an opposite effect of a slight increase in activity was observed. Taken together, our results indicate that the poly(A)

polymerase Tb927.7.3780 (annotated as putative) represents the major functional nuclear poly(A) polymerase in trypanosomes. In contrast, the poly(A) polymerase from the intron-containing gene Tb927.3.3160 localizes mainly in the cytoplasm and appears not to be functional in general 3´ polyadenylation.

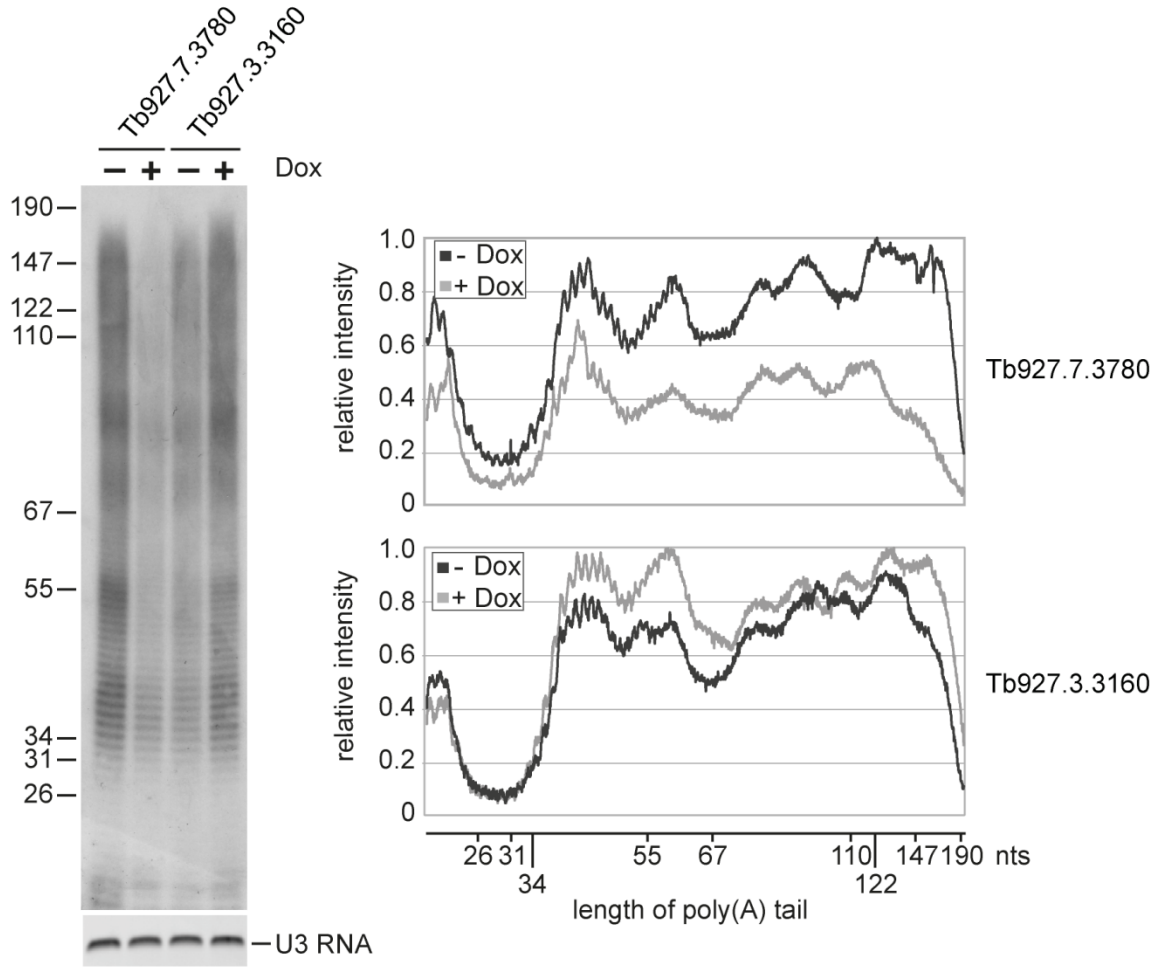

Figure 5.6 Only the putative poly(A) polymerase Tb927.7.3780 is active in polyadenylation *in vivo*. Depletion of poly(A) polymerase Tb927.7.3780, but not of Tb927.3.3160, impairs polyadenylation *in vivo*. RNA from uninduced (- Dox) and induced (+ Dox) cells was splint-labeled, digested with RNases A/T1, followed by separation of the labeled tails on a denaturing 15% polyacrylamide/urea gel. U3 RNA detected by RT-PCR served as loading control. Marker sizes are indicated in nucleotides. The relative intensities of both signals were measured with ImageJ and plotted. The black and grey lines represent the tail length distributions in uninduced and induced cells, respectively.

5.1.4 Identification of the constituents of the polyadenylation complex

To systematically investigate the composition of the trypanosomatid polyadenylation machinery, we used tandem affinity purification (TAP), based on the largest subunit of the CPSF complex, the putative CPSF160 [Tb927.11.14560]. We generated a clonal procyclic cell line, which stably expresses CPSF160 with a C terminal PTP tag (for Western blot analysis, see **Figure 5.7 A**; for

its cellular distribution, **Figure 5.7 B**). As expected, CPSF160-PTP predominantly localizes to the nucleus, with only minor staining of the cytoplasm.

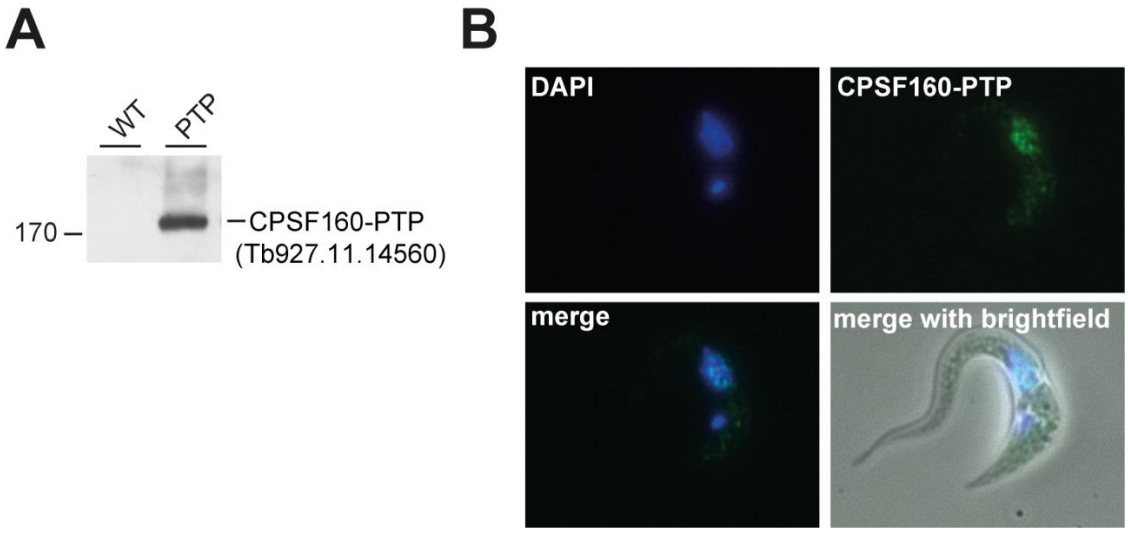

Figure 5.7 Expression and cellular localization of *T. brucei* CPSF160-PTP.
(A) Expression of PTP-tagged CPSF160 homolog [Tb927.11.14560; lane PTP] in *T. brucei* cells was detected by Western blotting, using polyclonal anti-protein A antibodies. As a control, *T. brucei* 427 wildtype (lane WT) cells were analyzed. Protein size marker in kDa.
(B) Nuclear localization of CPSF160-PTP. Cell lines stably expressing PTP-tagged *T. brucei* CPSF160 were fixed and stained with DAPI. The localization of tagged protein was assessed by indirect immunofluorescence, using anti-protein A antibodies (CPSF160-PTP). In addition, superimpositions of DAPI and PTP-tagged protein (merge) as well as with brightfield are shown (merge with brightfield).

Based on CPSF160-PTP, two independent tandem affinity purifications (TAP) were performed (prot C exp. 1 and 2); as control, wildtype *T. brucei* 427 cells (WT) were used (**Figure 5.8**; page 75). Factors co-purifying with CPSF160 were analyzed by mass spectrometry and are listed in **Figure 5.8** (page 75; for raw data, see **Supplementary Table 8.1**; page 131-133): Eight proteins were identified by homology search as putative factors of the polyadenylation complex in trypanosomes, including five CPSF subunits (CPSF160; CPSF100; CPSF73; CPSF30; Fip1), two constituents of CstF (CstF64 hinge domain [see below]; CstF50), and the scaffold protein Symplekin. Two additional proteins were found [Tb927.11.13860; Tb927.8.4480], which are likely associated with the polyadenylation complex, since they are clearly above the peptide counts of the background control (WT). However, neither the poly(A) polymerase Tb927.7.3780 nor Tb927.3.3160 was co-purified with CPSF160-PTP. In addition, we did homology-based databank searches for trypanosomatid homologs of other eukaryotic polyadenylation factors, which had not appeared in our mass spectrometry analysis. As a result, we identified potential homologs of the 25 kDa subunit of cleavage factor I (CFIm25) [Tb927.7.1620] and cleavage factor II (CFIIm) [Tb927.6.3690] (**Figure 5.8**; page 75).

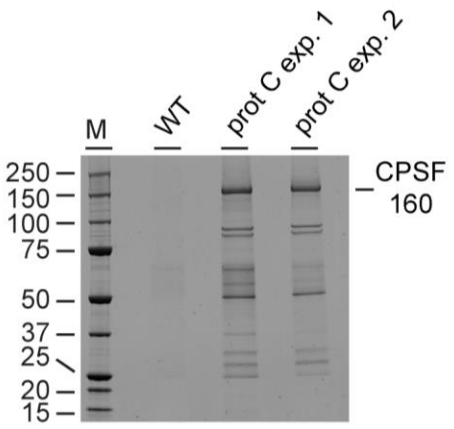

factor	annotation in *TriTrypDB*	mol. mass [kDa]	peptides experiment 1/2	reference
CPSF				
CPSF160	Tb927.11.14560	159.5	83/84	
CPSF100	Tb927.11.230	90.6	45/42	
CPSF73	Tb927.4.1340	85.3	37/33	Tkacz *et al.*, 2010
CPSF30	Tb927.11.12750	31.6	15/12	Hendriks *et al.*, 2003
Fip1	Tb927.5.4320	31.0	9/9	Bercovich *et al.*, 2009
CstF				
CstF64 (*hinge domain*)	Tb927.8.8210	14.7	3/7	
CstF50	Tb927.6.1830	49.9	2/5	
Others				
Symplekin	Tb927.8.7490	158.0	79/76	
hyp. protein	Tb927.11.13860	29.7	15/17	
hyp. protein	Tb927.8.4480	28.6	15/18	
identified by database search				
PAP	Tb927.7.3780	74.4		
CFI25m	Tb927.7.1620	32.7		
CFII	Tb927.6.3690	46.0		

Figure 5.8 Identification of components of the polyadenylation complex, based on TAP-tag purification of the nuclear localized trypanosomatid CPSF160 homolog.
CPSF160-associated proteins were identified by mass spectrometry. Extracts were prepared from *T. brucei* cell lines that stably express tagged CPSF160 (in two biological replicates; exp. 1/2), followed by TAP-tag affinity purification. Proteins after the second purification step (protein C elution) were analyzed by SDS-PAGE and Coomassie staining (lanes prot C experiment 1/2). As control, *T. brucei* 427 wildtype cells were used (lane WT). Protein size markers in kDa (M). Putative protein constituents of the *T. brucei* polyadenylation complex were identified by mass spectrometry. Each protein is described by name (factor), the TriTrypDB annotation number (http://tritrypdb.org/tritrypdb/), its molecular mass (in kDa), the number of exclusive unique peptide counts obtained by mass spectrometry, and, if applicable, by literature reference. Below, the three proteins identified only by database search (PAP, CFI25m, and CFII) are listed by name, TriTrypDB annotation number, and molecular mass.

In addition to MS-based homology search, we further confirmed our data by comparative InterProScan protein domain identification of the individual trypanosomatid factors and their respective human counterparts (**Figure 5.9**; page 78).

All CPSFs (see above) identified in our mass spectrometry analysis have a domain organization that is similar to their respective human homologs: For both CPSF160 subunits (sequence identity: 20.9%) the C-terminal CPSF A domain, whose function is unknown, could be identified.

Both the human as well as the trypanosomatid CPSF100 (sequence identity 22.0%) and CPSF73 (sequence identity 39.3%) have a ß-lactamase domain with a ß-caspase domain (ß-casp) inserted like a cassette with the active site of the protein at the interface of these two domains (Mandel *et al.*, 2006). In higher eukaryotes CPSF73 is the endonuclease in 3´ end processing, and the residues (mainly histidines) coordinating the two zinc atoms that are required for RNA cleavage are conserved in trypanosomes as well. In contrast, CPSF100 lacks the zinc-binding residues and cannot bind zinc, arguing against nuclease activity of the protein. In addition both CPSF 100 and CPSF73 have an RMMBL domain (RNA metabolizing metallo beta lactamase) and characteristic C-terminal domains, required for *in vivo* core cleavage complex formation composed of CPSF100, CPSF73 and Symplekin (Michalski & Steiniger, 2015).

The domain structure of *T. brucei* CPSF30 is compared to the human protein conserved (sequence identity 31.0%), harboring five C3H1 zinc fingers and a C-terminal C2HC zinc finger. The human protein was shown to bind (in cooperation with WDR33) the canonical AAUAAA hexamer polyadenylation signal via zinc fingers two and three, with a minor contribution of the C-terminal zinc finger (Chan *et al.*, 2014, Schönemann *et al.*, 2014, Shimberg *et al.*, 2016). Although, the AAUAAA polyadenylation signal was not found in trypanosomes, the conserved CPSF30 domain structure argues for a possible role in RNA binding.

Fip1 (sequence identity 12.7%), the fifth CPSF identified in our mass spectrometry analysis, contains the Fip1 domain (Fip1) present in the human homolog, which is required for the interaction with CPSF30 (zinc fingers four and five) in trypanosomes (Bercovich *et al.*, 2009). The C-terminal arginine-aspartate-rich region (RD-rich) of the human protein that binds to U-rich RNA sequences is not present in the trypanosomatid protein but it contains an additional C3H1 zinc finger (Kaufmann *et al.*, 2004).

All other identified proteins except for CstF64 display conserved domain architectures as well. CstF64 (sequence identity 4.9%) was only identified through a putative hinge domain present in both the trypanosomatid and human protein that was shown to interact with CstF77 and Symplekin in a mutual exclusive manner in humans (Takagaki & Manley, 2000, Ruepp *et al.*, 2011b). The N-terminal RRM binding the U-rich DSE and the highly conserved C-terminal

domain (CstF64-C) required for polyadenylation are absent in trypanosomes (MacDonald *et al.*, 1994, Gross & Moore, 2001, Qu *et al.*, 2007).

Both the *T. brucei* and the human CstF50 protein (sequence identity 17.2%) contain the WD40 repeat domain, which functions as a binding platform for CstF77 interaction (Takagaki & Manley, 2000). However, the N-terminal self-dimerization domain (CstF1-dd) of the human homolog is missing.

Trypanosomatid CFIm25 (sequence identity 23.7%) and CFIIm (sequence identity 26.6 %) have the same domain structure as their respective human counterparts, of which the CFIm25 NUDIX hydrolase domain is of special interest, since it binds the USE and regulates poly(A) site selection in humans (Yang *et al.*, 2010).

Symplekin (sequence identity 12.6%) functions as a scaffold protein and the C-terminal domain (Symplekin-C) is conserved in trypanosomes as well, but the ARM repeats (armadillo-type fold) are missing.

Take together our results suggest a general conservation of polyadenylation complex constituents among eukaryotes.

Figure 5.9 Domain conservation of polyadenylation factors.
Schematics of human polyadenylation factors and the *T. brucei* homologs. Domains were identified by InterProScan 5 scanning and are depicted in scale as colored boxes. CPSF A, cleavage and polyadenylation specificity factor, A subunit, C-terminal domain; ß-lactamase, beta-lactamase domain; ß-casp, beta-caspase domain; RMMBL, RNA metabolizing metallo beta lactamase domain (metal binding amino acid residues are colored in red); CPSF2-C, cleavage and polyadenylation specificity factor 2, C-terminal domain; CPSF73-C, cleavage and polyadenylation specificity factor 3 C-terminal domain; ZnF C3H1-type, zinc finger C3H1-type; ZnF C2HC, zinc finger type C2HC; Fip1, pre-mRNA polyadenylation factor Fip1 domain; RD-rich, arginine-aspartate-rich region; H-rich, histidine-rich region; P-rich, proline-rich region; CstF1-dd, cleavage stimulation factor subunit 1, dimerization domain; RRM, RNA recognition motif; hinge domain; CstF64-C, cleavage stimulating factor C-terminal domain; WD40 repeat, tryptophan-aspartate repeat; NUDIX, NUDIX hydrolase domain; MobB, MobB-type P-loop domain; Clp1, Pre-mRNA cleavage complex II cleavage and polyadenylation factor 1 domain; ARM repeat, armadillo-type fold; Symplekin-C, Symplekin C-terminal domain.

5.1.5 Characterization of the CPSF30 RNA-binding properties

To further analyze a possible RNA-binding function of CPSF30, suggested by the conserved domain structure (see 5.1.4), a SELEX-seq experiment was performed to identify an *in vitro* binding motif.

In brief: Recombinantly expressed and purified GST-CPSF30 and GST, as control, (**Figure 5.10**) was incubated with an *in vitro* T7 transcribed RNA, derived from a DNA oligonucleotide containing a random 20-mer sequence (**Figure 5.11 A**; page 80). Bound RNA was recovered, reverse-transcribed, PCR-amplified and used again for *in vitro* T7 transcription followed by another round of selection. Finally, libraries of all five rounds of selection (for GST, only round five) were prepared and subjected to high-throughput sequencing. We obtained between 0.55 mio and 0.87 mio reads (0.86 mio for GST) containing a 18 to 20-mer sequence that were used for CPSF30 RNA-binding motif analysis.

The representation of each of the possible tetramer (256) and hexamer (4096) motifs was determined after each SELEX cycle, and the enrichment of each tetramer and hexamer was evaluated by z-score values. **Figure 5.11 B** (page 80) shows heat maps for the top 20 and the bottom 10 tetramers (upper panel) and hexamers (lower panel) (ordered according to their z-score after the fifth SELEX round with GST-CPSF30 protein), especially how the motifs were enriched over the five cycles (CPSF30 R1 to R5).The most enriched tetramers and hexamers were long poly(U) stretches, whereas GC-rich sequences were most depleted, arguing for a oligo(U) *in vitro* RNA-binding motif of trypanosomatid CPSF30.

In addition, for further iCLIP-based *in vivo* analysis of CPSF30 RNA-binding a clonal procyclic cell line stably expressing a C-terminal PTP-tagged CPSF30 was generated (**Figure 5.12**; page 80).

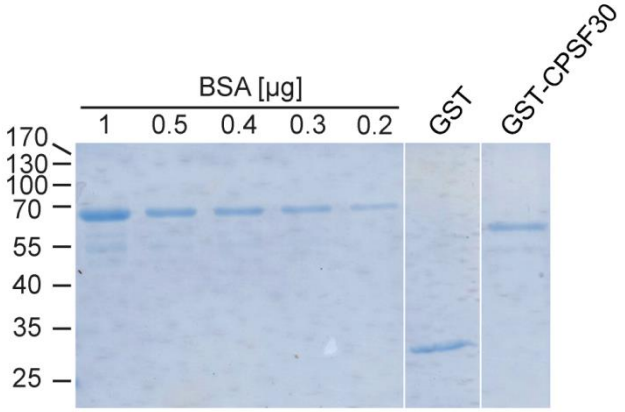

Figure 5.10 Quantification of *E. coli*-expressed GST-CPSF30 and GST.
Recombinant proteins were expressed in *E.coli* BL21 DE3 star cells, bound to glutathione sepharose and analyzed by SDS-PAGE and Coomassie staining. BSA standards (1-0.2 µg) were used for quantification. Protein size markers in kDa.

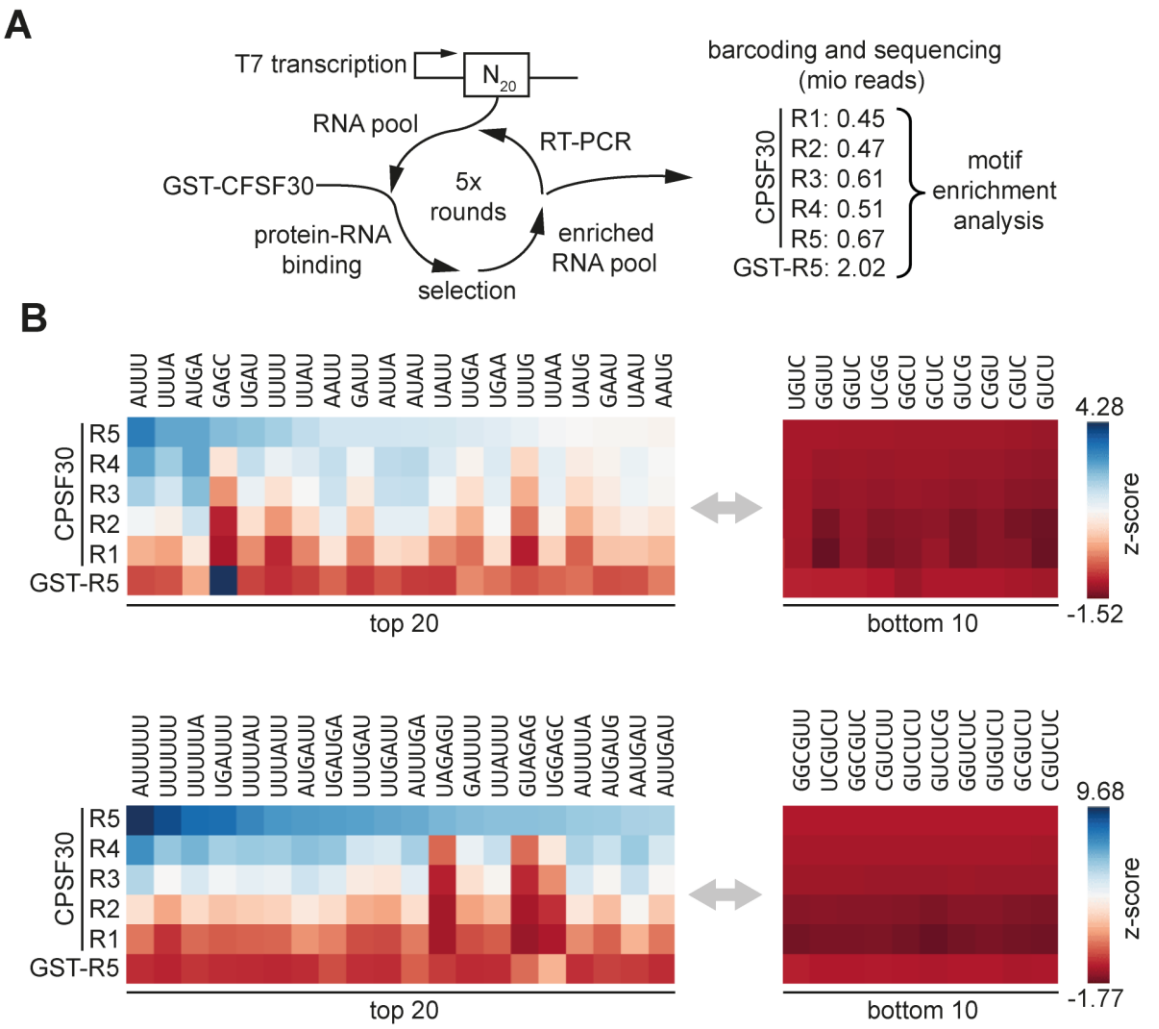

Figure 5.11 Identification of the CPSF30 *in vitro* RNA-binding motif by SELEX-seq.
(A) Schematic representation of the SELEX-seq procedure and data analysis. Using GST-CPSF30 (GST as control) and an N_{20} RNA pool, CPSF30 RNA-binding sequences were enriched through five SELEX rounds. After each selection round (CPSF30 R1-R5; GST control only R5), aliquots were taken for library preparation and high-throughput sequencing, followed by motif enrichment analysis (see panel B).
(B) Motif enrichment analysis of CPSF30 RNA-binding. The upper and lower panel shows the enrichment of tetramers and hexamers during the five SELEX rounds with GST-CPSF30 (R1-R5) and GST control (R5), respectively. Only the top 20 and the bottom 10 tetramers and hexamers are represented as colour-coded heat maps, showing z-scores of the motif frequencies for each round (ordered by z-score in R5 of GST-CPSF30).

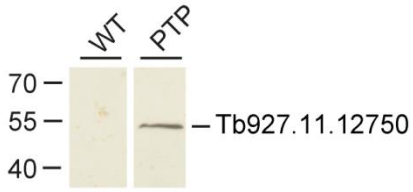

Figure 5.12 Validation of CPSF30-PTP expression.
The expression of PTP-tagged CPSF30 [Tb927.11.12750] in *T. brucei* cells was detected by Western blotting, using polyclonal anti-protein A antibodies (lane PTP). As control, *T. brucei* 427 wildtype (lane WT) cells were included. Protein size markers in kDa.

5.1.6 Polyadenylation factors are required for both polyadenylation and *trans* splicing

To assess the functional relevance of the proteins identified in the polyadenylation complex, we depleted each of them by inducible RNAi: Each of the individual knockdowns showed a severe growth defect in procyclic trypanosomes, with the exception of one of the two hypothetical proteins, Tb927.11.13860 (**Figure 5.13**; page 82). Following quality control of isolated total RNA by gel electrophoresis and silver staining, depletion of the individual factors was validated by semiquantitative RT-PCR (**Figure 5.14 A** and **B**; page 83). Afterwards the *in vivo* polyadenylation status was examined (**Figure 5.15 A**; page 84; for raw data, see **Figure 5.16**; page 85-86) as described for the two poly(A) polymerases (see 5.1.3).

Knockdown of CPSF100, CPSF73, and CPSF30 strongly reduced the overall poly(A) tail lengths. In contrast, depletion of CPSF160 and Fip1 -as part of the CPSF complex- did not cause significant changes. CstF50 depletion strongly affected polyadenylation, in contrast to CstF64 depletion. Note that the putative CstF64 analyzed here exhibits only a very low sequence similarity to its mammalian counterpart (see 5.1.4); it may represent a truncated homolog functionally different from the mammalian factor or a trypanosomatid-specific factor. Depletion of the scaffold factor Symplekin resulted in a severe polyadenylation phenotype. In contrast, depletion of the two cleavage factors CFIm25 and CFIIm did not significantly affect poly(A) tail length. Finally, when analyzing the two unannotated proteins [Tb927.11.13860 and Tb927.8.4480], small, but significant inhibitory and stimulatory effects were observed, respectively.

As several previous studies have indicated, both major pre-mRNA processing steps, *tran*s splicing and polyadenylation, are interconnected. Therefore we also analyzed *trans* splicing activities to compare them directly with the corresponding polyadenylation effects. Both spliced-leader (SL) RNA (**Figure 5.15 B**; page 84), which is known to accumulate upon inhibition of *trans* splicing (for example, see Tkacz *et al*., 2010), and a specific *trans*-spliced mRNA (PPIase) (**Figure 5.15 C**; page 84) were measured by quantitative RT-PCR after knockdown of the individual polyadenylation factors. Depletion of the CPSF complex subunits 160, 100, 73, and 30 resulted in spliced-leader accumulation and severe splicing deficiencies. However, for Fip1 only blocking of splicing was observed, but no effect on SL RNA accumulation (**Figure 5.15 C**; page 84). Knockdown of both CstF subunits 64 and 50, Symplekin, CFIIm, and the two hypothetical proteins Tb927.11.13860 and Tb927.8.4480 resulted in moderate effects on spliced-leader accumulation and in most cases also on inhibition of *trans* splicing. However, depletion of CFIm25 had neither an effect on SL RNA accumulation nor on *trans* splicing. These effects on PPIase *trans* splicing were largely confirmed with another gene, PRP8, analyzed by

semiquantitative RT-PCR (**Figure 5.17**; page 87). We conclude that the corresponding knockdown effects of most core polyadenylation factors on both polyadenylation and *trans* splicing, as well as splicing deficiencies after CPSF160 and Fip1 depletion, argue for a general coupling of these two major RNA processing steps.

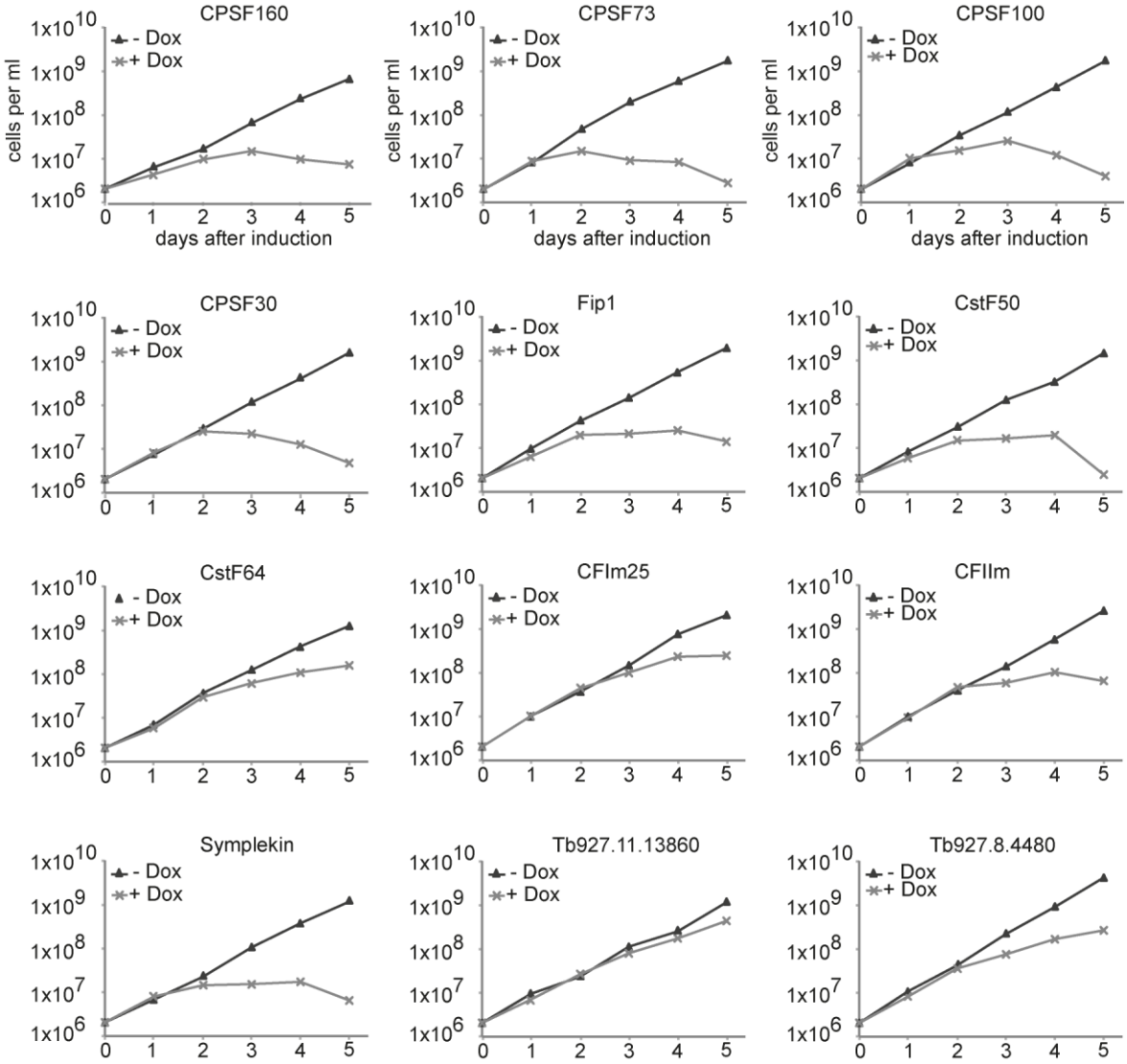

Figure 5.13 Growth curves of procyclic trypanosomes after RNAi depletion of polyadenylation complex constituents.

Growth curves of representative cell lines, in which RNAi was induced by doxycycline (+Dox, lines with asterisks) and respective uninduced controls (-Dox, lines with triangles). The following factors were subjected to RNAi induction (TriTrypDB numbers in brackets): CPSF160 [Tb927.11.14560]; CPSF100 [Tb927.11.230]; CPSF73 [Tb927.4.1340]; CPSF30 [Tb927.11.12750]; Fip1 [Tb927.5.4320]; CstF50 [Tb927.6.1830]; CstF64 [Tb927.8.8210]; CFIm25 [Tb927.7.1620]; CFIIm [Tb927.6.3690]; Symplekin [Tb927.8.7490]; Tb927.11.13860; Tb927.8.4480.

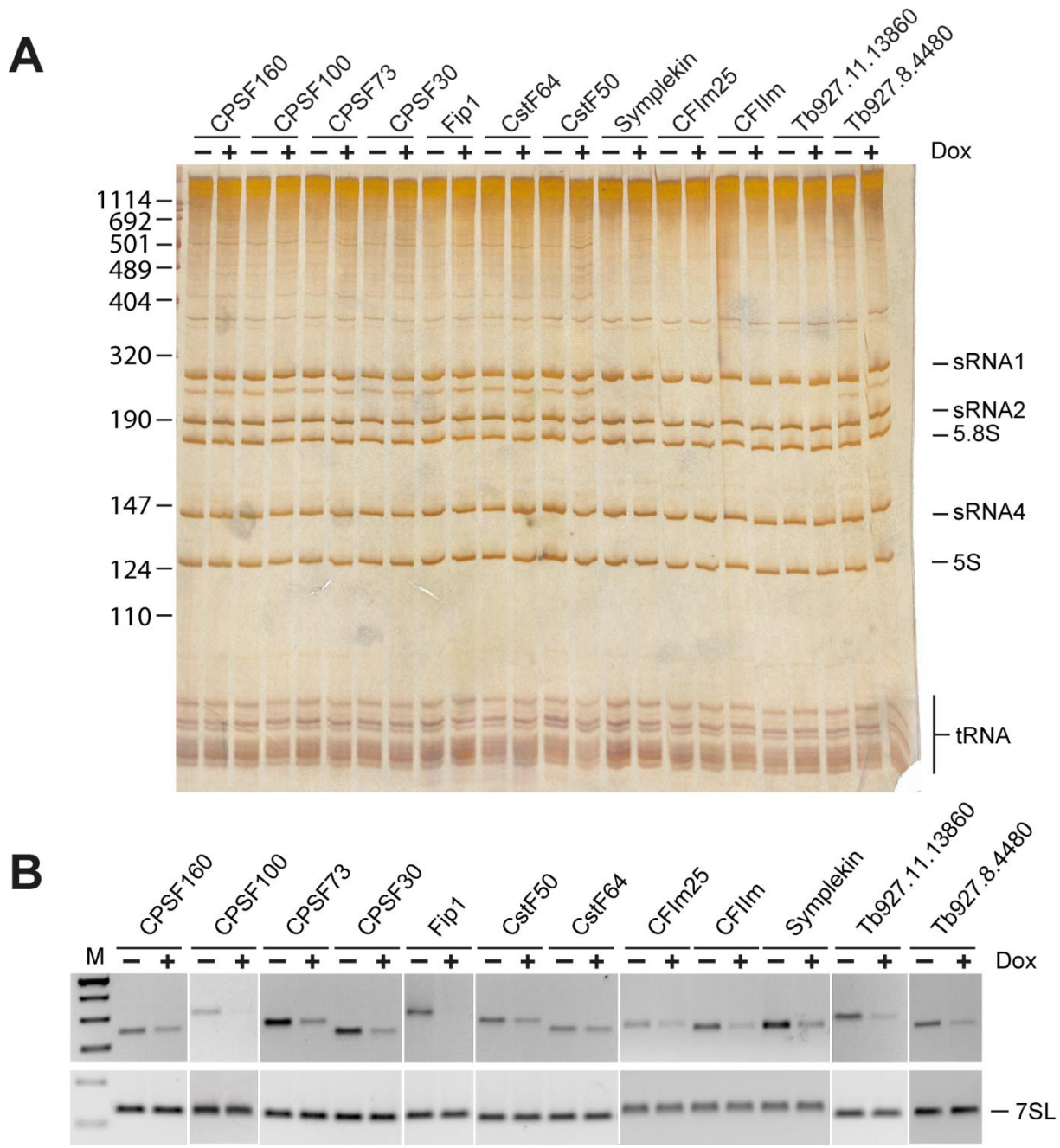

Figure 5.14 RNAi mediated knockdown of polyadenylation complex constituents.
(A) RNA was isolated from uninduced (-) and RNAi induced cells (+), separated on a denaturing 10% polyacrylamide/urea gel and visualized by silver staining. The ribosomal sRNA1, sRNA2, 5.8S, sRNA4 and 5S RNA as well as the tRNAs are indicated. The following factors were subjected to RNAi induction (TriTrypDB numbers in brackets): CPSF160 [Tb927.11.14560]; CPSF100 [Tb927.11.230]; CPSF73 [Tb927.4.1340]; CPSF30 [Tb927.11.12750]; Fip1 [Tb927.5.4320]; CstF64 [Tb927.8.8210]; CstF50 [Tb927.6.1830]; CFIm25 [Tb927.7.1620]; CFIIm [Tb927.6.3690]; Symplekin [Tb927.8.7490]; Tb927.11.13860; Tb927.8.4480.
(B) mRNA levels were analyzed by semiquantitative RT-PCR from uninduced cells (-) and after 3 days of RNAi induction (+). As control, 7SL RNA from the same samples was analyzed. M, markers (200, 300, 400, and 500 bp; for 7SL: 100 and 200 bp).

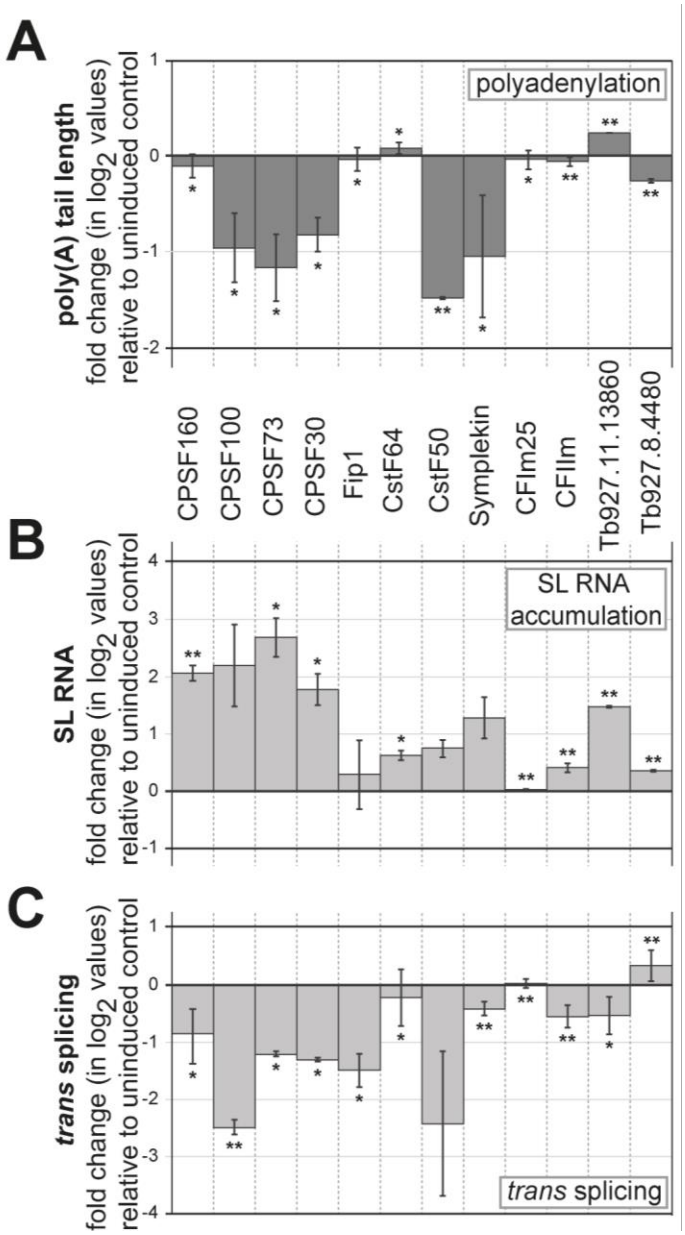

Figure 5.15 Polyadenylation factors required for both polyadenylation and splicing *in vivo*.
The following factors were subjected to RNAi knockdown (TriTrypDB numbers in brackets): CPSF160 [Tb927.11.14560]; CPSF100 [Tb927.11.230]; CPSF73 [Tb927.4.1340]; CPSF30 [Tb927.11.12750]; Fip1 [Tb927.5.4320]; CstF50 [Tb927.6.1830]; CstF64 [Tb927.8.8210]; CFIm25 [Tb927.7.1620]; CFIIm [Tb927.6.3690]; Symplekin [Tb927.8.7490]; Tb927.11.13860; Tb927.8.4480. Changes in the overall poly(A) tail length **(A)**, in SL RNA accumulation **(B)**, and in *trans* splicing of PPIase mRNA **(C)** upon depletion of individual polyadenylation factors are graphically shown. Poly(A) tail lengths were analyzed and quantitated by the "Riemann´s sum", comparing induced and uninduced cells (for raw data, see Figure 5.15; page 86/87). SL RNA accumulation and *trans*-splicing activities were determined by RT-qPCR on SL RNA and *trans* spliced PPIase mRNA, respectively, and normalized to U3 RNA. For both polyadenylation, SL RNA accumulation, and *trans* splicing, fold changes (in $\log_2$ values) of uninduced and induced levels were calculated, with standard deviations derived from three biological replicates (* for P values <0.05; ** for P values <0.01).

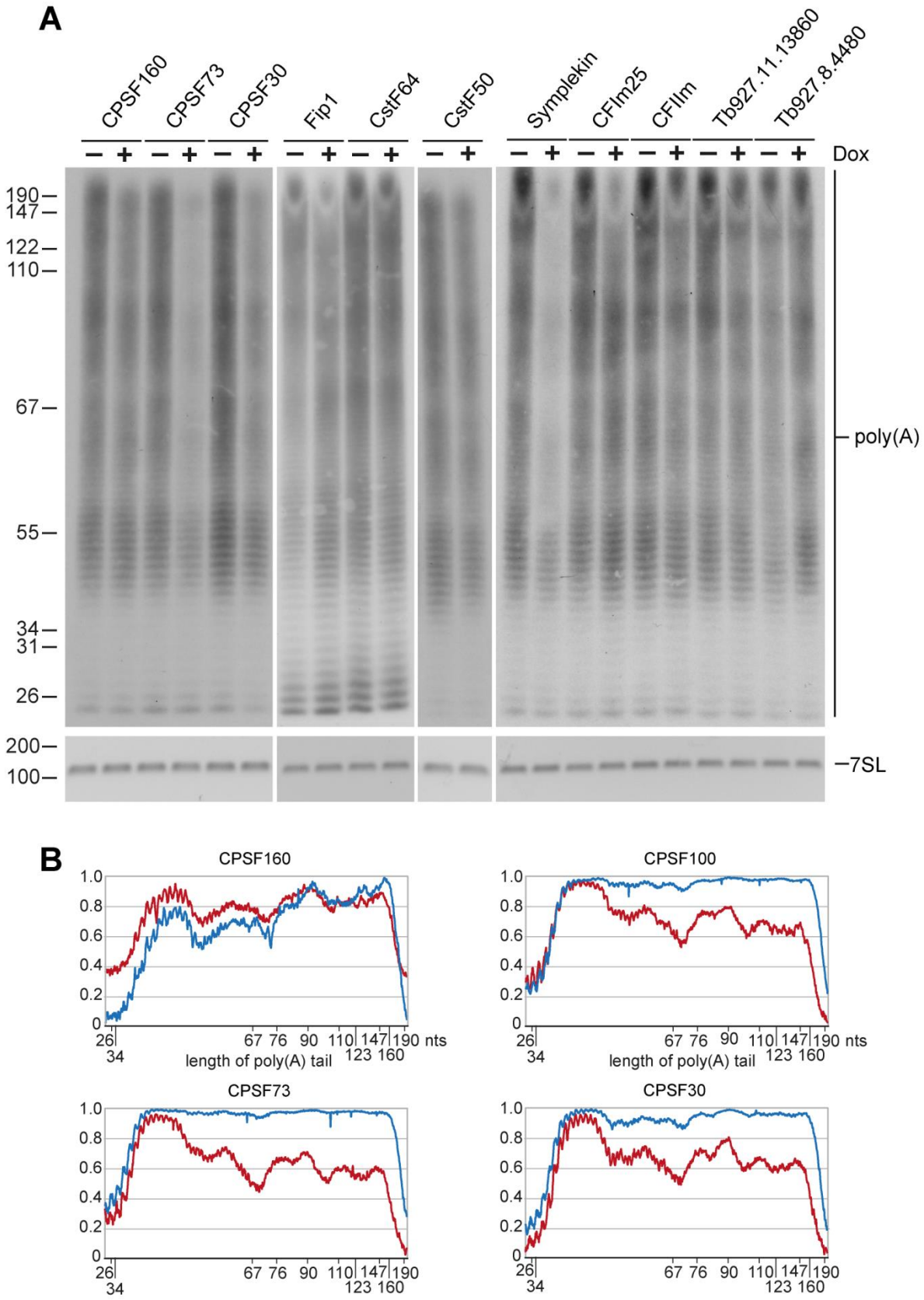
A
CPSF160
CPSF73
CPSF30
Fip1
CstF64
CstF50
Symplekin
CFIm25
CFIIm
Tb927.11.13860
Tb927.8.4480
– + – + – + – + – + – + – + – + – + – + – + Dox
190
147
122
110
67
55
34
31
26
poly(A)
200
100
7SL
B
CPSF160
CPSF100
CPSF73
CPSF30
1.0
0.8
0.6
0.4
0.2
0
26 34 67 76 90 110 147 190 nts
123 160
length of poly(A) tail

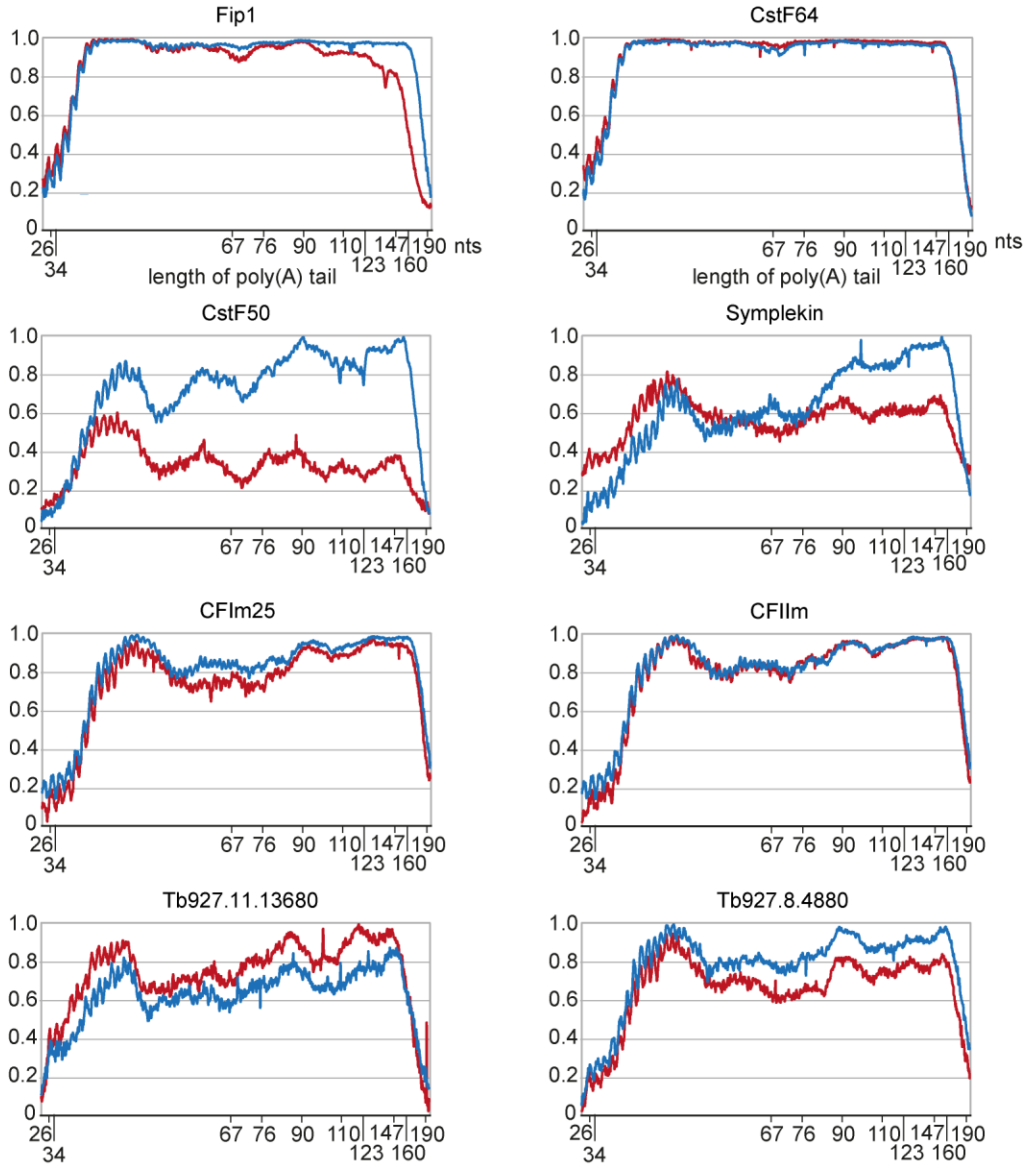

Figure 5.16 Changes in the poly(A) tail length upon depletion of 12 individual trypanosomatid polyadenylation factors.

(A and B; page 85-86**)** The following factors were subjected to RNAi induction (TriTrypDB numbers in brackets): CPSF160 [Tb927.11.14560]; CPSF100 [Tb927.11.230]; CPSF73 [Tb927.4.1340]; CPSF30 [Tb927.11.12750]; Fip1 [Tb927.5.4320]; CstF50 [Tb927.6.1830]; CstF64 [Tb927.8.8210]; CFIm25 [Tb927.7.1620]; CFIIm [Tb927.6.3690]; Symplekin [Tb927.8.7490]; Tb927.11.13860; Tb927.8.4480.

(A) RNA from uninduced (- Dox) and RNAi induced (+ Dox) cells was splint-labeled, digested with RNases A/T1, followed by separation of the ^{32}P-labeled tails [poly(A)] on a denaturing 15% polyacrylamide/urea gel. 7SL RNA detected by RT-PCR served as loading control. Marker sizes are indicated in nucleotides.

(B) The relative intensities of knockdown and uninduced control signals were measured with ImageJ and plotted. The tail length distributions in uninduced (blue lines) and induced cells (red lines) are represented.

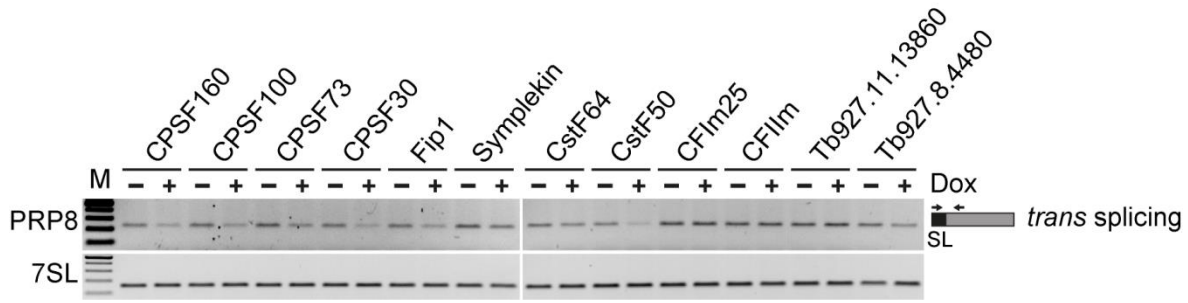

Figure 5.17 Changes in PRP8 mRNA *trans* splicing upon depletion of 12 individual trypanosomatid polyadenylation factors.

The respective splicing activities were monitored in uninduced (-Dox) and induced (+Dox) cells by semiquantitative RT-PCR. To detect the *trans* spliced PRP8 mRNA, SL- and PRP8 exon-specific primer were used. The primer positions and orientations are schematically represented on the right side. As control 7SL RNA was analyzed. M, marker (100, 200, 300, 400, and 500 bp). TriTrypDB numbers in brackets: CPSF160 [Tb927.11.14560]; CPSF100 [Tb927.11.230]; CPSF73 [Tb927.4.1340]; CPSF30 [Tb927.11.12750]; Fip1 [Tb927.5.4320]; CstF50 [Tb927.6.1830]; CstF64 [Tb927.8.8210]; CFIm25 [Tb927.7.1620]; CFIIm [Tb927.6.3690]; Symplekin [Tb927.8.7490]; Tb927.11.13860; Tb927.8.4480.

5.2 DRBD4-mediated regulation of mRNA polyadenylation in *Trypanosoma brucei*

5.2.1 DRBD4 binds *in vivo* preferentially to gene UTRs

To map DRBD4-RNA contacts at single-nucleotide resolution in procyclic *T. brucei* cells, we applied the iCLIP approach. Three individual experiments were performed, using a cell line expressing DRBD4 with a PTP tag (protein C epitope / TEV cleavage site / 2× protein A epitope), with wildtype *T. brucei* 427 (WT) cells as negative control. Trypanosomes were UV-crosslinked, and DRBD4-RNA complexes were purified by tandem affinity purification (TAP), separated by SDS-PAGE, and blotted onto nitrocellulose membrane (**Figure 5.18**). Subsequently, bound RNA was eluted and used for library preparation, followed by high-throughput sequencing.

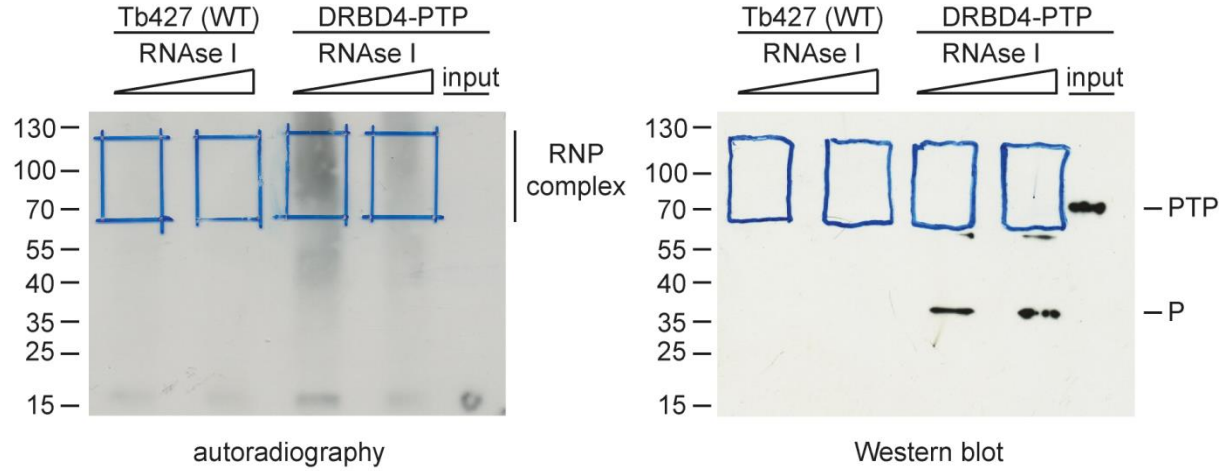

Figure 5.18 Representative DRBD4-PTP iCLIP experiment.
Protein-RNA interactions were crosslinked by UV-irradiation of DRBD4-PTP-expressing cells or Tb427 wildtype cells (WT; negative control), followed by lysate preparation, limited RNase digestion, immunoprecipitation of DRBD4-PTP RNA-protein (RNP) complexes, 3´ linker ligation, tobacco-etch-virus (TEV) protease cleavage and the second affinity step (anti-protein C immunoaffinity purification). 5′-terminal ^{32}P-labeled RNP-complexes were then gel-separated under denaturing conditions and visualized by autoradiography (left panel). In each case, RNase I amounts were titrated (as indicated). Boxed regions were cut out and subjected to RNA isolation and library preparation. Western blot analysis (right panel) of the same membrane was performed using anti-protein C antibodies including 2% input material. The gel positions of DRBD4 with the full PTP tag (PTP) and the remaining protein C epitope (P) after TEV-protease cleavage are indicated.

Approximately 3.6 mio of the 9.5 mio total DRBD4-PTP iCLIP sequences could be uniquely mapped to the *T. brucei* genome (**Figure 5.19**; page 89). After random-barcode filtering, the 387,577 crosslink tags from 255,063 crosslink sites were used for downstream analysis. Within the individual DRBD4 iCLIP crosslink tags, approximately 56% mapped to mRNAs, with a strong preference for the UTR regions (~42%, compared with ~14% in the coding regions). The large

proportion of not annotated iCLIP crosslink tags (~37%) can be most likely explained by the incomplete annotation of gene UTRs. In addition, the overall highly consistent distribution of iCLIP tags in the different RNA classes argues for the reproducibility of the individual experiments.

	sequenced reads	uniquely mapped reads	crosslink site counts	crosslink tags counts
Tb427 (WT)	828,656	83,965	1,264	2,677
DRBD4 (total)	**9,489,415**	**3,625,320**	**255,063**	**387,577**
DRBD4-PTP_1	2,435,834	392,110	23,128	**36,327**
DRBD4-PTP_2	4,187,648	1,838,268	164,787	**249,799**
DRBD4-PTP_3	2,865,933	1,394,942	67,148	**101,451**

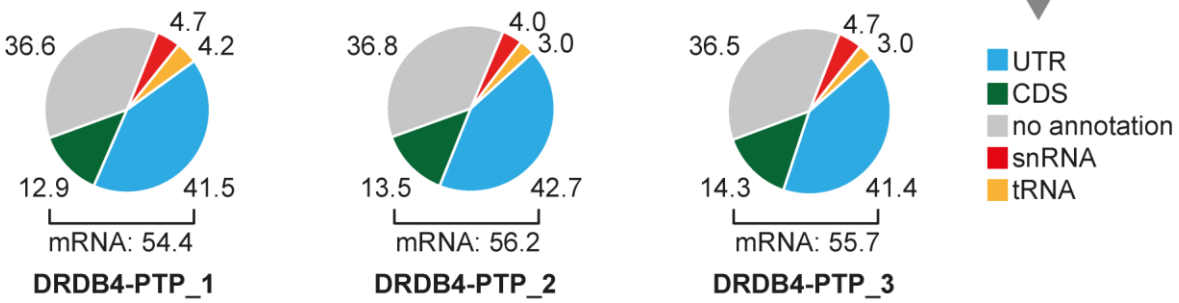

Figure 5.19 Genome-wide mapping of DRBD4-RNA interactions in *T. brucei* by iCLIP-seq.
Summary of sequenced/mapped iCLIP reads (upper panel) and the genomic distribution of barcode-filtered tag counts (in percent; lower panel), based on three individual DRBD4-PTP experiments.

In addition to the PTP-based iCLIP-approach (see above), a second iCLIP protocol using a YFP-tag was established. A single experiment was performed with a procyclic DRBD4-YFP cell line and wildtype *T. brucei* 427 (WT) cells served as negative control. The experimental procedure is as described above, with the exception that only a one step immunoprecipitation using anti-GFP antibodies is applied.

Approximately 1.1 mio of the 2.2 mio DRBD4-YFP iCLIP sequences were uniquely mapped to the *T. brucei* genome (**Figure 5.20**; page 90). After random-barcode filtering, the 954,953 crosslink tags from 739,861 crosslink sites were used for downstream analysis. The majority of YFP-DRBD4 iCLIP tags mapped -similar to the DRBD4-PTP iCLIP (see above)- to mRNAs (68.1%), displaying again a preference for UTR regions (~40.2%, compared with ~27.9% in the coding regions). Moreover, a large proportion of not annotated iCLIP crosslink tags (~30.5%) was observed (see above). A general reproducibility between both protocols is reflected by the constant distribution of iCLIP tags in the different classes of RNAs in the PTP-based and YFP-based experiments. However, the numbers of uniquely mapped reads, crosslink site counts and crosslink tag counts in the YFP-based experiment were strongly increased, when compared to

individual DRBD-PTP experiments with a similar number of total sequenced reads (DRBD4-PTP_1 and 3). This indicates that the YFP-library was more complex, compared to the individual DRDB4-PTP libraries, which can be most likely explained by a higher YFP-immunoprecipitation efficiency, since only a single-step method was used.

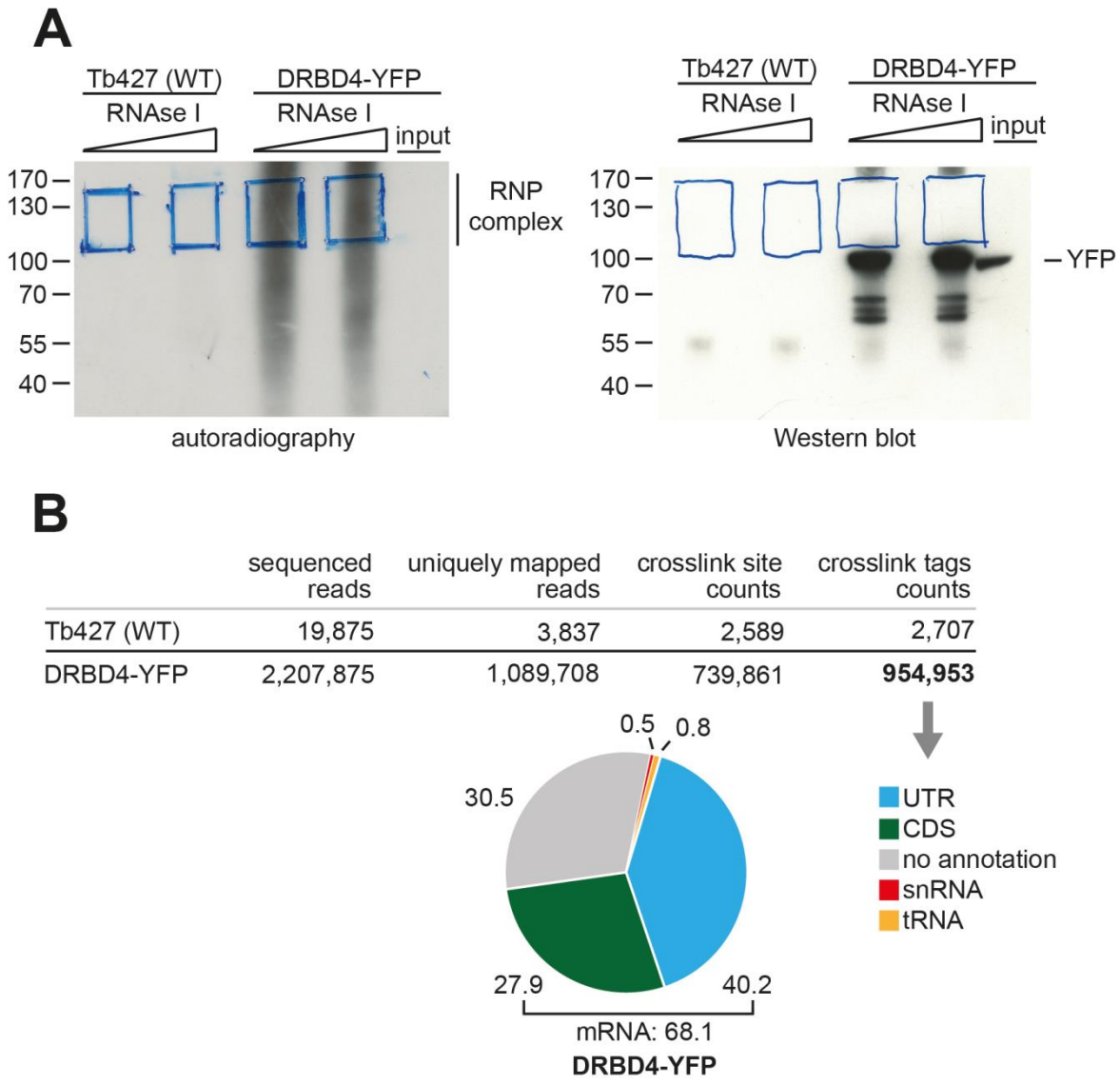

Figure 5.20 DRBD4-YFP iCLIP experiment.
(A) Protein-RNA interactions were crosslinked by UV-irradiation of DRBD4-YFP expressing cells or Tb427 wildtype cells (WT; negative control), followed by lysate preparation, limited RNase digestion, immunoprecipitation of DRBD4-YFP RNA-protein (RNP) complexes and 3´ linker ligation. 5′-terminal 32P-labeled RNP-complexes were then gel-separated under denaturing conditions and visualized by autoradiography (left panel). In each case, RNase I amounts were titrated (as indicated). Boxed regions were cut out and subjected to RNA isolation and library preparation. Western blot analysis (right panel) of the same membrane was performed using anti-protein GFP antibodies including 1.5% input material. The gel position of DRBD4-YFP is indicated.
(B) Summary of sequenced/mapped iCLIP reads (upper panel) and the genomic distribution of barcode-filtered tag counts (in percent; lower panel), in the DRBD4-YFP experiment.

5.2.2 DRBD4 binds purine-rich sequences containing AUGA elements *in vitro*

To further investigate the DRBD4 RNA-binding properties we next used a SELEX-seq approach to derive a minimal binding motif. Briefly, recombinant *T. brucei* GST-DRBD4 (with GST protein as negative control; **Figure 5.21 A**) was incubated with RNA T7-transcribed from a DNA oligonucleotide template containing a random 20-mer sequence (**Figure 5.21 B**). Bound RNA was recovered, reverse-transcribed, PCR-amplified, and used again for *in vitro* T7 transcription, followed by further rounds of selection. Finally, RNA-seq libraries were prepared from aliquots after each of the five selection rounds (for the GST control, only after the fifth round) and subjected to high-throughput sequencing.

Between 0.45 and 0.67 mio sequence tags per SELEX cycle were obtained for GST-DRBD4 (for GST control: 2.02 mio after the fifth cycle), with 20-mer sequences that were analyzed for the *in vitro* RNA-binding motif of DRBD4.

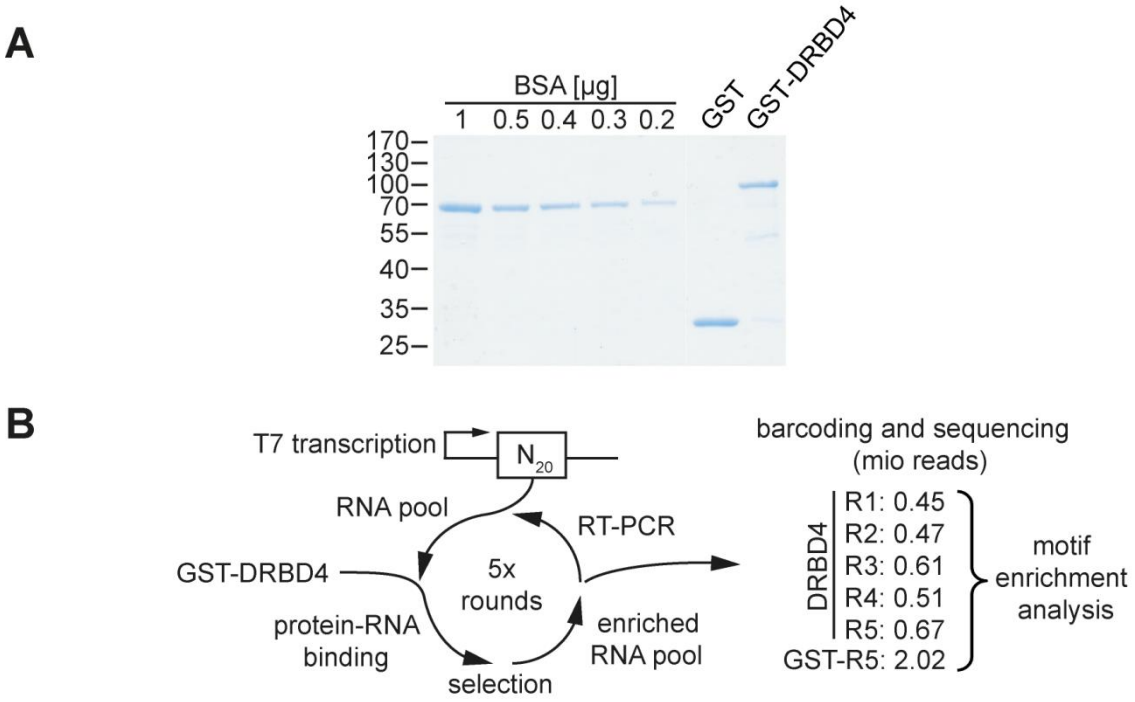

Figure 5.21 Identification of the RNA-binding motif of DRBD4 by SELEX-seq.
(A) Quantification of *E. coli*-expressed GST-DRBD4 and GST. Recombinant proteins were expressed in *E. coli* BL21 DE3 star cells, bound to glutathione sepharose and analyzed by SDS-PAGE and Coomassie staining. BSA standards (1-0.2 µg) were used for quantification.
(B) Schematic representation of the SELEX-seq procedure and data analysis. Using GST-DRBD4 (GST as control) and an N_{20} RNA pool, DRBD4 RNA-binding sequences were enriched through five SELEX rounds. After each selection round (DRBD4 R1-R5; GST control only R5), aliquots were taken for library preparation and high-throughput sequencing, followed by motif enrichment analysis (see Figure 5.22; page 93).

The representation of each of the possible tetramer (256) and hexamer (4096) motifs was determined after each cycle, and the enrichment of each tetramer and hexamer was evaluated by z-score values. **Figure 5.22** (page 93) shows heat maps for the top 20 and the bottom 10 tetramers (upper panel) and hexamers (middle panel) (ordered according to their z-score after the fifth SELEX round with GST-DRBD4 protein), especially how the motifs were enriched over the five cycles (DRBD4 R1 to R5).

Interestingly, sequences containing purines -in particular adenosines- were highly enriched during the selection process, with the AUGA tetramer being most enriched. This was further underlined by the hexamer analysis, where also AUGA flanked by two A nucleotides was most enriched. In contrast, pyrimidine-rich stretches appear to be depleted in both the tetramer and hexamer analyses.

Since a single RRM can recognize up to eight nucleotides and DRBD4 contains four RRMs, RNA binding of DRBD4 may be combinatorial and involve more than a single minimal motif. Therefore we also analyzed tetramer combinations: The eight most enriched tetramers from the final selection round with GST-DRBD4 were combined, allowing up to two nucleotides spacing between them, and ranked according to their representation in the SELEX-sequence tags. **Figure 5.22** (lower panel; page 93) shows a heat map of the top 20 and bottom 10 most enriched double-tetramer combinations, ordered according to their motif frequency (sum of 0/1/2-nts spacing). As the most enriched double-tetramer combinations AUGA-AUGA and GAAA-UGAA were identified, each without spacer (note that the latter one also contains an AUGA motif, with flanking adenosine nucleotides, as the most enriched hexamer).

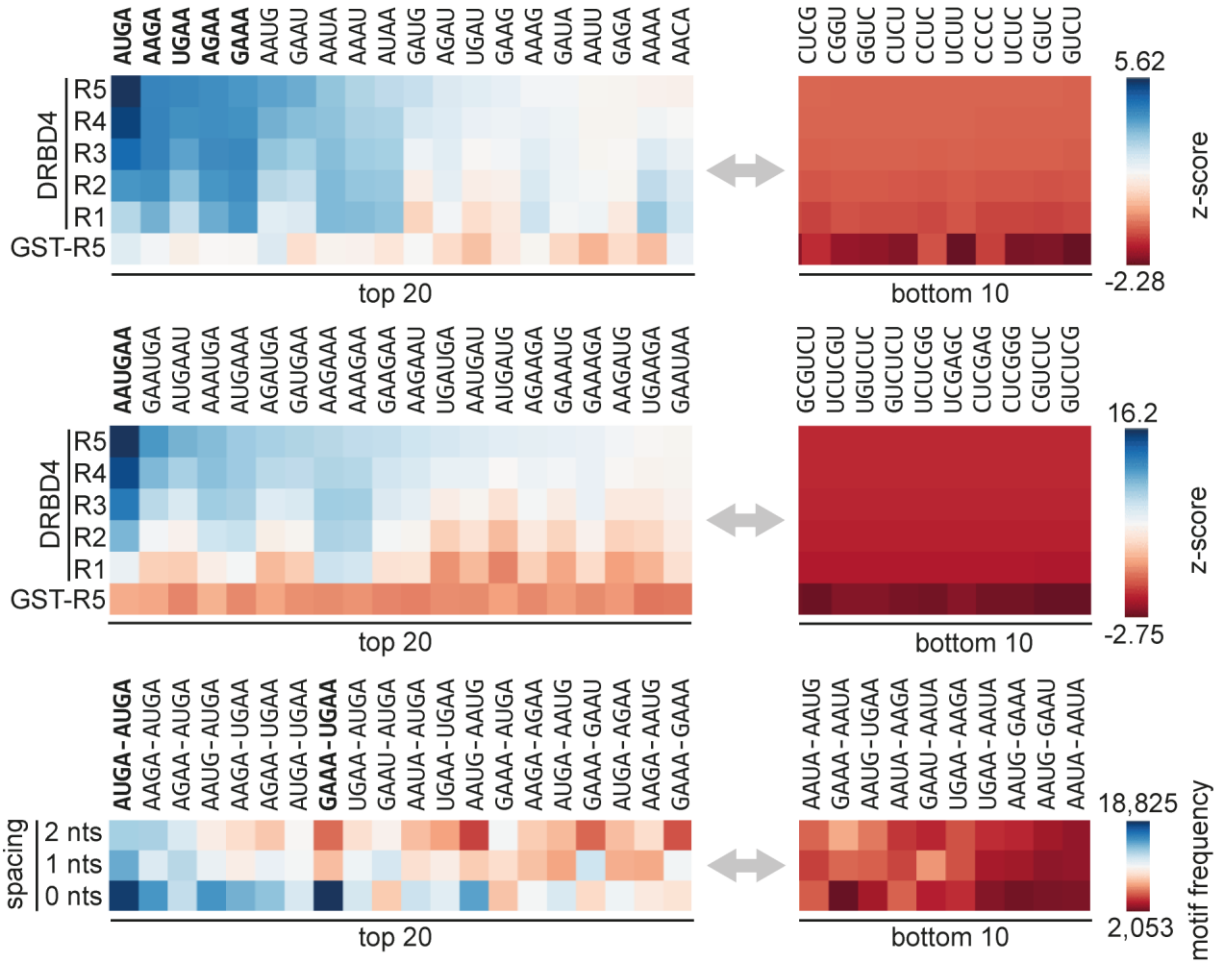

Figure 5.22 Motif enrichment analysis of DRBD4 RNA binding.
The upper and middle panel shows the enrichment of tetramers and hexamers during the five SELEX rounds with GST-DRBD4 (R1-R5) and GST control (R5). Only the top 20 and the bottom 10 tetramers and hexamers are represented as colour-coded heat maps, showing z-scores of the motif frequencies for each round (ordered by z-score in R5 of GST-DRBD4). The lower panel shows the enrichment for combinations of the top eight tetramers from the upper panel (with 0/1/2 nts spacing). Only the top 20 and the bottom 10 double-tetramers are displayed as colour-coded heat map, indicating motif frequencies in the R5 round of GST-DRBD4 (ordered by the sum of frequencies of 0/1/2 nts spacing). The motifs selected for experimental validation are highlighted in bold.

To biochemically validate the binding motif, we assayed for *in vitro* binding of GST-DRBD4 to selected ^{32}P-labeled RNA transcripts, using GST pulldown and analysis of associated RNAs by denaturing PAGE, followed by quantitation (**Figure 5.23 A**; page 95).

Surprisingly, the most enriched hexamer (motif #1; in two copies with an eight-nucleotide spacer in between, see **Figure 5.23 A** for context; page 95) and the double-tetramer combination GAAA-UGAA (motif #3; in a single copy) did not significantly bind DRBD4 above GST control levels. In contrast, the transcript with the double-AUGA sequence (motif #2) efficiently bound

and appears to represent a minimal functional binding motif. To further analyze a possible spacing tolerance of this minimal motif, which was suggested by a high motif frequency with one or two spacing nucleotides (see **Figure 5.22**; lower panel; page 93), adenosine nucleotides (which were overrepresented in our SELEX-derived, DRBD4-binding sequences; **Figure 5.22**; page 93), were inserted between the two AUGA tetramers (motifs #6-8): Compared with the minimal double-tetramer (motif #2), the insertion of two adenosine (A_2) nucleotides reduced, whereas four (A_4) or eight (A_8) adenosines enhanced binding. However, three adjacent AUGA motifs without spacing did not further increase the binding efficiency (motif #4). The specificity for and requirement of the AUGA unit was underlined by the strong effect of a single point mutation in the tetramer motif (AUGA to AUUA; compare motif #4 and #10). Moreover, another triple-tetramer combination (motif #5), with the high-affinity AUGA flanked by AAGA and AGAA, among the most enriched tetramers (see **Figure 5.23 A**; upper panel; page 95), bound almost as well as the triple-AUGA sequence. Surprisingly, even a simple oligo-adenosine stretch $(A)_{12}$ was bound with similar efficiency (motif #9).

In addition, to test a polypyrimidine-rich DRBD4 binding motif as suggested in a previous study (Stern *et al*., 2009), we also assayed DRBD4 binding to four *T. brucei* polypyrimidine tracts (**Figure 5.23 B**; page 95). However, the relatively high DRBD4 binding affinities we observed were in all cases similar to the GST control, arguing for unspecific background binding probably based on the GST moiety.

Taken together, our binding assays further confirmed and validated the SELEX-seq data: We conclude that DRBD4 binds *in vitro* RNA sequences that are purine-, in particular adenosine-rich, often harboring AUGA elements.

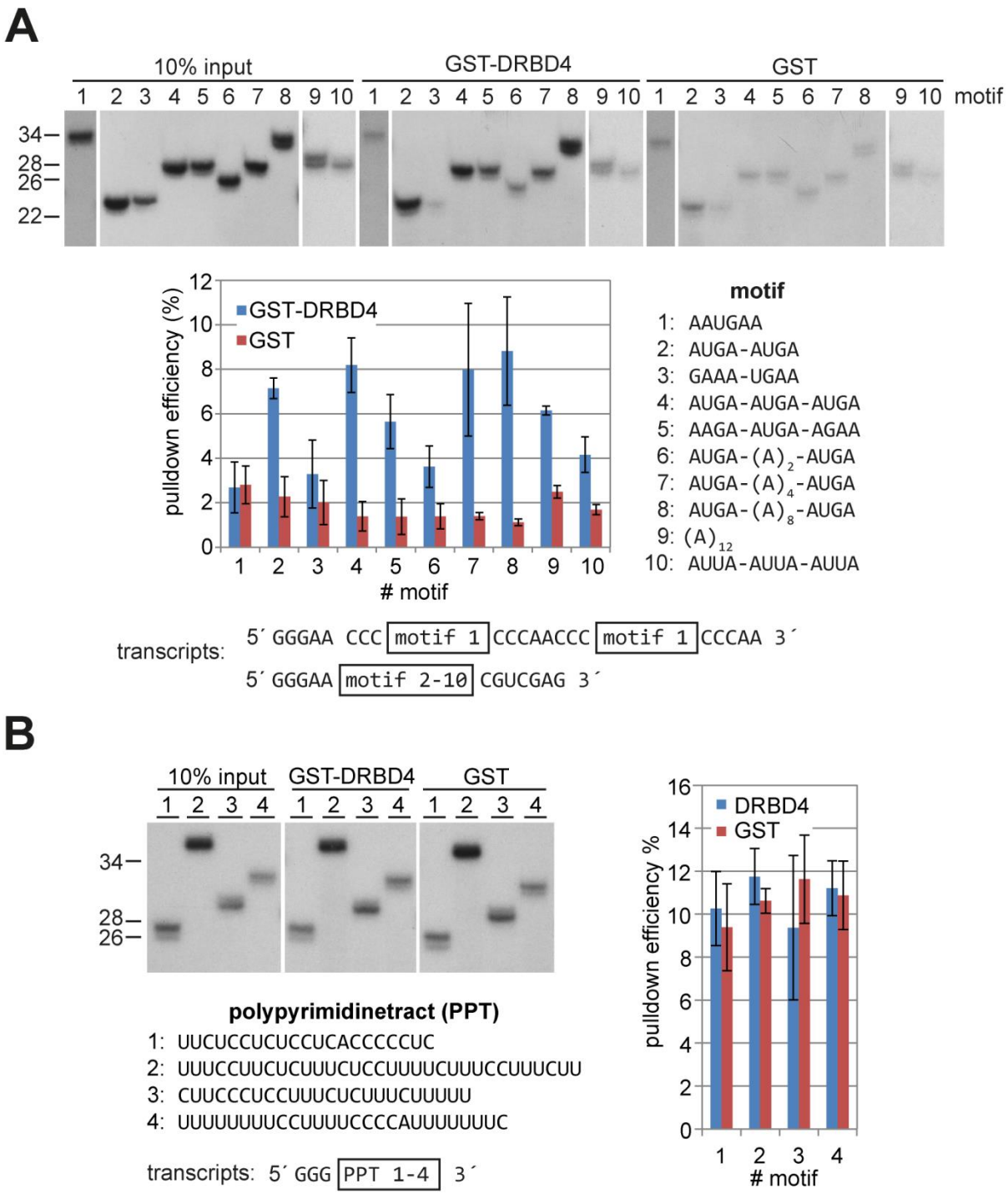

Figure 5.23 DRBD4 preferentially binds purine-rich sequences containing AUGA motifs.
^{32}P labeled short RNA transcripts containing different **(A)** SELEX-derived binding motifs (#1-10) or **(B)** polypyrimidine tracts form *T. brucei* genes (#1: Tb927.1.2340; # 2, 3: Tb927.11.3630; #4: Tb927.6.510) were incubated with GST-DRBD4 or GST (negative control), immobilized on glutathione sepharose. Bound RNA was recovered and analyzed by denaturing polyacrylamide gel electrophoresis (marker sizes in nucleotides). For each pulldown assay, 10% of the input and the total recovered RNA were loaded. The respective pulldown efficiencies including standard deviations were calculated from three replicates.

5.2.3 DRBD4 depletion affects polyadenylation site usage

In addition to the reported functions of the trypanosome DRBD4 in mRNA stability and splicing (Stern et al., 2009), DRBD4 was identified in a targeted RNAi screen for genes that were necessary for the instability of developmentally regulated mRNAs. In the course of this work, it was found that RNAi depletion of DRBD4 resulted in an altered poly(A) site location in the GPI-PLC (Tb927.2.6000) mRNA (see 5.2.4). As the human homolog PTB1 can also modulate polyadenylation efficiency (Castelo-Branco et al., 2004, Izquierdo et al., 2005, , Fred & Welsh, 2009) we assayed for a regulatory role of DRBD4 in trypanosomatid 3´ end processing of mRNAs. In a procyclic *T. brucei* cell line expressing endogenous YFP-tagged DRBD4, depletion was initiated for three days by doxycycline-inducible RNAi and monitored through flow cytometry (**Figure 5.24 A**); the cells continued to proliferate throughout the time course (**Figure 5.24 B**).

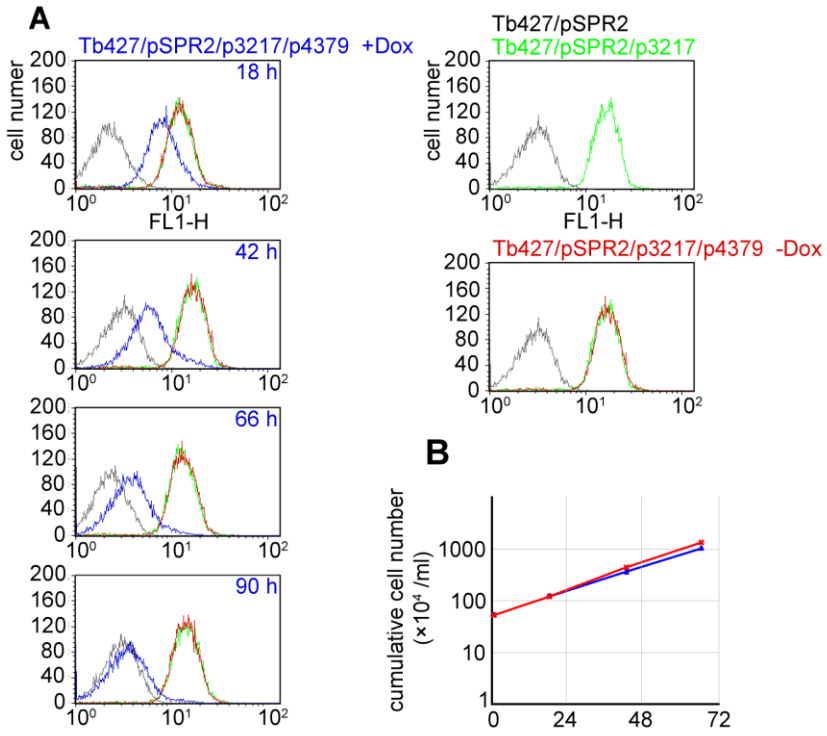

Figure 5.24 Validation of RNAi-mediated DRBD4 depletion.
(A) Flow cytometry measurements of YPF in cell lines expressing tet repressor (pSPR2, gray) and an additional endogenous YFP-tagged DRBD4 allele (p3217, green). DRBD4-YFP levels were measured in a time course after 18, 42, 66 and 90 hours of DRBD4-RNAi (p4376) induction (blue; +Dox), and uninduced cells served as control (red; -Dox). FL1-H indicates the relative intensity of the YFP fluorescence.
(B) Growth curve of the DRBD4-RNAi line (as in **A**), in which RNAi was induced by doxycycline (red line with asterisks), and the respective uninduced control (blue line with triangles).

Total RNA was isolated from cells after RNAi and from uninduced control, followed by poly(A)$^+$ RNA selection, library preparation for 3´ end mapping and RNA-seq (**Table 5.1**). Based on 6.86 mio and 10.48 mio total sequenced reads in control and knockdown cells, respectively, polyadenylation sites in both samples were mapped using the SLaP mapper tool: Based on 1.19 mio (in control) and 1.70 mio poly(A)-site-spanning reads (in knockdown cells), we identified in total 152,628 (control) and 200,141 (knockdown) individual polyadenylation sites. First, poly(A) sites from the uninduced control cells were clustered (to give 8,962 poly(A) site clusters) and second, the poly(A)-site reads in each cluster were summarized and compared with those in DRBD4-knockdown cells: As a result, we identified 234 down- and 248 up-regulated poly(A) site clusters (**Table 5.1**).

Table 5.1 DRBD-mediated poly(A) site choice.
Summary of poly(A)-site-spanning reads, poly(A) sites, poly(A) site clusters, and up-/down-regulated clusters, based on RNA-seq analysis of DRBD4 knockdown (kd) and control (ctr) cells.

	ctr	kd
total sequenced reads	6,863,039	10,482,225
poly(A)-site-spanning reads	1,186,940	1,699,656
poly(A) sites	**152,628**	200,141

5.2.4 DRBD4-regulated poly(A) site choice: integrating iCLIP and RNA-seq data

Next, we combined our DRBD4-PTP iCLIP and RNA-seq datasets, with the aim to correlate *in vivo* RNA binding and DRBD4-dependent poly(A) site choice. Based on the 234 down- and 248 up-regulated poly(A) site clusters, iCLIP crosslink tag counts in the region between -200 to +200 nts of the regulated poly(A) site clusters were summarized. Likewise, non-regulated poly(A) site clusters with similar expression levels were selected as background group (see *Materials and methods* for details). **Figure 5.25** (page 98, for DRBD4-YFP iCLIP see, **Supplementary Figure 8.2**; page 130) shows the accumulated distribution of DRBD4-PTP iCLIP tag counts (as smooth line in 21-nts windows) around the regulated poly(A) sites; a poly(A) site was defined as the position with the highest number of poly(A) site tags within the cluster, with the background group (dashed line) plotted for comparison. As a result, we found an enrichment of DRBD4 binding in the upstream region of regulated poly(A) sites (-20 to -140 nts for down-regulated, -100 to -180 nts for up-regulated sites).

In sum, these data provide evidence for a correlation between DRBD4 *in vivo* binding and DRBD4-dependent changes in poly(A) site selection, arguing for a DRBD4-mediated regulation of this process.

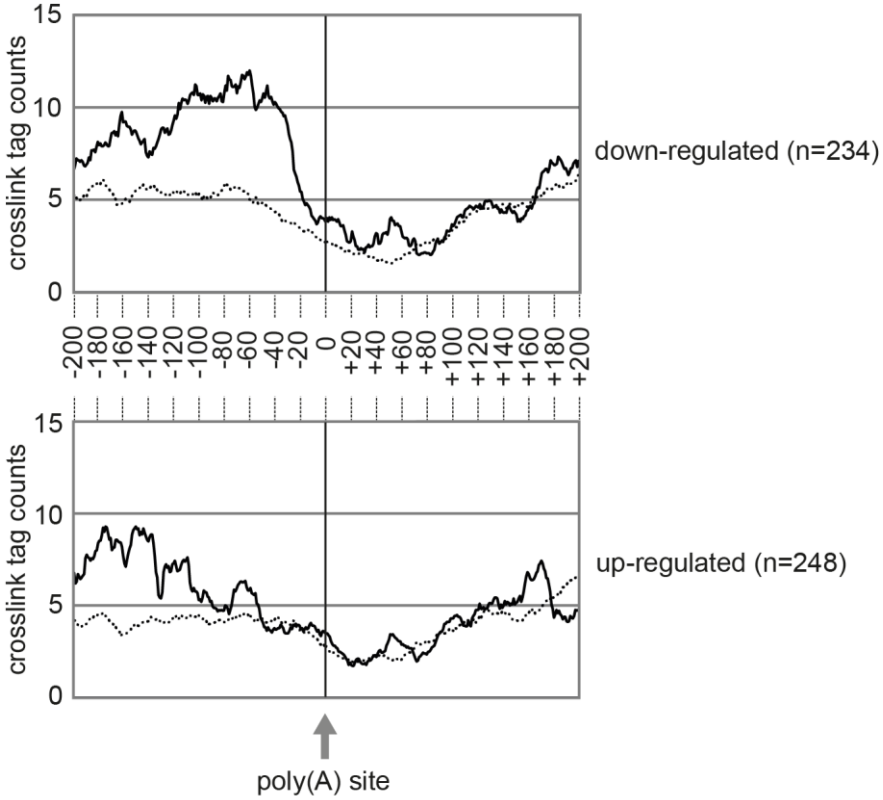

Figure 5.25 DRBD4 RNA binding around regulated poly(A) sites.
Accumulated DRBD4-PTP iCLIP crosslink-tag counts were plotted in the region between -200 to +200 nts relative to the poly(A) site of the down- and up-regulated clusters (top: down-regulated n=234; background n=936; bottom: up-regulated n=248; background n=992) and are depicted as solid lines. As background control, unaffected polyadenylation sites were used (dashed lines). Crosslink-tag counts were plotted with fitted values (21-nts windows) on the Y-axis and positions on the X-axis.

To validate individual cases of DRBD4-dependent poly(A) site choice, we analyzed by Northern blotting changes in transcript levels after DRBD4 knockdown (at 24, 48, and 72 hours; **Figure 5.26**; page 100; for sequences and crosslink sites, see **Figure 5.27**; page 101). We initially tested two individual genes, Tb927.8.760 and Tb927.8.770, each containing a single poly(A) site, which is down-regulated after DRBD4 depletion (based on our RNA-seq read numbers: for Tb927.8.760, from 692 to 470 reads; for Tb927.8.770, from 223 to 128 reads) and Northern blot analysis confirmed lower transcript levels (**Figure 5.26 A**; top and middle; page 100).
In contrast, Tb927.11.5440 is more complex since there are two reciprocally used poly(A) sites, separated by 350 nucleotides (tandem 3´ UTR APA; see 3.4): the distal one, which is down-regulated after DRBD4 depletion (200 to 69 reads), and a proximal one, which is up-regulated

(46 to 177 reads), causing a shift from a long to a short isoform (**Figure 5.26 A**; bottom; page 100). This shift in isoform levels, due to differential poly(A) site choice, could be nicely confirmed by Northern blotting, which showed after DRBD4 knockdown a decrease of the long and a parallel, approximately two-fold increase of the short isoform. Interestingly, in the bloodstream form, the opposite can be observed, that the short Tb927.11.5440 isoform is predominantly expressed (**Figure 5.28**; page 102).

In addition, we tested two genes with DRBD4 crosslink sites upstream of a poly(A) site that was up-regulated after DRBD4 knockdown (**Figure 5.26 B**; page 100; for sequences and crosslink sites, see **Figure 5.27**; page 101): First, Tb927.6.1470 contains two poly(A) sites with a 960-nucleotide distance (tandem 3´ UTR APA; see 3.4), of which the proximal site is up-regulated (62 to 270 reads) and the distal one down-regulated (52 to 32 reads). Northern blot analysis clearly confirmed this strong and reciprocal shift in poly(A) site use.

In the second example, Tb927.2.6000 encoding a developmentally regulated glycosylphosphatidylinositol-phospholipase C (GPI-PLC), DRBD4 depletion activated a cryptic poly(A) site (proximal; 0 to 27 reads), whereas the distal polyadenylation site was not strongly affected (18 to 25 reads). The GPI-PLC mRNA is normally unstable in procyclic cells (Webb *et al.*, 2005a) but the shortening of the 3´ UTR resulting from use of the cryptic polyadenylation sites removed the *cis*-elements necessary to most of the instability (Webb *et al.*, 2005b). The activation of the cryptic poly(A) site results in the expression of a transcript shortened by 2.5 kb (**Figure 5.26 B**; page 100), as validated by Northern blotting, which showed the respective band only after knockdown for 48 and 72 hours. The long transcript [using the distal poly(A) site] appears in three closely spaced bands, most likely due to alternative *trans* splicing; in combination, these long isoforms did not change significantly over the knockdown time course.

Taken together, our data clearly show that DRBD4 binds upstream of polyadenylation sites and is required for both their activation and repression. For the first time this provides evidence for a *trans*-acting RNA-binding protein regulating polyadenylation in trypanosomes.

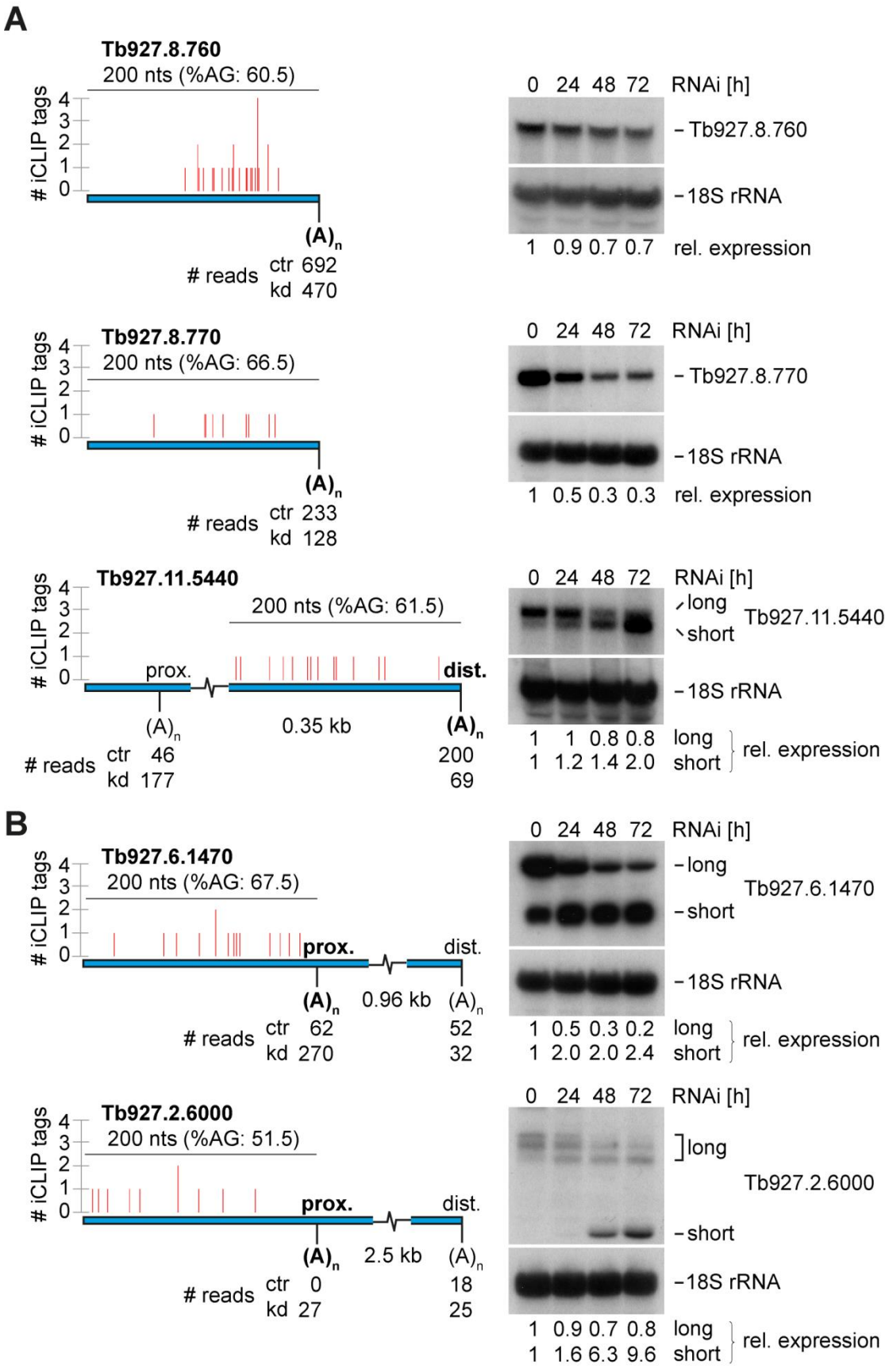
A
Tb927.8.760
200 nts (%AG: 60.5)
iCLIP tags
reads ctr 692 kd 470
0 24 48 72 RNAi [h]
Tb927.8.760
18S rRNA
1 0.9 0.7 0.7 rel. expression
Tb927.8.770
200 nts (%AG: 66.5)
reads ctr 233 kd 128
0 24 48 72 RNAi [h]
Tb927.8.770
18S rRNA
1 0.5 0.3 0.3 rel. expression
Tb927.11.5440
200 nts (%AG: 61.5)
prox.
dist.
0.35 kb
reads ctr 46 kd 177
200 69
0 24 48 72 RNAi [h]
long
short
Tb927.11.5440
18S rRNA
1 1 0.8 0.8 long
1 1.2 1.4 2.0 short
rel. expression
B
Tb927.6.1470
200 nts (%AG: 67.5)
prox.
dist.
0.96 kb
reads ctr 62 kd 270
52 32
0 24 48 72 RNAi [h]
long
short
Tb927.6.1470
18S rRNA
1 0.5 0.3 0.2 long
1 2.0 2.0 2.4 short
rel. expression
Tb927.2.6000
200 nts (%AG: 51.5)
prox.
dist.
2.5 kb
reads ctr 0 kd 27
18 25
0 24 48 72 RNAi [h]
long
short
Tb927.2.6000
18S rRNA
1 0.9 0.7 0.8 long
1 1.6 6.3 9.6 short
rel. expression

Figure 5.26 DRBD4 binding modulates alternative poly(A) site usage.
For each gene the DRBD4 iCLIP tag distribution, DRBD4-dependent alternative poly(A) site usage (based on RNA-seq read numbers), and validation by Northern blot analysis are shown together (page 100; panel **A**, three examples down-regulated after DRBD4 knockdown: Tb927.8.760; Tb927.8.770; Tb927.11.5440; panel **B**, two up-regulated examples: Tb927.6.1470; Tb927.2.6000).
First, in each case the distribution of DRBD4 iCLIP tags within 200 nts upstream of the DRBD4-regulated poly(A) site [**(A)$_n$**] is graphically represented, including the AG content of this region (in %). Gene bodies are marked as blue boxes, with distances between proximal (prox.) and distal (dist.) poly(A) sites indicated. Second, below the respective poly(A) sites the RNA-seq-based read counts are listed (DRBD4 knockdown at 0 versus 72 h). Third, for RNA-seq validation, DRBD4-dependent poly(A) site choice was directly analyzed by Northern blotting, showing four time points of DRBD4 knockdown (0-72 h) and using 18S rRNA as a loading control and for normalization. Below, the relative mRNA levels are listed.

nts upstream of poly(A) site	Tb927.8.760 mRNA sequence (% of purine crosslinks: 73)
-200 to -151	GUUGUAGUGCAACGUUUUUCUUGCGCUUGAAAUUAUGGACAGCGUUAGAG
-150 to -101	GACACUAAAGAAAUGGUUGAGUAAUAUAAGGAGAGA^{1}AAAUAUAAACG^{2}A^{1}UG
-100 to -51	AA^{1}UCAGCGUG^{1}A^{1}AUAAGAA^{1}UAAUAA^{1}UGA^{1}U^{2}AACAA^{1}AGGAUA^{1}A^{1}UGA^{1}U^{1}GAG^{1}AG^{4}U^{1}
-50 to 0	GAAUUCUU^{2}CCUAGCGUU^{1}ACUAUCGUAAGAAUGAUCGUUCGGAGUUUCUGA
nts upstream of poly(A) site	Tb927.8.770 mRNA sequence (% of purine crosslinks: 88)
-200 to -151	UGGACAGCGUUAGAGGACACUAAAGAAAUGGUUGAGUAAUAUAAGGAGAG
-150 to -101	AAAAUA^{1}UAAACGAUGAAUCAGCGUGAAUAAGAAUAAUAAUGAUAACAAAG^{1}
-100 to -51	G^{1}AUAAUGA^{1}UGAGAGUG^{1}GGAGGGACAGAGGAUGUGGA^{1}AG^{1}AAGGUGAUAGGU
-50 to 0	CGCUUU^{1}GCAUA^{1}UAAUGGAAUCUGUUUCCUGGUACUUACUUUUGGGUAAUA
nts upstream of poly(A) site	Tb927.11.5440 mRNA sequence (% of purine crosslinks: 69)
-200 to -151	GUUUUU^{1}GAAG^{1}AGAUAGGGUGGGCUCAGUGGGAAAA^{1}UAUUAUAUUCA^{1}AAAU
-150 to -101	AAACU^{1}AGGAGG^{1}AAGAAA^{1}UA^{1}AC^{1}UUAAGG^{1}AGAAAGCACAAUCA^{1}ACG^{1}AGGAGG
-100 to -51	AAGACGUU^{1}CAGAAACGCAAAAGACACACGA^{1}GCAGA^{1}UCCAAUAUCAUCAUA
-50 to 0	UCGCUUAUCACUACGAGAAUAAACUGUCACUU^{1}UUAUUUGUUCCCCCCUAU
nts upstream of poly(A) site	Tb927.6.1470 mRNA sequence (% of purine crosslinks: 86)
-200 to -151	AACUCUGAAGGCUGUUGAAGGGCGG^{1}AAAUGGGACUUCUACCACCAUAACA
-150 to -101	AAAGAGUGAACCAAAGAG^{1}GGAAAGAAGUA^{2}UAACUAUUAAUAAAGUGGGG^{1}A
-100 to -51	AAUGAGAACAAAC^{1}UUGUAAGUUAG^{1}UUGAA^{1}AG^{1}CAA^{1}AAAUGAUUAGGCGAGU
-50 to 0	GGUAACCAAA^{1}AGAAAAGUG^{1}UGGAGGAG^{1}UUGAAAUU^{1}UCAUCUAUGUAGGA
nts upstream of poly(A) site	Tb927.2.6000 mRNA sequence (% of purine crosslinks: 30)
-200 to -151	GUGCC^{1}AGUGG^{1}UACUGCU^{1}GCUAUAUUAAAAAAAAAAAU^{1}UAUACGGGU^{1}AUGG
-150 to -101	UGUGGAAGCAAAUGUGGGGGUUUUUAUU^{2}UUAAUCCUUAAAAAGCAA^{1}AAG
-100 to -51	CAAAAGCAAAAAACGGGA^{1}AACUAAUACGCUAUGCGUUUUGUGCCU^{1}AAAU
-50 to 0	GUACGGGCCCUCACAUGCUUUAUUUUCCAUUCUGGUUUUUACCCGUAUUC

Figure 5.27 mRNA sequences upstream of regulated poly(A) sites.
mRNA sequences with purine nucleotides (marked in grey) upstream of DRBD4-regulated poly(A) sites. The DRBD4 iCLIP crosslink sites are indicated as bold letters and the respective superscripts indicate the number of crosslink site counts. The number of crosslinked purine nucleotides (relative to the total crosslinks) in given in percent.

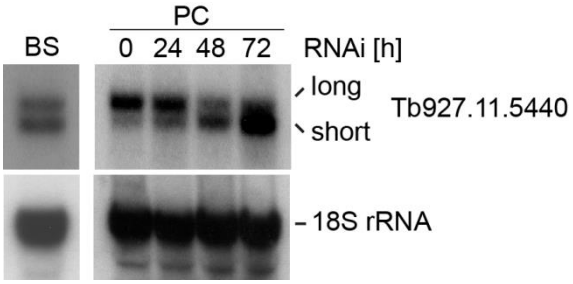

Figure 5.28 Life-cycle dependent expression of Tb927.11.5440 isoforms.
Expression levels of the long and short Tb927.11.5440 mRNA in wildtype bloodstream (BS) and procyclic (PC) trypanosomes after DRBD4 knockdown (0-72 hours). Transcript isoforms were detected by Northern blotting, and 18S rRNA served as loading control.

5.2.5 DRDB4 is associated with polyadenylation complex constituents

To get initial insights in the DRBD4-dependent regulation of polyadenylation we identified DRBD4-associated proteins. Two independent tandem affinity purifications (TAP) of DRBD4-PTP were performed, and co-purified factors were analyzed by mass spectrometry (**Figure 5.29**; page 103). Among the approximately 200 factors (data not shown) with more than one unique peptide count (as sum of both experiments), we identified five proteins of the *T. brucei* polyadenylation complex, which were also purified by CPSF160-PTP TAP (see 5.1.4): Three subunits of the CPSF complex (CPSF160, CPSF100 and CPSF73), one constituent of the CstF (CstF50) and the scaffold protein Symplekin. In addition, we also co-purified the polyadenylation factor PABP2, the homolog of the human PABPN1 protein, which displayed in comparison to the polyadenylation complex constituents a high number of unique peptides. Interestingly, also the functional poly(A) polymerase [Tb927.7.3780], which was not purified by TAP of CPSF160-PTP, was associated with DRBD4. However, in contrast to the polyadenylation complex (see 5.1.4), DRBD4 does not form large, stable protein complexes, as indicated by a high number of co-purified proteins with a very low unique peptide count. In sum, these data of DRDB4-associated polyadenylation factors provides further evidence for a DRBD4-dependent regulation of polyadenylation in trypanosomes.

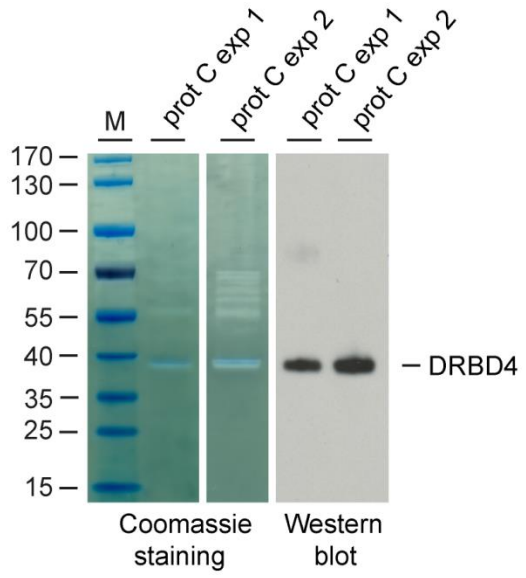

factor	annotation in *TriTrypDB*	mol. mass [kDa]	peptides exp 1+2	reference
CPSF				
CPSF160	Tb927.11.14560	159.5	11	
CPSF100	Tb927.11.230	90.6	4	
CPSF73	Tb927.4.1340	85.3	2	Tkacz *et al.*, 2010
CstF				
CstF50	Tb927.4.1340	49.9	3	
Others				
Symplekin	Tb927.8.7490	158.0	14	
PABP2	Tb927.9.10770	62.0	30	
PAP	Tb927.7.3780	74.4	3	

Figure 5.29 Identification of DRBD4-associated proteins by mass spectrometry.
Extracts were prepared from *T. brucei* cell lines that stably express tagged DRBD4 (in two biological replicates; exp 1/2), followed by TAP-tag affinity purification. Proteins after the second purification step (protein C elution) were analyzed by SDS-PAGE, Coomassie staining and Western blotting using polyclonal anti-protein A antibodies (lanes prot C exp 1/2). Protein size markers in kDa (M). Protein constituents involved in polyadenylation as well as putative factors were identified by mass spectrometry. Each protein is described by name (factor), the TriTrypDB annotation number (http://tritrypdb.org/tritrypdb/), its molecular mass (in kDa), the number of exclusive unique peptide counts obtained by mass spectrometry, and, if applicable, by literature reference.

6 Discussion

6.1 The poly(A) polymerase of *T. brucei*

Two genes Tb927.3.3160 and Tb927.7.3780 code for putative poly(A) polymerases in *T. brucei,* the first of which is peculiar in that it containis an intron requiring additional *cis* splicing for mRNA maturation. Both proteins share strong similarities in their domain structure with other eukaryotic poly(A) polymerases (see 5.1.1): The tripartite domain architecture of classical poly(A) polymerases consisting of the N-terminal catalytic domain, the central domain (also referred as PAP domain), and the C-terminal RNA-binding domain, which is conserved in both trypanosomatid paralogs (Martin *et al.*, 2000). Both Tb927.3.3160 and Tb927.7.3780 lack a clearly defined nuclear localization signal (NLS); however, some basic residues can be found near the C-terminus of the Tb927.7.3780 protein, which may act as an NLS (**Supplementary Figure 8.1**; page 128-129). Interestingly, only Tb927.7.3780 is located in the nucleus, whereas the putative poly(A) polymerase paralog Tb927.3.3160 has a cytoplasmic localization, specifically within distinct spots (see 5.1.1). Despite the fact that only the Tb927.7.3780 protein showed *in vitro* as well as *in vivo* polyadenylation activity, this argues for functions of the Tb927.3.3160 protein other than 3´ end processing of pre-mRNAs (see 5.1.2 and 5.1.3). However, due to our negative results in *in vitro* polyadenylation, we cannot rule out that Tb927.3.3160 may represent a functional poly(A) polymerase because additional factors might be required for activity even if Mg^{2+} is replaced by Mn^{2+} (Christofori & Keller, 1988). Moreover, we cannot exclude that Tb927.3.3160 has a limited, specialized set of targets, which our *in vivo* polyadenylation assay could not detect. For example, Tb927.3.3160 could function in cytoplasmic polyadenylation or uridylation regulating translation or mRNA stability (Norbury, 2013). During cytoplasmic polyadenylation a poly(A) tail is re-added to a transcript, which was exported from the nucleus with a very short poly(A) tail preventing translation since PABP (poly(A)-binding protein) cannot bind. Cytoplasmic polyadenylation depends on two *cis*-acting elements, the PAS, which is bound by the CPSF complex, and a less conserved cytoplasmic polyadenylation element (CPE) with a $UUUUUA_{1-3}U$ motif, which is bound by the CPE-binding protein. As a result, re-addition of the poly(A) tail activates the transcript for translation by the ribosome. In contrast, cytoplasmic uridylation of polyadenylated mRNAs leads to decapping, transcriptional silencing and degradation of the mRNA.

6.2 Importance of *cis* splicing in trypanosomes

An open question is the importance of *cis* splicing in trypanosomes, since only two genes contain a single intron with a highly conserved sequence in trypanosomes and require *cis* splicing for mRNA maturation (Tschudi & Ullu, 1990, Mair *et al.*, 2000, Liang *et al.*, 2003, Berriman *et al.*, 2005, Kolev *et al.*, 2010, Siegel *et al.*, 2010): A putative poly(A) polymerase, Tb927.3.3160, which is currently classified as non-functional in 3´ end processing (see 5.1.2 and 5.1.3) and an ATP-dependent DEAD box helicase Tb927.8.1510. However, RNAi-based depletion of Tb927.3.3160 (see 5.1.3) or Tb927.8.1510 had no effect on cell growth (Alsford *et al.*, 2011). A recent study from our group supports the hypothesis that *cis* splicing may be an evolutionary relic (Preußer *et al.*, 2014): Depletion of the U1 snRNP-specific U1C protein had no effect on cell growth and neither affected U1 snRNA levels nor the integrity of the U1 snRNP. U1C knockdown inhibited *cis*, but not *trans* splicing, which is in line with U1 snRNA binding at the 5´ *cis* splice site of both *cis*-spliced genes. Moreover, *cis* splicing was blocked with an antisense morpholino oligonucleotide that specifically binds the 5´ end of the U1 snRNA. After U1C depletion recovery from starvation stress was clearly impeded, indicating that *cis* splicing becomes essential only under stress conditions. Interestingly, Tb927.7.3780 is the major functional poly(A) polymerase in 3´ end processing, and for the intron-containing ATP-dependent DEAD box helicase Tb927.8.1510 an intronless putative counterpart may exist (Tb927.10.6630). However, this does not exclude that the two introns may fulfill an important, still unknown function, especially since the sequence is highly conserved in trypanosomes.

6.3 The trypanosomatid polyadenylation complex

Our identification and initial characterization of the components of the trypanosomatid polyadenylation complex provides an important initial step in understanding the evolution of mRNA processing mechanisms. There are considerable differences in the *cis*-acting polyadenylation elements between trypanosomes, yeast, and mammals. The mammalian polyadenylation signal consists of three elements (see 3.3): First, the highly conserved AAUAAA hexanucleotide PAS typically located 15 to 30 nts upstream of the cleavage site, which is in most cases a CA dinucleotide (Sheets *et al*., 1990, Beaudoing *et al*., 2000, Hu *et al*., 2005); second, the GU- (YGUGUUYY; Y=pyrimidine) or U-rich (UUUU) DSE within 20 nts downstream of the cleavage site (Hart *et al*., 1985, McLauchlan *et al*., 1985, Gil & Proudfoot, 1987, MacDonald *et al*., 1994, Hu *et al*., 2005); and third, the USE with a UGUA sequence, which is positioned 40 to 100 nts upstream of the cleavage site (Hu *et al*., 2005).

In contrast, the yeast signal is somewhat different in both its sequence and organization (Zhao *et al.*, 1999, Mandel *et al.*, 2008). It is less conserved and a minimum three elements are

needed. The UA-efficiency element (UAUAUA) is located at variable distances upstream of the cleavage site and is required for activation of the downstream positioning element. For functioning of the efficiency element, the first and the fifth U are most critical. However, this element only improves the efficiency of the cleavage reaction but is not essential. The A-rich positioning element is located approximately 20 nts upstream of the polyadenylation site and directs the cleavage site position. Mutations in this element disrupt only the position of the cleavage site, but not the efficiency of 3´ end processing, indicating that the function is less critical when compared to its mammalian PAS counterpart. Polyadenylation occurs in most cases at $Y(A)_n$ sequences (Y=pyrimidine) and the polyadenylation site is in comparison to humans less well defined, resulting in polyadenylation site clusters.

In trypanosomes the only known *cis*-acting sequence element is the polypyrimidine tract upstream of a *trans* splice site, which affects polyadenylation of the upstream gene and *trans* splicing of the downstream gene (LeBowitz *et al.*, 1993, Matthews *et al.*, 1994, Benz *et al.*, 2005). The polyadenylation site is similar to yeast (see above) less well defined, resulting in polyadenylation site clusters as well (Siegel *et al.*, 2011). These differences of *cis*-acting polyadenylation elements between trypanosomes, yeast, and mammals raised the question whether the protein factors involved in polyadenylation are correspondingly divergent in trypanosomes. For example, for some mammalian polyadenylation factors, such as CstF50, no counterpart could be identified in yeast (Takagaki & Manley, 1997).

In trypanosomes, only Fip1 and CPSF30 had previously been identified and functionally described so far (Hendriks *et al.*, 2003, Bercovich *et al.*, 2009). Specifically, CPSF30 is required for polycistronic mRNA processing (Hendriks *et al.*, 2003). In addition, the CPSF73 ortholog associates with the U1 snRNP specific U1A protein in trypanosomes (Tkacz *et al.*, 2010). Here we identified eight additional factors as part of the trypanosomatid polyadenylation machinery, based on mass spectrometry and database search: CPSF160, CPSF100, CPSF73, CstF64, CstF50, Symplekin, Tb927.11.13860 and Tb927.8.4480 (see 5.1.4). However, the poly(A) polymerase was not co-purified, which is in line with previous observations, suggesting that the poly(A) polymerase is not tightly associated with other processing factors; instead, there may be a dynamic or transient association with the core polyadenylation complex (Shi *et al.*, 2009). Even if the sequence similarity between these trypanosome polyadenylation factors and their human counterparts is low, they share for the most part their domain architectures. This becomes particularly obvious when comparing the conservation of the subunits of the CPSF complex (see 5.1.4). For example, the CPSF73 subunit, which attracted special attention as the functional endonuclease in the mammalian polyadenylation reaction, shares specific, catalytically important residues with the trypanosome homolog: The zinc-binding residues (mainly histidines) are

conserved in the trypanosomatid CPSF73, indicating that CPSF73 likely also acts as the endonuclease during polyadenylation in trypanosomes (Mandel *et al.*, 2006). Moreover, the domain structures of *T. brucei* CPSF30 and its mammalian homolog are strongly conserved, harboring five C3H1 zinc fingers and a C-terminal C2HC zinc finger. Human CPSF30 (together with WDR33) is required for PAS binding, and it was shown that CPSF30 binds poly(U) sequences *in vitro* (Barabino *et al.*, 1997, Chan *et al.*, 2014, Schönemann *et al.*, 2014, Shimberg *et al.*, 2016). These *in vitro* binding properties for poly(U) sequences were observed for trypanosomatid CPSF30 in our SELEX-seq experiment as well, arguing for similar RNA-binding properties of both proteins (see 5.1.5).

Some of the new trypanosome factors display only low sequence conservation. The putative trypanosome CstF64 strikingly differs from the human counterpart (compare the molecular masses of 14 kDa vs. 64 kDa for the *T. brucei* and the human CstF64, respectively) and could only be identified through a putative hinge domain required for CstF64 interaction with CstF77 and Symplekin (Takagaki & Manley, 2000, Ruepp *et al.*, 2011b). The otherwise conserved N-terminal RRM domain, however, is completely missing in trypanosomes. Therefore the trypanosomatid CstF64 may have retained only and function as a scaffolding protein required for the recruitment of other 3´ end processing factors. Moreover, we cannot exclude that the functions have been moved to another, still unknown factor or may be not essential in trypanosomes anymore.

Finally, some known mammalian polyadenylation factors could be identified neither in our mass spectrometry approach nor through extensive database homology search: As an example, we did not find a trypanosome homolog of WDR33, a subunit of the CPSF complex. Independent studies had recently identified WDR33 as the factor that together with CPSF30 recognizes the AAUAAA polyadenylation signal (Chan *et al.*, 2014, Schönemann *et al.*, 2014, Shimberg *et al.*, 2016). Since trypanosomes lack the classical hexameric polyadenylation signal, this appears plausible. In sum, our results argue for a general conservation of polyadenylation factors among eukaryotes.

6.4 Linkage of polyadenylation and *trans* splicing

Depletion of the individual factors of the polyadenylation complex identified in our study showed severe growth defects and inhibition of polyadenylation in most cases (see 5.1.6). Interestingly, the two hypothetical proteins, Tb927.11.13860 and Tb927.8.4480, of which no known homolog or conserved domain structure could be identified, activate or repress polyadenylation, respectively. Such effects have been described in higher eukaryotes for factors that are not constituents of the core polyadenylation complex, but are required for regulation of

polyadenylation. As an example, 14-3-3ε interacts directly with the C-terminus of the poly(A) polymerase and inhibits the polyadenylation activity, whereas the transcription activator GAL4 stimulates polyadenylation via an interaction with PAF1c (Kim *et al.*, 2003, Nagaike *et al.*, 2011). In addition, we observed *trans* splicing defects consistent with close coupling of both mRNA processing reactions in trypanosomes. Interestingly, we did not detect for all factors effects on polyadenylation and *trans* splicing: For example, knockdown of cleavage factor I m25 (CFIm25) neither affected poly(A) tail length nor splicing. In higher eukaryotes CFIm25 is involved in the regulation of alternative polyadenylation, especially in the repression of proximal polyadenylation sites leading to longer 3´ UTRs (Gruber *et al.*, 2012). Since alternative polyadenylation is common in trypanosomes as well, CFIm25 identified here, which also contains a NUDIX domain required for USE binding in humans, is a potential regulator of this process (Kolev *et al.*, 2010, Siegel *et al.*, 2010, Yang *et al.*, 2010).

In other eukaryotes, a direct linkage between spliceosomal and 3´ end processing components had been demonstrated by several studies (Vagner *et al.*, 2000, Kyburz *et al.*, 2006, Millevoi *et al.*, 2006). For example, U2AF65, which binds the polypyrimidine tract during splicing, interacts with CFIm59 (via an arginine-serine-rich region in both proteins) and stimulates 3´ end cleavage and polyadenylation. Moreover, the poly(A) polymerase interacts with U2AF65 and increases the binding affinity of the latter one to the polypyrimidine tract, which in turn enhances splicing. In addition, the U2 snRNP interacts via SF3b with the CPSF complex, and CPSF stimulates splicing, whereas the U2 snRNP activates mRNA cleavage. In trypanosomes, so far only the polypyrimidine tract is known to affect *trans* splicing and polyadenylation of two adjacent genes (LeBowitz *et al.*, 1993, Matthews *et al.*, 1994, Benz *et al.*, 2005). Until recently no factor could be identified, which directly links the polyadenylation complex and the *trans*-spliceosome in trypanosomes. This is in line with our result that no known spliceosomal factor co-purified with CPSF160. However, a recent study provided first evidence that the polyadenylation factor CPSF73 copurifies with the U1A protein, a specific component of the spliceosomal U1 snRNP (Tkacz *et al.*, 2010). The U1A protein was previously shown to autoregulate its own expression by binding of two U1A proteins to its own mRNA, regulating poly(A) polymerase activity in higher eukaryotes (Gunderson *et al.*, 1994). In addition, the U1A protein interacts with CPSF160 and can generally stimulate polyadenylation (Lutz *et al.*, 1996). Moreover, the whole U1 snRNP can inhibit polyadenylation due to an interaction between U1-70K and the poly(A) polymerase and is also involved in blocking cryptic polyadenylation signals in introns, thereby preventing premature cleavage and polyadenylation (Gunderson *et al.*, 1998, Kaida *et al.*, 2010, Berg *et al.*, 2012). Note that the spliceosomal U1 snRNP was thought to be required only for *cis* splicing, not for *trans* splicing in trypanosomes. However, we recently reported that the U1 snRNP may also

associate with the *trans*-spliceosome, indicating a physical linkage between *cis*- and *trans*-splicing (Preußer *et al.*, 2014). Taken together this suggests that the U1 snRNP functions in both splicing and polyadenylation in trypanosomes, likely linking both processes as described for other eukaryotes before.

6.5 Characterization of the DRBD4 RNA binding motif

We initially characterized *in vivo* RNA binding of DRBD4 by iCLIP, which demonstrated a strong preference for UTR regions (see 5.2.1). Earlier studies had mapped DRBD3, a close paralog of DRBD4, in 3´ UTR regions, underlining the important regulatory role of gene UTRs (Das *et al.*, 2015). The DRBD4 RNA-binding motif was further evaluated by *in vitro* SELEX-seq, followed by GST pulldown assays of short transcripts for validation: The DRBD4 RNA-binding motif is purine-, especially adenosine-rich, containing AUGA elements (see 5.2.2). In contrast, polypyrimidine stretches were depleted during the SELEX rounds of selection.

This was surprising, because human PTB binds, as indicated by the name, polypyrimidine stretches: First, two studies identified UCUUC and CUCUCU RNA-binding motifs, and second, follow-up experiments identified the RNA-binding motif of each RRM with four different consensus motifs (RRM1: YCU; RRM2: CU(N)N, RRM3: YCUNN, RRM4: YCN (1995, Perez *et al.*, 1997, Oberstrass *et al.*, 2005, Reid *et al.*, 2009). Third, *in vivo* CLIP delineated a UYUYU consensus motif for PTB (Xue *et al.*, 2009). In addition, a PTB-like, pyrimidine-rich binding motif had been identified for the second PTB homolog in trypanosomes, DRBD3 (Das *et al.*, 2015).

However, one has to consider that the sequence homology between DRBD4 and PTB is low and subtle changes in amino acids involved in RNA binding may change specificity (Maris *et al.*, 2005)

6.6 DRBD4-dependent poly(A) site choice

In trypanosomes gene expression is controlled mainly by post-transcriptional mechanisms (Clayton, 2014). Recent genome-wide approaches showed that most genes contain several *trans* splice and polyadenylation sites, indicating that the regulation of both processes provides another, still not very well explored level of post-transcriptional gene regulation in trypanosomes (Kolev *et al.*, 2010, Nilsson *et al.*, 2010, Siegel *et al.*, 2010, Veitch *et al.*, 2010).

We focussed on DRBD4 binding upstream of activated and repressed polyadenylation sites, as an attempt to derive a predictive map for this factor. Our results provide evidence for a regulatory role of DRBD4 in poly(A) site choice in *T. brucei* (see 5.2.3 and 5.2.4), although we cannot recognize distinct features of DRBD4 binding sites or positioning that would associate with poly(A) site activation versus repression. Position-dependent effects on alternative splicing have been described for splicing regulators in humans (Rossbach *et al.*, 2014): hnRNP L binds

at repressed exons preferential upstream of the 3´ splice site (peak at position -40), whereas hnRNP L activates exon splicing when bound in the intron further downstream of the 5´ splice site (positions +25 to +200). In sum, it was proposed that hnRNP L represses 3´ splice sites by blocking the recognition of the polypyrimidine tract and 3´ splice site region, and activates 5´ splice sites from downstream intronic positions.

However, in case of DRBD4-regulated polyadenylation additional protein factors may be required, or there are distinctive changes in the sequence elements involved. Interestingly, among the DRBD4-associated proteins we found several constituents of the trypanosomatid polyadenylation complex (CPSF160, CPSF100, CPSF73, CstF50 and Symplekin) including the functional poly(A) polymerase [Tb927.7.3780] (see 5.2.5). Moreover, trypanosomatid PABP2 the homolog of human PABPN1, which stimulates the poly(A) polymerase for efficient polyadenylation and also regulates APA, was co-purified (Wahle, 1991a, Bienroth *et al.*, 1993, Wahle, 1995b, Janal *et al*., 2012). The association of DRBD4 and PABP2 may provide a first protein factor that could be involved in a combinatorial regulation of polyadenylation as observed for human PTB (see below).

However, further analyses are required to characterize the biochemical mechanisms and protein interactions involved in DRBD4-dependent regulation of polyadenylation. The repression of a polyadenylation site, as observed for a cryptic site in the 3´ UTR of Tb927.2.6000 (see 5.2.4) can be mediated in principle by blocking the assembly of single or multiple constituents of the polyadenylation complex. As an example, PTB and CstF64 can compete for binding to the downstream GU/U-rich sequence element (Castelo-Branco *et al.*, 2004). In addition, it was reported that the U1 snRNP can block cryptic polyadenylation signals in introns, thereby preventing premature cleavage and polyadenylation (Kaida *et al.*, 2010, Berg *et al.*, 2012). Stimulatory effects on polyadenylation site choice, as observed in case of the gene Tb927.11.5440 (see 5.2.4), may be caused by recruitment of polyadenylation complex constituents like CstF or the poly(A) polymerase or by directly stimulating poly(A) polymerase activity as observed for PTB (Millevoi *et al.*, 2009).

6.7 Alternative polyadenylation in *T. brucei*

In other eukaryotes, alternative polyadenylation is often associated with proliferation and cellular differentiation (Elkon *et al.*, 2013). For example, activation of T-cell proliferation is linked to proximal poly(A) site usage as well as general shortening of 3´ UTRs in cancer cells (Sandberg *et al.*, 2008, Mayr & Bartel, 2009, Lin *et al.*, 2012, Morris *et al.*, 2012). Most likely this correlates with the deletion of binding sites for miRNAs or *trans*-acting proteins that can negatively affect mRNA stability or translation efficiency. Moreover, many tissues show a specific bias in poly(A)

site choice, for instance a preference for distal poly(A) sites in brain and nervous system (Zhang *et al.*, 2005). In procyclic trypanosomes, mainly the distal of the two polyadenylation sites in the transcript of Tb927.11.5440 (malic enzyme) is used, resulting in an almost exclusive expression of the long mRNA isoform: Upon DRBD4 depletion, the distal poly(A) site is down-regulated, whereas the proximal one is up-regulated, causing a shift to the short isoform (see 5.2.4). Interestingly, in the bloodstream form, the opposite can be observed, that the short Tb927.11.5440 isoform is predominantly expressed (see 5.2.4). In addition, a previous study showed that expression of Tb927.11.5440 is developmentally regulated, with malic enzyme levels higher in the procyclic than the bloodstream form (Leroux *et al.*, 2011). Therefore the DRBD4-dependent poly(A) site choice and isoform expression in procyclic cells may be directly linked to differential regulation of developmental genes in the trypanosomatid life-cycle.

6.8 Further perspectives

Here we initially identified the functional poly(A) polymerase (see 5.1.1, 5.1.2 and 5.1.3) and the constituents of the polyadenylation complex in *T. brucei* (see 5.1.4). Moreover, we could show that depletion of most polyadenylation factors impaired both polyadenylation and *trans* splicing *in vivo*, arguing for close coupling of these processes (see 5.1.6).

However, further work is required to study the polyadenylation complex in trypanosomes in more details. For example, RNA binding of the complex remains still elusive, since the canonical *cis*-acting elements (PAS and DSE) and the WDR33 protein, which directly binds the PAS, are missing in trypanosomes (Proudfoot, 2011, Chan *et al.*, 2014, Schönemann *et al.*, 2014). Moreover, trypanosomatid CstF64 lacks the N-terminal RRM required for DSE recognition and was only identified through a putative hinge domain (see 5.1.4) (Takagaki *et al.*, 1992, MacDonald *et al.*, 1994, Takagaki & Manley, 1997, Perez Canadillas & Varani, 2003). Most likely the best candidate to analyze RNA binding of the *T. brucei* polyadenylation complex is CPSF30, since the mammalian protein is involved in PAS binding and the domain structure is highly conserved between the human and the trypanosomatid proteins (Chan *et al.*, 2014, Schönemann *et al.*, 2014, Shimberg *et al.*, 2016). We initially identified a poly(U) *in vitro* binding motif for *T. brucei* CPSF30 in our SELEX-seq experiment, which was also observed for the mammalian protein (Barabino *et al.*, 1997). However, this motif needs to be further analyzed biochemically by GST pulldown experiments of various RNA transcripts. To generally investigate *in vivo* RNA binding of the polyadenylation complex, CPSF30 iCLIP experiments can be used, and correlated with poly(A) sites identified in various RNA-seq datasets.

CPSF73 is the endonuclease in the cleavage and polyadenylation reaction and the domain structures of both the human and the trypanosomatid proteins are highly conserved, including the zinc-binding residues (mainly histidines), which are required for cleavage activity (Mandel *et al.*, 2006). To assay the trypanosomatid protein for cleavage activity, CPSF73 can be recombinantly expressed, purified and tested for *in vitro* cleavage. In addition, the conserved residues for zinc-binding can be mutated to further analyze the catalytic mechanism.

Moreover, the protein-protein interactions between the identified factors of the *T. brucei* polyadenylation complex remain elusive, but they have been well characterized for the mammalian system (see 3.3) (Chan *et al.*, 2011, Xiang *et al.*, 2014). Since the domain structures of most mammalian and trypanosomatid proteins are highly conserved (see 5.1.4) it appears likely that the interaction between the proteins is conserved as well. Indeed, the interaction between Fip1 and CPSF30 has been described in both trypanosomes and mammals (Bercovich *et al.*, 2009, Kaufmann *et al.*, 2004). To further identify the protein-protein interactions in the trypanosomatid polyadenylation complex, the factors can be recombinantly expressed, purified and tested for *in vitro* binding in pulldown experiments.

Furthermore, we identified the trypanosomatid PTB homolog DRBD4 as first *trans*-acting regulator of polyadenylation. DRBD4 binds upstream of regulated polyadenylation sites, has a purine, in particular adenosine, -rich binding motif and is required for both activation and repression of polyadenylation sites affecting general transcript and isoform expression levels (see 5.2.1, 5.2.2, 5.2.3 and 5.2.4).

To further analyze the DRBD4 RNA-binding motif and address the influence of single RRMs, truncated versions of the protein lacking individual RRMs can be recombinantly expressed and used in both SELEX-seq and pulldown assays.

We analyzed the DRBD4-dependent poly(A) site choice only in procyclic trypanosomes and have evidence for a life-cycle-dependent regulation, as observed for the differential isoform expression of Tb927.11.5440 (malic enzyme). For further characterization of a life-cycle-dependent regulation, DRBD4 binding sites need to be identified in the bloodstream form by iCLIP and correlated with poly(A) site choice after DRBD4 depletion or overexpression.

Another putative regulator of polya(A) site choice is the trypanosomatid CFIm25 homolog, since the mammalian protein is involved in the repression of proximal polyadenylation sites leading to longer 3´ UTRs (Gruber *et al.*, 2012). To assess CFIm25-dependent poly(A) site choice in *T. brucei,* the same combinatorial iCLIP/RNA-seq strategy as applied here can be used.

The cross-regulation between *trans* splicing and polyadenylation is still an open question in trypanosomes. To analyze a *trans* splice-dependent polyadenylation site choice, splicing can be blocked by various methods (knockdown of splicing factors, antisense morpholino

oligonucleotides for against specific snRNAs and Sinefungin treatment) and poly(A) site usage can be assayed by RNA-seq.

7 References

Achcar, F., Kerkhoven, E.J., Barrett, M.P. (2014) *Trypanosoma brucei*: meet the system. *Curr Opin Microbiol* **20**: 162-169.

Agabian, N. (1990) *Trans* splicing of nuclear pre-mRNAs. *Cell* **61**: 1157-1160.

Alsford, S., Turner, D.J., Obado, S.O., Sanchez-Flores, A., Glover, L., Berriman, M., *et al.* (2011) High-throughput phenotyping using parallel sequencing of RNA interference targets in the African trypanosome. *Genome Res* **21**: 915-924.

Altschul, S.F., Gish, W., Miller, W., Myers, E.W., Lipman, D.J. (1990) Basic local alignment search tool. *J Mol Biol* **215**: 403-410.

An, J.J., Gharami, K., Liao, G.Y., Woo, N.H., Lau, A.G., Vanevski, F., *et al.* (2008) Distinct role of long 3´ UTR BDNF mRNA in spine morphology and synaptic plasticity in hippocampal neurons. *Cell* **134**: 175-187.

Anders, S., Huber, W. (2010) Differential expression analysis for sequence count data. *Genome Biol* **11**: 106.

Andrade, M.A., Petosa, C., O'donoghue, S.I., Muller, C.W., Bork, P. (2001) Comparison of ARM and HEAT protein repeats. *J Mol Biol* **309**: 1-18.

Andreassi, C., Riccio, A. (2009) To localize or not to localize: mRNA fate is in 3´ UTR ends. *Trends Cell Biol* **19**: 465-474.

Aslett, M., Aurrecoechea, C., Berriman, M., Brestelli, J., Brunk, B.P., Carrington, M., *et al.* (2010) TriTrypDB: a functional genomic resource for the Trypanosomatidae. *Nucleic Acids Res* **38**: 457-462.

Auweter, S.D., Allain, F.H. (2008) Structure-function relationships of the polypyrimidine tract binding protein. *Cell Mol Life Sci* **65**: 516-527.

Bai, Y., Auperin, T.C., Chou, C.Y., Chang, G.G., Manley, J.L., Tong, L. (2007) Crystal structure of murine CstF-77: dimeric association and implications for polyadenylation of mRNA precursors. *Mol Cell* **25**: 863-875.

Bangs, J.D., Crain, P.F., Hashizume, T., Mccloskey, J.A., Boothroyd, J.C. (1992) Mass spectrometry of mRNA cap 4 from trypanosomatids reveals two novel nucleosides. *J Biol Chem* **267**: 9805-9815.

Barabino, S.M., Hubner, W., Jenny, A., Minvielle-Sebastia, L., Keller, W. (1997) The 30-kD subunit of mammalian cleavage and polyadenylation specificity factor and its yeast homolog are RNA-binding zinc finger proteins. *Genes Dev* **11**: 1703-1716.

Beaudoing, E., Freier, S., Wyatt, J.R., Claverie, J.M., Gautheret, D. (2000) Patterns of variant polyadenylation signal usage in human genes. *Genome Res* **10**: 1001-1010.

Benz, C., Nilsson, D., Andersson, B., Clayton, C.E., Guilbride, D.L. (2005) Messenger RNA processing sites in *Trypanosoma brucei*. *Mol Biochem Parasitol* **143**: 125-134.

Bercovich, N., Levin, M.J., Vazquez, M.P. (2009) The FIP-1 like polyadenylation factor in trypanosomes and the structural basis for its interaction with CPSF30. *Biochem Biophys Res Commun* **380**: 850-855.

Berg, M.G., Singh, L.N., Younis, I., Liu, Q., Pinto, A.M., Kaida, D., *et al.* (2012) U1 snRNP determines mRNA length and regulates isoform expression. *Cell* **150**: 53-64.

Berriman, M., Ghedin, E., Hertz-Fowler, C., Blandin, G., Renauld, H., Bartholomeu, D.C., *et al.* (2005) The genome of the African trypanosome *Trypanosoma brucei*. *Science* **309**: 416-422.

Bienroth, S., Keller, W., Wahle, E. (1993) Assembly of a processive messenger RNA polyadenylation complex. *EMBO J* **12**: 585-594.

Bienroth, S., Wahle, E., Suter-Crazzolara, C., Keller, W. (1991) Purification of the cleavage and polyadenylation factor involved in the 3'-processing of messenger RNA precursors. *J Biol Chem* **266**: 19768-19776.

Bolivar, F., Rodriguez, R.L., Greene, P.J., Betlach, M.C., Heyneker, H.L., Boyer, H.W., *et al.* (1977) Construction and characterization of new cloning vehicles. II. A multipurpose cloning system. *Gene* **2**: 95-113.

Boothroyd, J.C., Cross, G.A. (1982) Transcripts coding for variant surface glycoproteins of *Trypanosoma brucei* have a short, identical exon at their 5´ end. *Gene* **20**: 281-289.

Brawerman, G. (1981) The Role of the poly(A) sequence in mammalian messenger RNA. *CRC Crit Rev Biochem* **10**: 1-38.

Brown, S.J., Stoilov, P., Xing, Y. (2012) Chromatin and epigenetic regulation of pre-mRNA processing. *Hum Mol Genet* **21**: 90-96.

Callebaut, I., Moshous, D., Mornon, J.P., De Villartay, J.P. (2002) Metallo-beta-lactamase fold within nucleic acids processing enzymes: the beta-CASP family. *Nucleic Acids Res* **30**: 3592-3601.

Castelo-Branco, P., Furger, A., Wollerton, M., Smith, C., Moreira, A., Proudfoot, N. (2004) Polypyrimidine tract binding protein modulates efficiency of polyadenylation. *Mol Cell Biol* **24**: 4174-4183.

Chan, S., Choi, E.A., Shi, Y. (2011) Pre-mRNA 3´-end processing complex assembly and function. *Wiley Interdiscip Rev RNA* **2**: 321-335.

Chan, S.L., Huppertz, I., Yao, C., Weng, L., Moresco, J.J., Yates, J.R., 3rd, *et al.* (2014) CPSF30 and WDR33 directly bind to AAUAAA in mammalian mRNA 3´ processing. *Genes Dev* **28**: 2370-2380.

Christofori, G., Keller, W. (1988) 3´ cleavage and polyadenylation of mRNA precursors *in vitro* requires a poly(A) polymerase, a cleavage factor, and a snRNP. *Cell* **54**: 875-889.

Clayton, C.E. (2013) The regulation of trypanosome gene expression by RNA-binding proteins. *PLoS Pathog* **9**: e1003680.

Clayton, C.E., Estevez, A. (2011) The exosomes of trypanosomes and other protists. *Adv Exp Med Biol* **702**: 39-49.

Clayton, C.E., Shapira, M. (2007) Post-transcriptional regulation of gene expression in trypanosomes and leishmanias. *Mol Biochem Parasitol* **156**: 93-101.

Clayton, C.E. (2014) Networks of gene expression regulation in *Trypanosoma brucei*. *Mol Biochem Parasitol* **2**: 96-106.

Colgan, D.F., Manley, J.L. (1997) Mechanism and regulation of mRNA polyadenylation. *Genes Dev* **11**: 2755-2766.

Coseno, M., Martin, G., Berger, C., Gilmartin, G., Keller, W., Doublie, S. (2008) Crystal structure of the 25 kDa subunit of human cleavage factor Im. *Nucleic Acids Res* **36**: 3474-3483.

Cowley, M., Wood, A.J., Bohm, S., Schulz, R., Oakey, R.J. (2012) Epigenetic control of alternative mRNA processing at the imprinted Herc3/Nap1l5 locus. *Nucleic Acids Res* **40**: 8917-8926.

Dantonel, J.C., Murthy, K.G., Manley, J.L., Tora, L. (1997) Transcription factor TFIID recruits factor CPSF for formation of 3´ end of mRNA. *Nature* **389**: 399-402.

Das, A., Bellofatto, V., Rosenfeld, J., Carrington, M., Romero-Zaliz, R., Del Val, C*., et al.* (2015) High throughput sequencing analysis of *Trypanosoma brucei* DRBD3/PTB1-bound mRNAs. *Mol Biochem Parasitol* **199**: 1-4.

Das, A., Zhang, Q., Palenchar, J.B., Chatterjee, B., Cross, G.A., Bellofatto, V. (2005) Trypanosomal TBP functions with the multisubunit transcription factor tSNAP to direct spliced-leader RNA gene expression. *Mol Cell Biol* **25**: 7314-7322.

Davis, R., Shi, Y. (2014) The polyadenylation code: a unified model for the regulation of mRNA alternative polyadenylation. *J Zhejiang Univ Sci B* **15**: 429-437.

De Gaudenzi, J., Frasch, A.C., Clayton, C.E. (2005) RNA-binding domain proteins in Kinetoplastids: a comparative analysis. *Eukaryot Cell* **4**: 2106-2114.

De Vries, H., Ruegsegger, U., Hubner, W., Friedlein, A., Langen, H., Keller, W. (2000) Human pre-mRNA cleavage factor II(m) contains homologs of yeast proteins and bridges two other cleavage factors. *EMBO J* **19**: 5895-5904.

Delhi, P., Queiroz, R., Inchaustegui, D., Carrington, M., Clayton, C.E. (2011) Is there a classical nonsense-mediated decay pathway in trypanosomes? *PLoS One* **6**: e25112.

Dettwiler, S., Aringhieri, C., Cardinale, S., Keller, W., Barabino, S.M. (2004) Distinct sequence motifs within the 68-kDa subunit of cleavage factor Im mediate RNA binding, protein-protein interactions, and subcellular localization. *J Biol Chem* **279**: 35788-35797.

Dominski, Z. (2007) Nucleases of the metallo-beta-lactamase family and their role in DNA and RNA metabolism. *Crit Rev Biochem Mol Biol* **42**: 67-93.

Droll, D., Minia, I., Fadda, A., Singh, A., Stewart, M., Queiroz, R., *et al.* (2013) Post-transcriptional regulation of the trypanosome heat shock response by a zinc finger protein. *PLoS Pathog* **9**: e1003286.

Edmonds, M. (1990) Polyadenylate polymerases. *Methods Enzymol* **181**: 161-170.

El-Sayed, N.M., Myler, P.J., Blandin, G., Berriman, M., Crabtree, J., Aggarwal, G*., et al.* (2005) Comparative genomics of trypanosomatid parasitic protozoa. *Science* **309**: 404-409.

Elkon, R., Drost, J., Van Haaften, G., Jenal, M., Schrier, M., Oude Vrielink, J.A., *et al.* (2012) E2F mediates enhanced alternative polyadenylation in proliferation. *Genome Biol* **13**: R59.

Elkon, R., Ugalde, A.P., Agami, R. (2013) Alternative cleavage and polyadenylation: extent, regulation and function. *Nat Rev Genet* **14**: 496-506.

Erben, E., Chakraborty, C., Clayton, C.E. (2014) The CAF1-NOT complex of trypanosomes. *Front Genet* **4**: 299.

Estevez, A.M. (2008) The RNA-binding protein TbDRBD3 regulates the stability of a specific subset of mRNAs in trypanosomes. *Nucleic Acids Res* **36**: 4573-4586.

Fabian, M.R., Sonenberg, N., Filipowicz, W. (2010) Regulation of mRNA translation and stability by microRNAs. *Annu Rev Biochem* **79**: 351-379.

Farber, V., Erben, E., Sharma, S., Stoecklin, G., Clayton, C.E. (2013) Trypanosome CNOT10 is essential for the integrity of the NOT deadenylase complex and for degradation of many mRNAs. *Nucleic Acids Res* **41**: 1211-1222.

Fernandez-Moya, S.M., Garcia-Perez, A., Kramer, S., Carrington, M., Estevez, A.M. (2012) Alterations in DRBD3 ribonucleoprotein complexes in response to stress in *Trypanosoma brucei*. *PLoS One* **7**: e48870.

Fiebig, M., Gluenz, E., Carrington, M., Kelly, S. (2014) SLaP mapper: a webserver for identifying and quantifying spliced-leader addition and polyadenylation site usage in kinetoplastid genomes. *Mol Biochem Parasitol* **196**: 71-74.

Fred, R.G., Welsh, N. (2009) The importance of RNA binding proteins in preproinsulin mRNA stability. *Mol Cell Endocrinol* **297**: 28-33.

Gassen, A., Brechtefeld, D., Schandry, N., Arteaga-Salas, J.M., Israel, L., Imhof, A., *et al.* (2012) DOT1A-dependent H3K76 methylation is required for replication regulation in *Trypanosoma brucei*. *Nucleic Acids Res* **40**: 10302-10311.

Ghosh, A., Lima, C.D. (2010) Enzymology of RNA cap synthesis. *Wiley Interdiscip Rev RNA* **1**: 152-172.

Gil, A., Proudfoot, N.J. (1987) Position-dependent sequence elements downstream of AAUAAA are required for efficient rabbit beta-globin mRNA 3´ end formation. *Cell* **49**: 399-406.

Gilmartin, G.M., Nevins, J.R. (1989) An ordered pathway of assembly of components required for polyadenylation site recognition and processing. *Genes Dev* **3**: 2180-2190.

Gilmartin, G.M., Nevins, J.R. (1991) Molecular analyses of two poly(A) site-processing factors that determine the recognition and efficiency of cleavage of the pre-mRNA. *Mol Cell Biol* **11**: 2432-2438.

Gooding, C., Roberts, G.C., Smith, C.W. (1998) Role of an inhibitory pyrimidine element and polypyrimidine tract binding protein in repression of a regulated alpha-tropomyosin exon. *RNA* **4**: 85-100.

Gross, S., Moore, C. (2001) Five subunits are required for reconstitution of the cleavage and polyadenylation activities of *Saccharomyces cerevisiae* cleavage factor I. *Proc Natl Acad Sci U S A* **98**: 6080-6085.

Gruber, A.R., Martin, G., Keller, W., Zavolan, M. (2012) Cleavage factor Im is a key regulator of 3´ UTR length. *RNA Biol* **9**: 1405-1412.

Gunderson, S.I., Beyer, K., Martin, G., Keller, W., Boelens, W.C., Mattaj, L.W. (1994) The human U1A snRNP protein regulates polyadenylation via a direct interaction with poly(A) polymerase. *Cell* **76**: 531-541.

Gunderson, S.I., Polycarpou-Schwarz, M., Mattaj, I.W. (1998) U1 snRNP inhibits pre-mRNA polyadenylation through a direct interaction between U1 70K and poly(A) polymerase. *Mol Cell* **1**: 255-264.

Günzl, A. (2010) The pre-mRNA splicing machinery of trypanosomes: complex or simplified? *Eukaryot Cell* **9**: 1159-1170.

Gupta, S.K., Kosti, I., Plaut, G., Pivko, A., Tkacz, I.D., Cohen-Chalamish, S., *et al.* (2013) The hnRNP F/H homologue of *Trypanosoma brucei* is differentially expressed in the two life cycle stages of the parasite and regulates splicing and mRNA stability. *Nucleic Acids Res* **41**: 6577-6594.

Haile, S., Papadopoulou, B. (2007) Developmental regulation of gene expression in trypanosomatid parasitic protozoa. *Current Opinion in Microbiology* **10**: 569-577.

Han, S.P., Tang, Y.H., Smith, R. (2010) Functional diversity of the hnRNPs: past, present and perspectives. *Biochem J* **430**: 379-392.

Hang, J., Wan, R., Yan, C., Shi, Y. (2015) Structural basis of pre-mRNA splicing. *Science* **349**: 1191-1198.

Hart, R.P., Mcdevitt, M.A., Ali, H., Nevins, J.R. (1985) Definition of essential sequences and functional equivalence of elements downstream of the adenovirus E2A and the early simian virus 40 polyadenylation sites. *Mol Cell Biol* **5**: 2975-2983.

Hassan, A.H., Prochasson, P., Neely, K.E., Galasinski, S.C., Chandy, M., Carrozza, M.J., *et al.* (2002) Function and selectivity of bromodomains in anchoring chromatin-modifying complexes to promoter nucleosomes. *Cell* **111**: 369-379.

Hastings, K.E. (2005) SL *trans*-splicing: easy come or easy go? *Trends Genet* **21**: 240-247.

Hendriks, E.F., Abdul-Razak, A., Matthews, K.R. (2003) tbCPSF30 depletion by RNA interference disrupts polycistronic RNA processing in *Trypanosoma brucei*. *J Biol Chem* **278**: 26870-26878.

Higgs, D.R., Goodbourn, S.E., Lamb, J., Clegg, J.B., Weatherall, D.J., Proudfoot, N.J. (1983) Alpha-thalassaemia caused by a polyadenylation signal mutation. *Nature* **306**: 398-400.

Hirose, Y., Manley, J.L. (1998) RNA polymerase II is an essential mRNA polyadenylation factor. *Nature* **395**: 93-96.

Hockert, J.A., Yeh, H.J., Macdonald, C.C. (2010) The hinge domain of the cleavage stimulation factor protein CstF-64 is essential for CstF-77 interaction, nuclear localization, and polyadenylation. *J Biol Chem* **285**: 695-704.

Hofmann, I., Schnolzer, M., Kaufmann, I., Franke, W.W. (2002) Symplekin, a constitutive protein of karyo- and cytoplasmic particles involved in mRNA biogenesis in *Xenopus laevis* oocytes. *Mol Biol Cell* **13**: 1665-1676.

Houseley, J., Tollervey, D. (2009) The many pathways of RNA degradation. *Cell* **136**: 763-776.

Hu, J., Lutz, C.S., Wilusz, J.Tian, B. (2005) Bioinformatic identification of candidate *cis*-regulatory elements involved in human mRNA polyadenylation. *RNA* **11**: 1485-1493.

Huang, J., Van Der Ploeg, L.H. (1991a) Maturation of polycistronic pre-mRNA in *Trypanosoma brucei*: analysis of *trans* splicing and poly(A) addition at nascent RNA transcripts from the hsp70 locus. *Mol Cell Biol* **11**: 3180-3190.

Huang, J., Van Der Ploeg, L.H. (1991b) Requirement of a polypyrimidine tract for *trans*-splicing in trypanosomes: discriminating the PARP promoter from the immediately adjacent 3´ splice acceptor site. *EMBO J* **10**: 3877-3885.

Hui, J., Bindereif, A. (2005) Alternative pre-mRNA splicing in the human system: unexpected role of repetitive sequences as regulatory elements. *Biol Chem* **386**: 1265-1271.

Hull, M.W., Erickson, J., Johnston, M., Engelke, D.R. (1994) tRNA genes as transcriptional repressor elements. *Mol Cell Biol* **14**: 1266-1277.

Ito, S., Sakai, A., Nomura, T., Miki, Y., Ouchida, M., Sasaki, J., *et al.* (2001) A novel WD40 repeat protein, WDC146, highly expressed during spermatogenesis in a stage-specific manner. *Biochem Biophys Res Commun* **280**: 656-663.

Izquierdo, J.M., Majos, N., Bonnal, S., Martinez, C., Castelo, R., Guigo, R., *et al.* (2005) Regulation of Fas alternative splicing by antagonistic effects of TIA-1 and PTB on exon definition. *Mol Cell* **19**: 475-484.

Jenal, M., Elkon, R., Loayza-Puch, F., Van Haaften, G., Kuhn, U., Menzies, F.M., *et al.* (2012) The poly(A)-binding protein nuclear 1 suppresses alternative cleavage and polyadenylation sites. *Cell* **149**: 538-553.

Jenny, A., Minvielle-Sebastia, L., Preker, P.J., Keller, W. (1996) Sequence similarity between the 73-kilodalton protein of mammalian CPSF and a subunit of yeast polyadenylation factor I. *Science* **274**: 1514-1517.

Jin, C., Felsenfeld, G. (2007) Nucleosome stability mediated by histone variants H3.3 and H2A.Z. *Genes Dev* **21**: 1519-1529.

Johnson, P.J., Kooter, J.M., Borst, P. (1987) Inactivation of transcription by UV irradiation of *T. brucei* provides evidence for a multicistronic transcription unit including a VSG gene. *Cell* **51**: 273-281.

Jones, P., Binns, D., Chang, H.Y., Fraser, M., Li, W., Mcanulla, C.*, et al.* (2014) InterProScan 5: genome-scale protein function classification. *Bioinformatics* **30**: 1236-1240.

Kaida, D., Berg, M.G., Younis, I., Kasim, M., Singh, L.N., Wan, L.*, et al.* (2010) U1 snRNP protects pre-mRNAs from premature cleavage and polyadenylation. *Nature* **468**: 664-668.

Kaufmann, I., Martin, G., Friedlein, A., Langen, H., Keller, W. (2004) Human Fip1 is a subunit of CPSF that binds to U-rich RNA elements and stimulates poly(A) polymerase. *EMBO J* **23**: 616-626.

Keller, R.W., Kuhn, U., Aragon, M., Bornikova, L., Wahle, E., Bear, D.G. (2000) The nuclear poly(A) binding protein, PABP2, forms an oligomeric particle covering the length of the poly(A) tail. *J Mol Biol* **297**: 569-583.

Kennedy, S.A., Frazier, M.L., Steiniger, M., Mast, A.M., Marzluff, W.F., Redinbo, M.R. (2009) Crystal structure of the HEAT domain from the pre-mRNA processing factor Symplekin. *J Mol Biol* **392**: 115-128.

Kerwitz, Y., Kuhn, U., Lilie, H., Knoth, A., Scheuermann, T., Friedrich, H., *et al.* (2003) Stimulation of poly(A) polymerase through a direct interaction with the nuclear poly(A) binding protein allosterically regulated by RNA. *EMBO J* **22**: 3705-3714.

Kibbe, W.A. (2007) OligoCalc: an online oligonucleotide properties calculator. *Nucleic Acids Res* **35**: 43-46.

Kim, H., Lee, J.H., Lee, Y. (2003) Regulation of poly(A) polymerase by 14-3-3epsilon. *EMBO J* **22**: 5208-5219.

Kim, S., Yamamoto, J., Chen, Y., Aida, M., Wada, T., Handa, H., *et al.* (2010) Evidence that cleavage factor Im is a heterotetrameric protein complex controlling alternative polyadenylation. *Genes Cells* **15**: 1003-1013.

Knoch, K.P., Bergert, H., Borgonovo, B., Saeger, H.D., Altkruger, A., Verkade, P., *et al.* (2004) Polypyrimidine tract-binding protein promotes insulin secretory granule biogenesis. *Nat Cell Biol* **6**: 207-214.

Kohler, A., Hurt, E. (2007) Exporting RNA from the nucleus to the cytoplasm. *Nat Rev Mol Cell Biol* **8**: 761-773.

Kolev, N.G., Franklin, J.B., Carmi, S., Shi, H., Michaeli, S., Tschudi, C. (2010) The transcriptome of the human pathogen *Trypanosoma brucei* at single-nucleotide resolution. *PLoS Pathog* **6**: e1001090.

Kolev, N.G., Ullu, E., Tschudi, C. (2014) The emerging role of RNA-binding proteins in the life cycle of *Trypanosoma brucei*. *Cell Microbiol* **4**: 482-489.

Kramer, S. (2012) Developmental regulation of gene expression in the absence of transcriptional control: The case of kinetoplastids. *Mol Biochem Parasitol* **181**: 61-72.

Kramer, S., Carrington, M. (2011) *Trans*-acting proteins regulating mRNA maturation, stability and translation in trypanosomatids. *Trends Parasitol* **27**: 23-30.

Kuehner, J.N., Pearson, E.L., Moore, C. (2011) Unravelling the means to an end: RNA polymerase II transcription termination. *Nat Rev Mol Cell Biol* **12**: 283-294.

Kuhn, U., Gundel, M., Knoth, A., Kerwitz, Y., Rudel, S., Wahle, E. (2009) Poly(A) tail length is controlled by the nuclear poly(A)-binding protein regulating the interaction between poly(A) polymerase and the cleavage and polyadenylation specificity factor. *J Biol Chem* **284**: 22803-22814.

Kurowski, M.A., Bujnicki, J.M. (2003) GeneSilico protein structure prediction meta-server. *Nucleic Acids Res* **31**: 3305-3307.

Kyburz, A., Friedlein, A., Langen, H., Keller, W. (2006) Direct interactions between subunits of CPSF and the U2 snRNP contribute to the coupling of pre-mRNA 3' end processing and splicing. *Mol Cell* **23**: 195-205.

Lackford, B., Yao, C., Charles, G.M., Weng, L., Zheng, X., Choi, E.A., *et al.* (2014) Fip1 regulates mRNA alternative polyadenylation to promote stem cell self-renewal. *EMBO J* **33**: 878-889.

Laemmli, U.K. (1970) Cleavage of structural proteins during the assembly of the head of bacteriophage T4. *Nature* **227**: 680-685.

Lamichhane, R., Daubner, G.M., Thomas-Crusells, J., Auweter, S.D., Manatschal, C., Austin, K.S., *et al.* (2010) RNA looping by PTB: Evidence using FRET and NMR spectroscopy for a role in splicing repression. *Proc Natl Acad Sci U S A* **107**: 4105-4110.

Lau, A.G., Irier, H.A., Gu, J., Tian, D., Ku, L., Liu, G., *et al.* (2010) Distinct 3´ UTRs differentially regulate activity-dependent translation of brain-derived neurotrophic factor (BDNF). *Proc Natl Acad Sci U S A* **107**: 15945-15950.

Lebowitz, J.H., Smith, H.Q., Rusche, L., Beverley, S.M. (1993) Coupling of poly(A) site selection and *trans*-splicing in Leishmania. *Genes Dev* **7**: 996-1007.

Lee, J.H., Jung, H.S., Günzl, A. (2009) Transcriptionally active TFIIH of the early-diverged eukaryote *Trypanosoma brucei* harbors two novel core subunits but not a cyclin-activating kinase complex. *Nucleic Acids Res* **37**: 3811-3820.

Lee, J.H., Nguyen, T.N., Schimanski, B., Günzl, A. (2007) Spliced leader RNA gene transcription in *Trypanosoma brucei* requires transcription factor TFIIH. *Eukaryot Cell* **6**: 641-649.

Lee, Y., Rio, D.C. (2015) Mechanisms and regulation of alternative pre-mRNA splicing. *Annu Rev Biochem* **84**: 291-323.

Lejon, V., Bentivoglio, M., Franco, J.R. (2013) Human African trypanosomiasis. *Handb Clin Neurol* **114**: 169-181.

Leroux, A.E., Maugeri, D.A., Opperdoes, F.R., Cazzulo, J.J., Nowicki, C. (2011) Comparative studies on the biochemical properties of the malic enzymes from *Trypanosoma cruzi* and *Trypanosoma brucei*. *FEMS Microbiol Lett* **314**: 25-33.

Li, H., Tong, S., Li, X., Shi, H., Ying, Z., Gao, Y., *et al.* (2011) Structural basis of pre-mRNA recognition by the human cleavage factor Im complex. *Cell Res* **21**: 1039-1051.

Li, W., Yeh, H.J., Shankarling, G.S., Ji, Z., Tian, B., Macdonald, C.C. (2012) The tauCstF-64 polyadenylation protein controls genome expression in testis. *PLoS One* **7**: e48373.

Liang, X.H., Haritan, A., Uliel, S., Michaeli, S. (2003) *trans* and *cis* splicing in trypanosomatids: mechanism, factors, and regulation. *Eukaryot Cell* **2**: 830-840.

Lin, Y., Li, Z., Ozsolak, F., Kim, S.W., Arango-Argoty, G., Liu, T.T., *et al.* (2012) An in-depth map of polyadenylation sites in cancer. *Nucleic Acids Res* **40**: 8460-8471.

Liu, H., Zhang, W., Reed, R.B., Liu, W., Grabowski, P.J. (2002) Mutations in RRM4 uncouple the splicing repression and RNA-binding activities of polypyrimidine tract binding protein. *RNA* **8**: 137-149.

Luo, H., Gilinger, G., Mukherjee, D., Bellofatto, V. (1999) Transcription initiation at the TATA-less spliced leader RNA gene promoter requires at least two DNA-binding proteins and a tripartite architecture that includes an initiator element. *J Biol Chem* **274**: 31947-31954.

Lutz, C.S., Murthy, K.G., Schek, N., O'connor, J.P., Manley, J.L., Alwine, J.C. (1996) Interaction between the U1 snRNP-A protein and the 160-kD subunit of cleavage-polyadenylation specificity factor increases polyadenylation efficiency *in vitro*. *Genes Dev* **10**: 325-337.

Macdonald, C.C., Wilusz, J., Shenk, T. (1994) The 64-kilodalton subunit of the CstF polyadenylation factor binds to pre-mRNAs downstream of the cleavage site and influences cleavage site location. *Mol Cell Biol* **14**: 6647-6654.

Mair, G., Shi, H., Li, H., Djikeng, A., Aviles, H.O., Bishop, J.R., *et al.* (2000) A new twist in trypanosome RNA metabolism: *cis*-splicing of pre-mRNA. *RNA* **6**: 163-169.

Malvy, D., Chappuis, F. (2011) Sleeping sickness. *Clin Microbiol Infect* **17**: 986-995.

Mandel, C.R., Bai, Y., Tong, L. (2008) Protein factors in pre-mRNA 3´-end processing. *Cell Mol Life Sci* **65**: 1099-1122.

Mandel, C.R., Kaneko, S., Zhang, H., Gebauer, D., Vethantham, V., Manley, J.L., *et al.* (2006) Polyadenylation factor CPSF-73 is the pre-mRNA 3´-end-processing endonuclease. *Nature* **444**: 953-956.

Manful, T., Fadda, A., Clayton, C.E. (2011) The role of the 5´-3´ exoribonuclease XRNA in transcriptome-wide mRNA degradation. *RNA* **17**: 2039-2047.

Maris, C., Dominguez, C., Allain, F.H. (2005) The RNA recognition motif, a plastic RNA-binding platform to regulate post-transcriptional gene expression. *FEBS J* **272**: 2118-2131.

Markovtsov, V., Nikolic, J.M., Goldman, J.A., Turck, C.W., Chou, M.Y., Black, D.L. (2000) Cooperative assembly of an hnRNP complex induced by a tissue-specific homolog of polypyrimidine tract binding protein. *Mol Cell Biol* **20**: 7463-7479.

Martin, G., Gruber, A.R., Keller, W., Zavolan, M. (2012) Genome-wide analysis of pre-mRNA 3´ end processing reveals a decisive role of human cleavage factor I in the regulation of 3´ UTR length. *Cell Rep* **1**: 753-763.

Martin, G., Jeno, P., Keller, W. (1999) Mapping of ATP binding regions in poly(A) polymerases by photoaffinity labeling and by mutational analysis identifies a domain conserved in many nucleotidyltransferases. *Protein Sci* **8**: 2380-2391.

Martin, G., Keller, W. (1996) Mutational analysis of mammalian poly(A) polymerase identifies a region for primer binding and catalytic domain, homologous to the family X polymerases, and to other nucleotidyltransferases. *EMBO J* **15**: 2593-2603.

Martin, G., Keller, W., Doublie, S. (2000) Crystal structure of mammalian poly(A) polymerase in complex with an analog of ATP. *EMBO J* **19**: 4193-4203.

Martinez-Calvillo, S., Yan, S., Nguyen, D., Fox, M., Stuart, K., Myler, P.J. (2003) Transcription of *Leishmania major* Friedlin chromosome 1 initiates in both directions within a single region. *Mol Cell* **11**: 1291-1299.

Marzluff, W.F., Wagner, E.J., Duronio, R.J. (2008) Metabolism and regulation of canonical histone mRNAs: life without a poly(A) tail. *Nat Rev Genet* **9**: 843-854.

Matera, A.G., Wang, Z. (2014) A day in the life of the spliceosome. *Nat Rev Mol Cell Biol* **15**: 108-121.

Matthews, K.R., Tschudi, C., Ullu, E. (1994) A common pyrimidine-rich motif governs *trans*-splicing and polyadenylation of tubulin polycistronic pre-mRNA in trypanosomes. *Genes Dev* **8**: 491-501.

Maynard, C.M., Hall, K.B. (2010) Interactions between PTB RRMs induce slow motions and increase RNA binding affinity. *J Mol Biol* **397**: 260-277.

Mayr, C., Bartel, D.P. (2009) Widespread shortening of 3´ UTRs by alternative cleavage and polyadenylation activates oncogenes in cancer cells. *Cell* **138**: 673-684.

Mccracken, S., Fong, N., Yankulov, K., Ballantyne, S., Pan, G., Greenblatt, J., *et al.* (1997) The C-terminal domain of RNA polymerase II couples mRNA processing to transcription. *Nature* **385**: 357-361.

Mclauchlan, J., Gaffney, D., Whitton, J.L., Clements, J.B. (1985) The consensus sequence YGTGTTYY located downstream from the AATAAA signal is required for efficient formation of mRNA 3´ termini. *Nucleic Acids Res* **13**: 1347-1368.

Merrick, W.C. (2010) Eukaryotic protein synthesis: still a mystery. *J Biol Chem* **285**: 21197-21201.

Michalski, D., Steiniger, M. (2015) *In vivo* characterization of the Drosophila mRNA 3´ end processing core cleavage complex. *RNA* **21**: 1404-1418.

Migchelsen, S.J., Buscher, P., Hoepelman, A.I., Schallig, H.D., Adams, E.R. (2011) Human African trypanosomiasis: a review of non-endemic cases in the past 20 years. *Int J Infect Dis* **15**: 517-524.

Millevoi, S., Decorsiere, A., Loulergue, C., Iacovoni, J., Bernat, S., Antoniou, M., *et al.* (2009) A physical and functional link between splicing factors promotes pre-mRNA 3´ end processing. *Nucleic Acids Res* **37**: 4672-4683.

Millevoi, S., Loulergue, C., Dettwiler, S., Karaa, S.Z., Keller, W., Antoniou, M., *et al.* (2006) An interaction between U2AF 65 and CF I(m) links the splicing and 3´ end processing machineries. *EMBO J* **25**: 4854-4864.

Millevoi, S., Vagner, S. (2010) Molecular mechanisms of eukaryotic pre-mRNA 3´ end processing regulation. *Nucleic Acids Res* **38**: 2757-2774.

Milone, J., Wilusz, J.Bellofatto, V. (2002) Identification of mRNA decapping activities and an ARE-regulated 3´ to 5´ exonuclease activity in trypanosome extracts. *Nucleic Acids Res* **30**: 4040-4050.

Morris, A.R., Bos, A., Diosdado, B., Rooijers, K., Elkon, R., Bolijn, A.S., *et al.* (2012) Alternative cleavage and polyadenylation during colorectal cancer development. *Clin Cancer Res* **18**: 5256-5266.

Murthy, K.G., Manley, J.L. (1992) Characterization of the multisubunit cleavage-polyadenylation specificity factor from calf thymus. *J Biol Chem* **267**: 14804-14811.

Murthy, K.G., Manley, J.L. (1995) The 160-kD subunit of human cleavage-polyadenylation specificity factor coordinates pre-mRNA 3´-end formation. *Genes Dev* **9**: 2672-2683.

Nag, A., Narsinh, K., Martinson, H.G. (2007) The poly(A)-dependent transcriptional pause is mediated by CPSF acting on the body of the polymerase. *Nat Struct Mol Biol* **14**: 662-669.

Nagaike, T., Logan, C., Hotta, I., Rozenblatt-Rosen, O., Meyerson, M., Manley, J.L. (2011) Transcriptional activators enhance polyadenylation of mRNA precursors. *Mol Cell* **41**: 409-418.

Nemeth, A., Krause, S., Blank, D., Jenny, A., Jeno, P., Lustig, A., *et al.* (1995) Isolation of genomic and cDNA clones encoding bovine poly(A) binding protein II. *Nucleic Acids Res* **23**: 4034-4041.

Neuwald, A.F., Poleksic, A. (2000) PSI-BLAST searches using hidden markov models of structural repeats: prediction of an unusual sliding DNA clamp and of beta-propellers in UV-damaged DNA-binding protein. *Nucleic Acids Res* **28**: 3570-3580.

Ni, J.Z., Grate, L., Donohue, J.P., Preston, C., Nobida, N., O'brien, G., *et al.* (2007) Ultraconserved elements are associated with homeostatic control of splicing regulators by alternative splicing and nonsense-mediated decay. *Genes Dev* **21**: 708-718.

Nilsson, D., Gunasekera, K., Mani, J., Osteras, M., Farinelli, L., Baerlocher, L., *et al.* (2010) Spliced leader trapping reveals widespread alternative splicing patterns in the highly dynamic transcriptome of *Trypanosoma brucei*. *PLoS Pathog* **6**: e1001037.

Norbury, C.J. (2013) Cytoplasmic RNA: a case of the tail wagging the dog. *Nat Rev Mol Cell Biol* **14**: 643-653.

Oberstrass, F.C., Auweter, S.D., Erat, M., Hargous, Y., Henning, A., Wenter, P., *et al.* (2005) Structure of PTB bound to RNA: specific binding and implications for splicing regulation. *Science* **309**: 2054-2057.

Orkin, S.H., Cheng, T.C., Antonarakis, S.E., Kazazian, H.H., Jr. (1985) Thalassemia due to a mutation in the cleavage-polyadenylation signal of the human beta-globin gene. *EMBO J* **4**: 453-456.

Palenchar, J.B., Bellofatto, V. (2006) Gene transcription in trypanosomes. *Mol Biochem Parasitol* **146**: 135-141.

Patel, A.A., Steitz, J.A. (2003) Splicing double: insights from the second spliceosome. *Nat Rev Mol Cell Biol* **4**: 960-970.

Pauws, E., Van Kampen, A.H., Van De Graaf, S.A., De Vijlder, J.J., Ris-Stalpers, C. (2001) Heterogeneity in polyadenylation cleavage sites in mammalian mRNA sequences: implications for SAGE analysis. *Nucleic Acids Res* **29**: 1690-1694.

Perez Canadillas, J.M., Varani, G. (2003) Recognition of GU-rich polyadenylation regulatory elements by human CstF-64 protein. *EMBO J* **22**: 2821-2830.

Perez, I., Lin, C.H., Mcafee, J.G., Patton, J.G. (1997) Mutation of PTB binding sites causes misregulation of alternative 3´ splice site selection *in vivo*. *RNA* **3**: 764-778.

Pfaffl, M.W. (2001) A new mathematical model for relative quantification in real-time RT-PCR. *Nucleic Acids Res* **29**: 45.

Pinto, P.A., Henriques, T., Freitas, M.O., Martins, T., Domingues, R.G., Wyrzykowska, P.S., *et al.* (2011) RNA polymerase II kinetics in polo polyadenylation signal selection. *EMBO J* **30**: 2431-2444.

Preker, P.J., Keller, W. (1998) The HAT helix, a repetitive motif implicated in RNA processing. *Trends Biochem Sci* **23**: 15-16.

Preußer, C., Jae, N., Bindereif, A. (2012) mRNA splicing in trypanosomes. *Int J Med Microbiol* **302**: 221-224.

Preußer, C., Jae, N., Günzl, A., Bindereif, A. (2012) RNA Metabolism in Trypanosomes. *Springer-Verlag*.

Preußer, C., Rossbach, O., Hung, L.H., Li, D., Bindereif, A. (2014) Genome-wide RNA-binding analysis of the trypanosome U1 snRNP proteins U1C and U1-70K reveals *cis*/*trans*-spliceosomal network. *Nucleic Acids Res* **42**: 6603-6615.

Proudfoot, N.J. (2011) Ending the message: poly(A) signals then and now. *Genes Dev* **25**: 1770-1782.

Qu, X., Perez-Canadillas, J.M., Agrawal, S., De Baecke, J., Cheng, H., Varani, G., *et al.* (2007) The C-terminal domains of vertebrate CstF-64 and its yeast orthologue Rna15 form a new structure critical for mRNA 3´-end processing. *J Biol Chem* **282**: 2101-2115.

Raabe, T., Bollum, F.J., Manley, J.L. (1991) Primary structure and expression of bovine poly(A) polymerase. *Nature* **353**: 229-234.

Raabe, T., Murthy, K.G., Manley, J.L. (1994) Poly(A) polymerase contains multiple functional domains. *Mol Cell Biol* **14**: 2946-2957.

Rahman, L., Bliskovski, V., Reinhold, W., Zajac-Kaye, M. (2002) Alternative splicing of brain-specific PTB defines a tissue-specific isoform pattern that predicts distinct functional roles. *Genomics* **80**: 245-249.

Ray, D., Kazan, H., Chan, E.T., Pena Castillo, L., Chaudhry, S., Talukder, S., *et al.* (2009) Rapid and systematic analysis of the RNA recognition specificities of RNA-binding proteins. *Nat Biotechnol* **27**: 667-670.

Reid, D.C., Chang, B.L., Gunderson, S.I., Alpert, L., Thompson, W.A., Fairbrother, W.G. (2009) Next-generation SELEX identifies sequence and structural determinants of splicing factor binding in human pre-mRNA sequence. *RNA* **15**: 2385-2397.

Rettig, J., Wang, Y., Schneider, A., Ochsenreiter, T. (2012) Dual targeting of isoleucyl-tRNA synthetase in *Trypanosoma brucei* is mediated through alternative *trans*-splicing. *Nucleic Acids Res* **40**: 1299-1306.

Reynolds, D., Hofmeister, B.T., Cliffe, L., Alabady, M., Siegel, T.N., Schmitz, R.J., *et al.* (2016) Histone H3 variant regulates RNA polymerase II transcription termination and dual strand transcription of siRNA Loci in *Trypanosoma brucei*. *PLoS Genet* **12**: e1005758.

Robinson, J.T., Thorvaldsdottir, H., Winckler, W., Guttman, M., Lander, E.S., Getz, G., *et al.* (2011) Integrative genomics viewer. *Nat Biotechnol* **29**: 24-26.

Romanelli, M.G., Diani, E., Lievens, P.M. (2013) New insights into functional roles of the polypyrimidine tract-binding protein. *Int J Mol Sci* **14**: 22906-22932.

Rossbach, O., Hung, L.H., Khrameeva, E., Schreiner, S., König, J., Curk, T., *et al.* (2014) Crosslinking-immunoprecipitation (iCLIP) analysis reveals global regulatory roles of hnRNP L. *RNA Biology* **11**: 146-155.

Rozen, S., Skaletsky, H. (2000) Primer3 on the WWW for general users and for biologist programmers. *Methods Mol Biol* **132**: 365-386.

Ruan, J.P., Arhin, G.K., Ullu, E., Tschudi, C. (2004) Functional characterization of a *Trypanosoma brucei* TATA-binding protein-related factor points to a universal regulator of transcription in trypanosomes. *Mol Cell Biol* **24**: 9610-9618.

Rüegsegger, U., Beyer, K., Keller, W. (1996) Purification and characterization of human cleavage factor Im involved in the 3´ end processing of messenger RNA precursors. *J Biol Chem* **271**: 6107-6113.

Rüegsegger, U., Blank, D., Keller, W. (1998) Human pre-mRNA cleavage factor Im is related to spliceosomal SR proteins and can be reconstituted *in vitro* from recombinant subunits. *Mol Cell* **1**: 243-253.

Ruepp, M.D., Aringhieri, C., Vivarelli, S., Cardinale, S., Paro, S., Schümperli, D., *et al.* (2009) Mammalian pre-mRNA 3´ end processing factor CF I m 68 functions in mRNA export. *Mol Biol Cell* **20**: 5211-5223.

Ruepp, M.D., Schümperli, D., Barabino, S.M. (2011a) mRNA 3´ end processing and more-multiple functions of mammalian cleavage factor I-68. *Wiley Interdiscip Rev RNA* **2**: 79-91.

Ruepp, M.D., Schweingruber, C., Kleinschmidt, N., Schümperli, D. (2011b) Interactions of CstF-64, CstF-77, and symplekin: implications on localisation and function. *Mol Biol Cell* **22**: 91-104.

Sandberg, R., Neilson, J.R., Sarma, A., Sharp, P.A., Burge, C.B. (2008) Proliferating cells express mRNAs with shortened 3´ untranslated regions and fewer microRNA target sites. *Science* **320**: 1643-1647.

Schimanski, B., Brandenburg, J., Nguyen, T.N., Caimano, M.J., Günzl, A. (2006) A TFIIB-like protein is indispensable for spliced leader RNA gene transcription in *Trypanosoma brucei*. *Nucleic Acids Res* **34**: 1676-1684.

Schimanski, B., Nguyen, T.N., Günzl, A. (2005a) Characterization of a multisubunit transcription factor complex essential for spliced-leader RNA gene transcription in *Trypanosoma brucei*. *Mol Cell Biol* **25**: 7303-7313.

Schimanski, B., Nguyen, T.N., Günzl, A. (2005b) Highly efficient tandem affinity purification of trypanosome protein complexes based on a novel epitope combination. *Eukaryot Cell* **4**: 1942-1950.

Schneider, C.A., Rasband, W.S., Eliceiri, K.W. (2012) NIH Image to ImageJ: 25 years of image analysis. *Nat Methods* **9**: 671-675.

Schönemann, L., Kuhn, U., Martin, G., Schafer, P., Gruber, A.R., Keller, W., *et al.* (2014) Reconstitution of CPSF active in polyadenylation: recognition of the polyadenylation signal by WDR33. *Genes Dev* **28**: 2381-2393.

Schrader, M., Reuber, B.E., Morrell, J.C., Jimenez-Sanchez, G., Obie, C., Stroh, T.A., *et al.* (1998) Expression of PEX11beta mediates peroxisome proliferation in the absence of extracellular stimuli. *J Biol Chem* **273**: 29607-29614.

Schulz, D., Zaringhalam, M., Papavasiliou, F.N., Kim, H.S. (2016) Base J and H3.V regulate transcriptional termination in *Trypanosoma brucei*. *PLoS Genet* **12**: e1005762.

Schwede, A., Ellis, L., Luther, J., Carrington, M., Stoecklin, G., Clayton, C.E. (2008) A role for Caf1 in mRNA deadenylation and decay in trypanosomes and human cells. *Nucleic Acids Res* **36**: 3374-3388.

Schwede, A., Manful, T., Jha, B.A., Helbig, C., Bercovich, N., Stewart, M., *et al.* (2009) The role of deadenylation in the degradation of unstable mRNAs in trypanosomes. *Nucleic Acids Res* **37**: 5511-5528.

Schweingruber, C., Rufener, S.C., Zund, D., Yamashita, A., Muhlemann, O. (2013) Nonsense-mediated mRNA decay - mechanisms of substrate mRNA recognition and degradation in mammalian cells. *Biochim Biophys Acta* **1829**: 612-623.

Scrima, A., Konickova, R., Czyzewski, B.K., Kawasaki, Y., Jeffrey, P.D., Groisman, R., *et al.* (2008) Structural basis of UV DNA-damage recognition by the DDB1-DDB2 complex. *Cell* **135**: 1213-1223.

Shankarling, G.S., Macdonald, C.C. (2013) Polyadenylation site-specific differences in the activity of the neuronal betaCstF-64 protein in PC-12 cells. *Gene* **529**: 220-227.

Sharp, P.A. (1994) Split genes and RNA splicing. *Cell* **77**: 805-815.

Sheets, M.D., Ogg, S.C., Wickens, M.P. (1990) Point mutations in AAUAAA and the poly (A) addition site: effects on the accuracy and efficiency of cleavage and polyadenylation *in vitro*. *Nucleic Acids Res* **18**: 5799-5805.

Shepard, P.J., Hertel, K.J. (2009) The SR protein family. *Genome Biol* **10**: 242.

Shi, H., Djikeng, A., Mark, T., Wirtz, E., Tschudi, C., Ullu, E. (2000) Genetic interference in *Trypanosoma brucei* by heritable and inducible double-stranded RNA. *RNA* **6**: 1069-1076.

Shi, Y. (2012) Alternative polyadenylation: new insights from global analyses. *RNA* **18**: 2105-2117.

Shi, Y., Di Giammartino, D.C., Taylor, D., Sarkeshik, A., Rice, W.J., Yates, J.R., 3rd, *et al.* (2009) Molecular architecture of the human pre-mRNA 3´ processing complex. *Mol Cell* **33**: 365-376.

Shimberg, G.D., Michalek, J.L., Oluyadi, A.A., Rodrigues, A.V., Zucconi, B.E., Neu, H.M., *et al.* (2016) Cleavage and polyadenylation specificity factor 30: An RNA-binding zinc-finger protein with an unexpected 2Fe-2S cluster. *Proc Natl Acad Sci U S A* **113**: 4700-4705

Siegel, T.N., Gunasekera, K., Cross, G.A., Ochsenreiter, T. (2011) Gene expression in *Trypanosoma brucei*: lessons from high-throughput RNA sequencing. *Trends Parasitol* **27**: 434-441.

Siegel, T.N., Hekstra, D.R., Kemp, L.E., Figueiredo, L.M., Lowell, J.E., Fenyo, D., *et al.* (2009) Four histone variants mark the boundaries of polycistronic transcription units in *Trypanosoma brucei*. *Genes Dev* **23**: 1063-1076.

Siegel, T.N., Hekstra, D.R., Wang, X., Dewell, S., Cross, G.A. (2010) Genome-wide analysis of mRNA abundance in two life-cycle stages of *Trypanosoma brucei* and identification of splicing and polyadenylation sites. *Nucleic Acids Res* **38**: 4946-4957.

Singh, A., Minia, I., Droll, D., Fadda, A., Clayton, C.E., Erben, E. (2014) Trypanosome MKT1 and the RNA-binding protein ZC3H11: interactions and potential roles in post-transcriptional regulatory networks. *Nucleic Acids Res* **42**: 4652-4668.

Smibert, P., Miura, P., Westholm, J.O., Shenker, S., May, G., Duff, M.O., *et al.* (2012) Global patterns of tissue-specific alternative polyadenylation in *Drosophila*. *Cell Rep* **1**: 277-289.

Spellman, R., Rideau, A., Matlin, A., Gooding, C., Robinson, F., Mcglincy, N., *et al.* (2005) Regulation of alternative splicing by PTB and associated factors. *Biochem Soc Trans* **33**: 457-460.

Stern, M.Z., Gupta, S.K., Salmon-Divon, M., Haham, T., Barda, O., Levi, S., *et al.* (2009) Multiple roles for polypyrimidine tract binding (PTB) proteins in trypanosome RNA metabolism. *RNA* **15**: 648-665.

Stirnimann, C.U., Petsalaki, E., Russell, R.B., Muller, C.W. (2010) WD40 proteins propel cellular networks. *Trends Biochem Sci* **35**: 565-574.

Stothard, P. (2000) The sequence manipulation suite: JavaScript programs for analyzing and formatting protein and DNA sequences. *Biotechniques* **28**: 1102, 1104.

Sullivan, K.D., Steiniger, M., Marzluff, W.F. (2009) A core complex of CPSF73, CPSF100, and Symplekin may form two different cleavage factors for processing of poly(A) and histone mRNAs. *Mol Cell* **34**: 322-332.

Takagaki, Y., Macdonald, C.C., Shenk, T.Manley, J.L. (1992) The human 64-kDa polyadenylylation factor contains a ribonucleoprotein-type RNA binding domain and unusual auxiliary motifs. *Proc Natl Acad Sci U S A* **89**: 1403-1407.

Takagaki, Y., Manley, J.L. (1992) A human polyadenylation factor is a G protein beta-subunit homologue. *J Biol Chem* **267**: 23471-23474.

Takagaki, Y., Manley, J.L. (1994) A polyadenylation factor subunit is the human homologue of the *Drosophila* suppressor of forked protein. *Nature* **372**: 471-474.

Takagaki, Y., Manley, J.L. (1997) RNA recognition by the human polyadenylation factor CstF. *Mol Cell Biol* **17**: 3907-3914.

Takagaki, Y., Manley, J.L. (1998) Levels of polyadenylation factor CstF-64 control IgM heavy chain mRNA accumulation and other events associated with B cell differentiation. *Mol Cell* **2**: 761-771.

Takagaki, Y., Manley, J.L. (2000) Complex protein interactions within the human polyadenylation machinery identify a novel component. *Mol Cell Biol* **20**: 1515-1525.

Takagaki, Y., Manley, J.L., Macdonald, C.C., Wilusz, J.Shenk, T. (1990) A multisubunit factor, CstF, is required for polyadenylation of mammalian pre-mRNAs. *Genes Dev* **4**: 2112-2120.

Takagaki, Y., Ryner, L.C., Manley, J.L. (1989) Four factors are required for 3´-end cleavage of pre-mRNAs. *Genes Dev* **3**: 1711-1724.

Takagaki, Y., Seipelt, R.L., Peterson, M.L., Manley, J.L. (1996) The polyadenylation factor CstF-64 regulates alternative processing of IgM heavy chain pre-mRNA during B cell differentiation. *Cell* **87**: 941-952.

Thorvaldsdottir, H., Robinson, J.T., Mesirov, J.P. (2013) Integrative Genomics Viewer (IGV): high-performance genomics data visualization and exploration. *Brief Bioinform* **14**: 178-192.

Tian, B., Graber, J.H. (2012) Signals for pre-mRNA cleavage and polyadenylation. *Wiley Interdiscip Rev RNA* **3**: 385-396.

Timmusk, T., Palm, K., Metsis, M., Reintam, T., Paalme, V., Saarma, M., *et al.* (1993) Multiple promoters direct tissue-specific expression of the rat BDNF gene. *Neuron* **10**: 475-489.

Tkacz, I.D., Gupta, S.K., Volkov, V., Romano, M., Haham, T., Tulinski, P., *et al.* (2010) Analysis of spliceosomal proteins in trypanosomatids reveals novel functions in mRNA processing. *J Biol Chem* **285**: 27982-27999.

Tresaugues, L., Stenmark, P., Schuler, H., Flodin, S., Welin, M., Nyman, T., *et al.* (2008) The crystal structure of human cleavage and polyadenylation specific factor-5 reveals a dimeric Nudix protein with a conserved catalytic site. *Proteins* **73**: 1047-1052.

Tschudi, C., Ullu, E. (1990) Destruction of U2, U4, or U6 small nuclear RNA blocks *trans* splicing in trypanosome cells. *Cell* **61**: 459-466.

Ullu, E., Matthews, K.R., Tschudi, C. (1993) Temporal order of RNA-processing reactions in trypanosomes: rapid *trans* splicing precedes polyadenylation of newly synthesized tubulin transcripts. *Mol Cell Biol* **13**: 720-725.

Vagner, S., Vagner, C., Mattaj, I.W. (2000) The carboxyl terminus of vertebrate poly(A) polymerase interacts with U2AF 65 to couple 3´-end processing and splicing. *Genes Dev* **14**: 403-413.

Van Hoof, A., Wagner, E.J. (2011) A brief survey of mRNA surveillance. *Trends Biochem Sci* **36**: 585-592.

Van Luenen, H.G., Farris, C., Jan, S., Genest, P.A., Tripathi, P., Velds, A., *et al.* (2012) Glucosylated hydroxymethyluracil, DNA base J, prevents transcriptional readthrough in Leishmania. *Cell* **150**: 909-921.

Veitch, N.J., Johnson, P.C., Trivedi, U., Terry, S., Wildridge, D., Macleod, A. (2010) Digital gene expression analysis of two life cycle stages of the human-infective parasite, *Trypanosoma brucei gambiense* reveals differentially expressed clusters of co-regulated genes. *BMC Genomics* **11**: 124.

Venkataraman, K., Brown, K.M., Gilmartin, G.M. (2005) Analysis of a noncanonical poly(A) site reveals a tripartite mechanism for vertebrate poly(A) site recognition. *Genes Dev* **19**: 1315-1327.

Wahle, E. (1991a) A novel poly(A)-binding protein acts as a specificity factor in the second phase of messenger RNA polyadenylation. *Cell* **66**: 759-768.

Wahle, E. (1991b) Purification and characterization of a mammalian polyadenylate polymerase involved in the 3´ end processing of messenger RNA precursors. *J Biol Chem* **266**: 3131-3139.

Wahle, E. (1995a) 3´-end cleavage and polyadenylation of mRNA precursors. *Biochim Biophys Acta* **1261**: 183-194.

Wahle, E. (1995b) Poly(A) tail length control is caused by termination of processive synthesis. *J Biol Chem* **270**: 2800-2808.

Wahle, E., Martin, G., Schiltz, E., Keller, W. (1991) Isolation and expression of cDNA clones encoding mammalian poly(A) polymerase. *EMBO J* **10**: 4251-4257.

Wallace, A.M., Dass, B., Ravnik, S.E., Tonk, V., Jenkins, N.A., Gilbert, D.J., *et al.* (1999) Two distinct forms of the 64,000 Mr protein of the cleavage stimulation factor are expressed in mouse male germ cells. *Proc Natl Acad Sci U S A* **96**: 6763-6768.

Wang, Z., Morris, J.C., Drew, M.E., Englund, P.T. (2000) Inhibition of *Trypanosoma brucei* gene expression by RNA interference using an integratable vector with opposing T7 promoters. *J Biol Chem* **275**: 40174-40179.

Webb, H., Burns, R., Ellis, L., Kimblin, N.Carrington, M. (2005a) Developmentally regulated instability of the GPI-PLC mRNA is dependent on a short-lived protein factor. *Nucleic Acids Res* **33**: 1503-1512.

Webb, H., Burns, R., Kimblin, N., Ellis, L.Carrington, M. (2005b) A novel strategy to identify the location of necessary and sufficient *cis*-acting regulatory mRNA elements in trypanosomes. RNA 11: 1108-1116.

West, S., Proudfoot, N.J. (2008) Human Pcf11 enhances degradation of RNA polymerase II-associated nascent RNA and transcriptional termination. *Nucleic Acids Res* **36**: 905-914.

Will, C.L., Lührmann, R. (2011) Spliceosome structure and function. *Cold Spring Harb Perspect Biol* **3**.

Wirtz, E., Leal, S., Ochatt, C., Cross, G.A. (1999) A tightly regulated inducible expression system for conditional gene knock-outs and dominant-negative genetics in *Trypanosoma brucei*. *Mol Biochem Parasitol* **99**: 89-101.

Wollerton, M.C., Gooding, C., Wagner, E.J., Garcia-Blanco, M.A., Smith, C.W. (2004) Autoregulation of polypyrimidine tract binding protein by alternative splicing leading to nonsense-mediated decay. *Mol Cell* **13**: 91-100.

Wood, A.J., Schulz, R., Woodfine, K., Koltowska, K., Beechey, C.V., Peters, J., *et al.* (2008) Regulation of alternative polyadenylation by genomic imprinting. *Genes Dev* **22**: 1141-1146.

Wright, J.R., Siegel, T.N., Cross, G.A. (2010) Histone H3 trimethylated at lysine 4 is enriched at probable transcription start sites in *Trypanosoma brucei*. *Mol Biochem Parasitol* **172**: 141-144.

Xiang, K., Nagaike, T., Xiang, S., Kilic, T., Beh, M.M., Manley, J.L., *et al.* (2010) Crystal structure of the human symplekin-Ssu72-CTD phosphopeptide complex. *Nature* **467**: 729-733.

Xiang, K., Tong, L., Manley, J.L. (2014) Delineating the structural blueprint of the pre-mRNA 3´-end processing machinery. *Mol Cell Biol* **34**: 1894-1910.

Xue, Y., Zhou, Y., Wu, T., Zhu, T., Ji, X., Kwon, Y.S., *et al.* (2009) Genome-wide analysis of PTB-RNA interactions reveals a strategy used by the general splicing repressor to modulate exon inclusion or skipping. *Mol Cell* **36**: 996-1006.

Yang, Q., Coseno, M., Gilmartin, G.M., Doublie, S. (2011) Crystal structure of a human cleavage factor CFI(m)25/CFI(m)68/RNA complex provides an insight into poly(A) site recognition and RNA looping. *Structure* **19**: 368-377.

Yang, Q., Gilmartin, G.M., Doublie, S. (2010) Structural basis of UGUA recognition by the Nudix protein CFI(m)25 and implications for a regulatory role in mRNA 3´ processing. *Proc Natl Acad Sci U S A* **107**: 10062-10067.

Yao, C., Biesinger, J., Wan, J., Weng, L., Xing, Y., Xie, X., *et al.* (2012) Transcriptome-wide analyses of CstF64-RNA interactions in global regulation of mRNA alternative polyadenylation. *Proc Natl Acad Sci U S A* **109**: 18773-18778.

Yao, C., Choi, E.A., Weng, L., Xie, X., Wan, J., Xing, Y., *et al.* (2013) Overlapping and distinct functions of CstF64 and CstF64tau in mammalian mRNA 3´ processing. *RNA* **19**: 1781-1790.

Yu, L., Volkert, M.R. (2013) UV damage regulates alternative polyadenylation of the RPB2 gene in yeast. *Nucleic Acids Res* **41**: 3104-3114.

Zhang, H., Lee, J.Y., Tian, B. (2005) Biased alternative polyadenylation in human tissues. *Genome Biol* **6**: 100.

Zhao, J., Hyman, L., Moore, C. (1999) Formation of mRNA 3´ ends in eukaryotes: mechanism, regulation, and interrelationships with other steps in mRNA synthesis. *Microbiol Mol Biol Rev* **63**: 405-445.

Zhelkovsky, A.M., Kessler, M.M., Moore, C.L. (1995) Structure-function relationships in the *Saccharomyces cerevisiae* poly(A) polymerase. Identification of a novel RNA binding site and a domain that interacts with specificity factor(s). *J Biol Chem* **270**: 26715-26720.

8 Supplementary Information

8.1 Figures and Tables

A

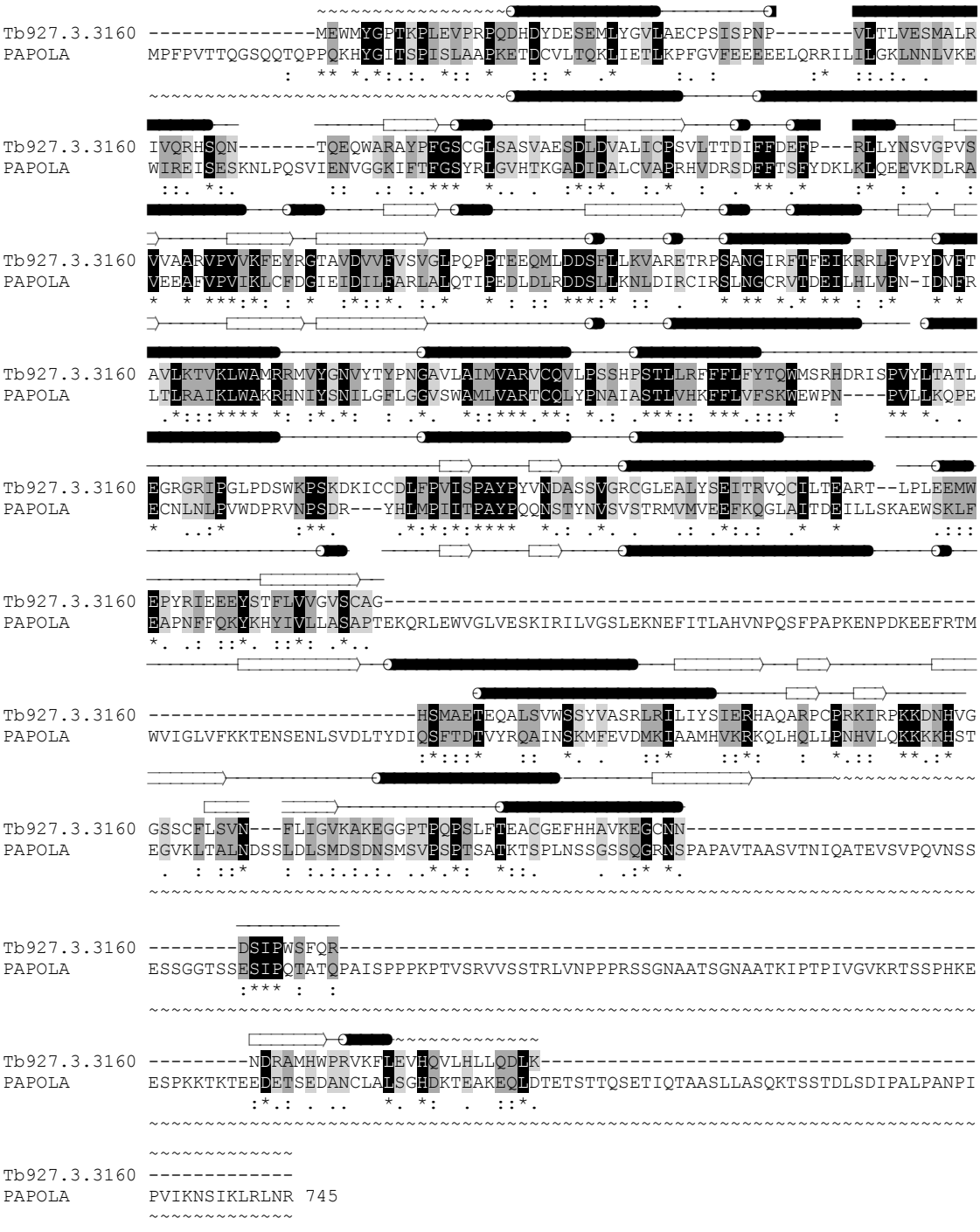

B

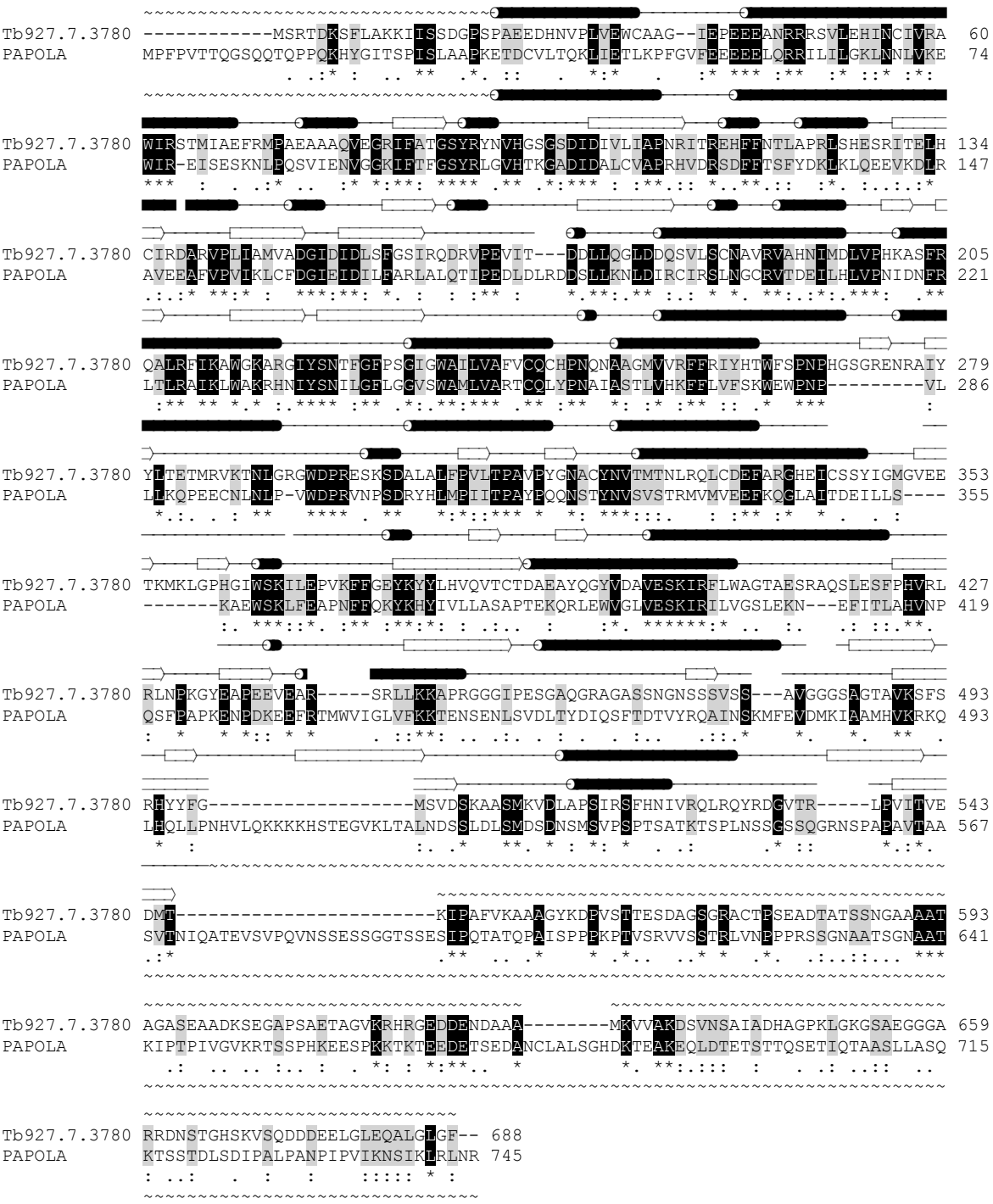

Supplementary Figure 8.1 Alignment of the human poly(A) polymerase (PAPOLA) to the two putative *T. brucei* poly(A) polymerases, (A) Tb927.3.3160, and (B) Tb927.7.3780.

Residues (page 128-129) that are conserved or have a similar physicochemical character in more than 50% of sequences are highlighted in black and gray, respectively. The predicted secondary structures of PAP from *T. brucei* and *H. sapiens* are shown above and below the alignments, respectively. α-helices are represented as tubes, and β-strands as arrows, while disordered regions are shown as "~".

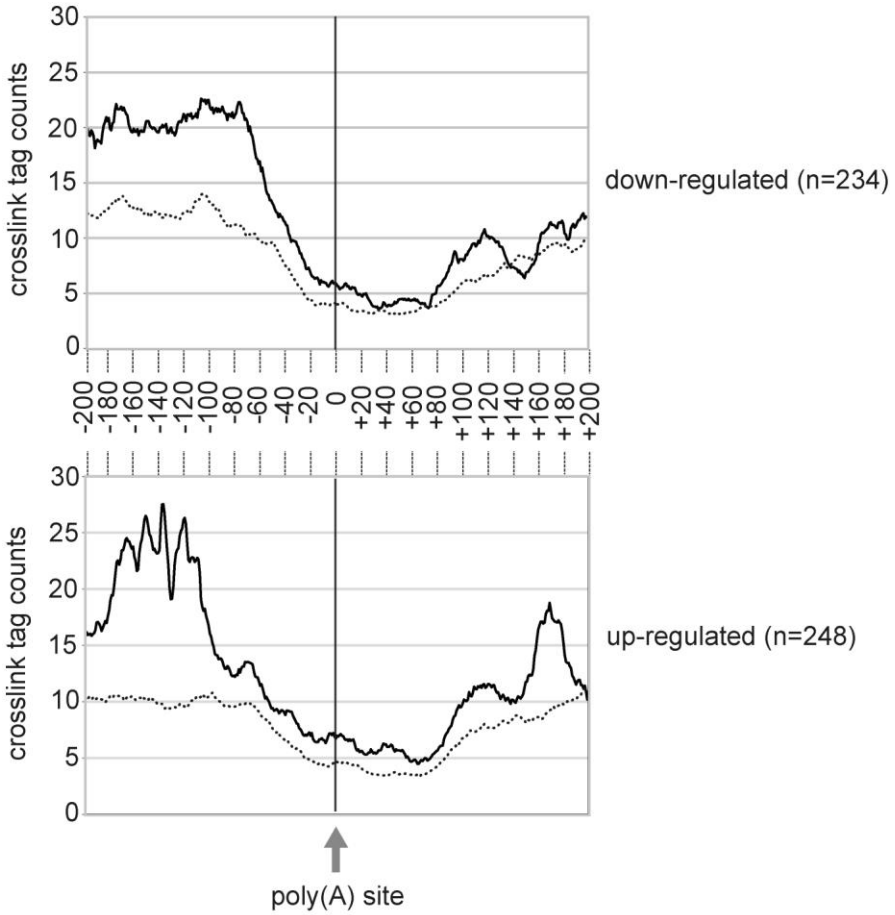

Figure 8.2 DRBD4 RNA binding around regulated poly(A) sites.
Accumulated DRBD4-YFP iCLIP crosslink-tag counts were plotted in the region between -200 to +200 nts relative to the poly(A) site of the down- and up-regulated clusters (top: down-regulated n=234; background n=936; bottom: up-regulated n=248; background n=992) and are depicted as solid lines. As background control, unaffected polyadenylation sites were used (dashed lines). Crosslink-tag counts were plotted with fitted values (21-nts windows) on the Y-axis and positions on the X-axis.

Supplementary Table 8.1 CPSF160-associated proteins identified by mass spectrometry after tandem affinity purification.

Extracts were prepared from *T. brucei* cell lines that stably express tagged CPSF160 (in two biological replicates; experiment 1/2), followed by TAP-tag affinity purification. Proteins after the second purification step (protein C elution) were identified by mass spectrometry. Each protein is described by name (factor), the TriTrypDB annotation number (http://tritrypdb.org/tritrypdb/), its molecular mass (in kDa), the number of exclusive unique peptide counts obtained by mass spectrometry. As control, *T. brucei* wildtype cells were used.

Database Name: the T_brucei database	
Version: unknown	
Taxonomy: All Entries	
Number of Proteins: 38057	
Search Engine Set: 1 Search Engine	
Search Engine: Mascot	
Version: 2.3.02	
Samples: All Samples	
Fragment Tolerance: 0,60 Da (Monoisotopic)	
Parent Tolerance: 10,0 PPM (Monoisotopic)	
Fixed Modifications:	
Variable Modifications: +16 on M (Oxidation), +57 on C (Carbamidomethyl)	
Database: the T_brucei database (unknown version, 38057 entries)	
Digestion Enzyme: Trypsin	
Max Missed Cleavages: 2	
Scaffold: Version: Scaffold_4.4.1.1	
Modification Metadata Set: 1541 modifications	
Comment:	
Protein Grouping Strategy: Experiment-wide grouping with binary peptide-protein weights	
Peptide Thresholds: 95,0% minimum	
Protein Thresholds: 95,0% minimum and 3 peptides minimum	
Peptide FDR: 0,7% (Prophet)	
Protein FDR: 0,0% (Prophet)	

	Displaying: Exclusive Unique Peptide Count						
#	Identified Proteins (51)	Accession Number	Molecular mass (kDa)	ctr (WT)	CPSF160 prot C experiment 1	CPSF160 prot C experiment 2	factor
1	cleavage and polyadenylation specificity factor-like protein	Tb927.11.14560	159	0	83	84	CPSF160
2	hypothetical protein	Tb927.8.7490	158	0	79	76	Symplekin
3	cleavage and polyadenylation specificity factor, putative	Tb927.11.230	91	0	45	42	CPSF100
4	cleavage and polyadenylation specificity factor subunit, putative	Tb927.4.1340	85	0	37	33	CstF50
5	hypothetical protein	Tb927.6.1830	50	0	23	25	CPSF73
6	beta tubulin	Tb927.1.2330	50	10	23	23	
7	alpha tubulin	Tb927.1.2340	50	9	20	20	
8	heat shock protein 70	Tb927.11.11330	71	2	16	19	
9	hypothetical protein	Tb927.11.13860	30	0	15	17	hyp. protein
10	cleavage and polyadenylation specificity factor 30 kDa subunit	Tb927.11.12750	32	0	15	12	CPSF30
11	hypothetical protein	Tb927.8.4480	29	0	15	18	hyp. protein
12	elongation factor 1-alpha, EF-1-alpha (TEF1)	Tb927.10.2100	49	2	13	9	
13	hypothetical protein, conserved	Tb927.5.4320	31	0	9	9	Fip1
14	unspecified product	Tb927.9.5750	22	1	5	3	
15	chaperonin Hsp60, mitochondrial precursor	Tb927.10.6400	60	1	4	5	
16	hypothetical protein	Tb927.8.7490	158	0	3	3	
17	heat shock protein 83, putative	Tb927.10.10890	81	0	3	8	
18	heat shock 70 kDa protein, putative	Tb927.7.710	70	0	3	6	
19	60S acidic ribosomal subunit protein, putative	Tb927.11.2050	35	0	3	2	
20	heat shock 70 kDa protein, mitochondrial precursor, putative	Tb927.6.3740	72	1	2	7	
21	hypothetical protein, conserved	Tb927.8 .8210	15	0	2	5	CstF64
22	actin A	Tb927.9.8850	45	0	2	4	
23	peroxidoxin (TRYP2)	Tb927.8.1990	26	0	2	4	
24	chaperone protein DnaJ, putative	Tb927.2.5160	45	0	2	3	
25	GTP-binding nuclear protein rtb2, putative	Tb927.3.1120	24	0	2	3	
26	glutamine synthetase, putative	Tb927.7.4970	47	0	1	12	
27	40S ribosomal protein S3, putative	Tb927.9.6070	30	0	1	3	
28	40S ribosomal protein S4, putative	Tb927.11.3590	31	0	1	3	
29	t-complex protein 1 gamma subunit, putative	Tb927.8.3150	61	0	1	3	
30	elongation factor 2	Tb10.70.2650	94	2	0	9	
31	glutamate dehydrogenase (GDH)	Tb927.9.5900	112	0	0	10	
32	succinyl-CoA ligase [GDP-forming] beta-chain,putative	Tb927.9.5900	55	2	0	7	
33	enolase	Tb927.10.2890	47	0	0	10	
34	T-complex protein 1, alpha subunit, putative (TCP-1-alpha)	Tb927.11.16760	53	0	0	4	
35	retrotransposon hot spot protein 5 (RHS5), putative	Tb927.2.240	95	0	0	3	
36	ATP-dependent DEAD box helicase, putative, eukaryotic initiation factor 4a, putative	Tb927.9.4680	45	0	0	4	

37	2-amino-3-ketobutyrate coenzyme A ligase,putative	Tb927.8.6060	44	0	0	5		
38	DHH1	Tb927.10.3990	46	0	0	4		
39	hypothetical protein, conserved	Tb927.4.1300	42	0	0	5		
40	phosphoglycerate kinase	Tb927.1.710	45	0	0	5		
41	delta-1-pyrroline-5-carboxylate dehydrogenase,putative	Tb927.10.3210	62	0	0	4		
42	T-complex protein 1, beta subunit, putative	Tb927.11.1900	58	0	0	3		
43	unspecified product	Tb927.9.6230	42	0	0	4		
44	T-complex protein 1, zeta subunit, putative	Tb927.11.3240	60	0	0	3		
45	ATP-dependent DEAD/H RNA helicase, putative	Tb927.10.540	49	0	0	4		
46	cystathionine beta-synthase, putative	Tb11.02.5400	39	0	0	4		
47	chain A, s-adenosyl homocysteine hydrolase (Sahh)	Tb927.11.9590	48	0	0	3		
48	ADP-ribosylation factor-like protein 3A, putative	Tb927.3.3450	20	0	0	3		
49	prostaglandin f synthase	Tb927.11.4700	32	0	0	3		
50	L-threonine 3-dehydrogenase, putative	Tb927.6.2790	37	0	0	3		
51	malic enzyme	Tb927.11.5440	62	0	0	3		

8.2 Abbreviations and Symbols

~	approximately
<	less than
>	more than
+	plus
-	minus
%	percent
×	times
× g	times gravity
°C	degree Celsius
µ	micro
2´	bonds to the C-2 carbon of ribose in nucleic acids
3´	directionality in nucleic acids: in the direction of the C-3 ribose carbon
5´	directionality in nucleic acids: in the direction of the C-5 ribose carbon
α	alpha
β	beta
ε	eplison
γ	gamma
Δ	delta, without / lacking
A	adenosine
aa	amino acids
AcTEV	tobacco etch virus protease
APA	alternative polyadenylation
APS	ammonium persulfate
ARM	armadillo-type fold
As	anti-sense
ATP	adenosine triphosphate
ß-casp	beta-caspase domain
Bdf3	bomodomain factor 3 protein
bp	base pairs
BP	branch point
BSA	bovine serum albumin
C	cytidine
cDNA	complementary DNA
CF	cleavage factor

Ci	Curie
CLIP	cross-linking and immunoprecipitation
CPSF	cleavage and polyadenylation specificity factor
CstF	cleavage stimulation factor
CstF1-dd	cleavage stimulation factor subunit 1, dimerization domain
CstF64-C	cleavage stimulating factor C-terminal domain
C_T	cycle of threshold
CTD	carboxyl-terminal domain of RNA polymerase II
C-terminal	carboxyl-terminal
CTP	cytidine triphosphate
ctr	control
DAPI	4´,6-diamidino-2-phenylindole
dCTP	deoxycytidine triphosphate
DIG	digoxigenin
DMPC	dimethyl pyrocarbonate
DMSO	dimethyl sulfoxide
DNA	deoxyribonucleic acid
dNTP	deoxynucleoside triphosphate
Dox	doxycyclin
DRBD	double-stranded RNA-binding domain
DSE	downstream sequence element
dT	deoxythymidine triphosphate
DTT	dithiothreitol
E. coli	*Escherichia coli*
EDTA	ethylenediaminetetraacetic acid
e.g.	*exempli gratia* (for the sake of example)
EGTA	ethyleneglycoltetraacetic acid
et al.	*et alii* (and others)
f	femto
FBS	fetal bovine serum
fw.	forward (primer)
g	gram
G	guanosine
GST	glutathione S-transferase
GTP	guanosine triphosphate

h	hour(s)
HEPES	N-2-hydroxyethylpiperazine
His	polyhistidine-tag
hnRNP	heterogeneous ribonucleoprotein particle
hPAPOLA	human poly(A) polymerase alpha
HPLC	high-performance liquid chromatography
H. sapiens	*Homo sapiens*
iCLIP	individual-nucleotide resolution cross-linking and immunoprecipitation
IgG	immunoglobulin G
IPTG	isopropyl-β-D-thiogalactopyranosid
k	kilo
kb	kilobases
kd	knockdown
kDa	kilodalton
l	liter
L-	L-confirmation
LB	Luria/Miller
LC-MS/MS	liquid chromatography-tandem mass spectrometry
M	marker
m	milli
M	molar
mA	milliampere
min	minute(s)
miRNA	micro RNA
mRNA	messenger RNA
MS	mass spectrometry
(n)	poly
n	nano
N	random / any nucleotide
NCBI	National center for biotechnology information
NLS	nuclear localization signal
NP-40	Nonidet P-40
nPTB	neuronal polypyrimidine tract binding protein
N-terminal	amino-terminal
nts	nucleotides

NUDIX	NUDIX hydrolase domain
OH	hydroxyl (-group)
ORF	open reading frame
p	pico
P, p	phosphate
PABPN1	nuclear poly(A)-binding protein 1
PAGE	polyacrylamide gel electrophoresis
PAP	poly(A) polymerase
PAS	polyadenylation signal
PBS	phosphate-buffered saline
PCR	polymerase chain reaction
PK	proteinase K
PNK	polynucleotide kinase
Pol II	DNA-dependent RNA-polymerases II
PPIase	prolyl isomerase
PPT	polypyrimidine tract
PRP8	pre-mRNA processing factor 8
PTB	polypyrimidine tract binding protein
PTP	protein C epitope / TEV cleavage site / 2× protein A epitope
PTU	polycistronic transcription unit
PVA	polyvinyl alcohol
®	registered trade mark
RNA	ribonucleic acid
RNAi	RNA interference
RNP	ribonucleoprotein (-particle)
RRM	RNA recognition motif
rRNA	ribosomal RNA
RT	reverse transcription
RT-qPCR	quantitative RT-PCR
Rv.	reverse (primer)
S	Svedberg; sedimentation coefficient
SAP	shrimp alkaline phosphatase
SDS	sodium dodecyl sulfate
sec	second
SELEX-seq	systematic evolution of ligands by exponential enrichment-sequencing

seq	sequencing
SL	spliced-leader
snRNA	small nuclear RNA
snRNP	small nuclear ribonucleoprotein (-particle)
ss	splice site
SSR	strand switch region
T	thymidine
t	time point
T4	enterobacteria phage T4
T7	bacteriophage T7
TAP	tandem affinity purification
TBE	Tris-Borate-EDTA
T. brucei	*Trypanosoma brucei*
TEMED	N,N,N´,N´-tetramethylenediamine
TM	Trade Mark
Tris	Tris-hydroxymethylaminomethane
tRNA	transfer RNA
TSS	transcription start site
TTS	transcription termination site
Tween 20	Polyoxyethylene (20) sorbitan monolaurate
U	uridine
U	unit
USE	upstream sequence element
UTP	uridine triphosphate
UTR	untranslated region
UV	ultraviolet
V	volt
V	A, G or C
W	watt
WD40 repeat	tryptophan-aspartate repeat
WT	wildtype
Y	pyrimidine

Der Lebenslauf wurde aus der elektronischen Version der Arbeit entfernt.

The curriculum vitae was removed from the electronic version of the paper.

10 Danksagung

Ich danke zunächst Prof. Dr. Albrecht Bindereif für die Möglichkeit diese Arbeit in seinem Labor anfertigen zu können. Vor allem möchte ich mich für die sehr gute Betreuung bei allen theoretischen und praktischen Fragestellungen bedanken. Außerdem möchte ich mich herzlich bei meinem IRTG Co-Supervisor Prof. Dr. Roland Hartmann bedanken, der zudem das Zweitgutachten für diese Arbeit angefertigt hat.

Weiterer Dank gilt allen aus der AG Bindereif, die an diesem Projekt beteiligt waren. Zunächst einmal Dr. Christian Preußer, der einen Großteil der direkten Betreuung übernommen hat und unter anderem diese Arbeit kritisch gelesen hat. Des Weiteren Lee-Hsueh Hung, die die zahlreichen bioinformatischen Analysen durchgeführt hat.

Moreover, I want to thank Prof. Dr. Mark Carrington for the opportunity to participate in the DRBD4 project and to visit his laboratory in Cambridge (UK). In addition, I want to thank Janina from the Carrington lab, who helped me with Glyoxal-Northern blotting and performed essential experiments. Finally, I want to thank Dr. Steven Kelly, who analyzed the DRBD4 RNA-seq data.

Großer Dank gilt natürlich auch allen anderen Kollegen aus dem Labor, ohne die es nicht so viel Spaß gemacht hätte, wenn es einmal nicht so rund lief: Silke, die das Labor am Laufen erhält und für alles einen guten Rat hat, Oliver, Tim, Isabelle, Stefan und den Ehemaligen Heinrich und Patrick. Außerdem danke ich natürlich auch dem IRTG, das mir unter anderem den Laboraufenthalt in England sowie die Teilnahme an zahlreichen Konferenzen und Fortbildungen ermöglicht hat.

Vielen Dank auch allen Freunden aus benachbarten Arbeitsgruppen: Dennis, Lennart, Bernhard und vielen anderen für all die lustigen Abende.

Ein ganz besonderer Dank gilt natürlich meiner gesamten Familie, die mich immer unterstützt hat.

Und zu guter Letzt danke an: RSC, Fightclub, BK, BB, BG, Pizza-Nord sowie das zugehörige PL, UVP, Marböbchen, Ritzcarlton, Abaum, Sowiesx, Brick, Klim, Börse, Express, Affen, Ulo, Scara, Harlem, Aramäer Klaus, Tante Emma, Tegue und die Göttin der Weisheit: Öttexia -nebst ihrer anderen zahlreichen Erscheinungen.

11 Eidesstattliche Erklärung

Ich erkläre: Ich habe die vorgelegte Dissertation selbständig und ohne unerlaubte fremde Hilfe und nur mit den Hilfen angefertigt, die ich in der Dissertation angegeben habe. Alle Textstellen, die wörtlich oder sinngemäß aus veröffentlichten Schriften entnommen sind, und alle Angaben, die auf mündlichen Auskünften beruhen, sind als solche kenntlich gemacht. Bei den von mir durchgeführten und in der Dissertation erwähnten Untersuchungen habe ich die Grundsätze guter wissenschaftlicher Praxis, wie sie in der „Satzung der Justus-Liebig-Universität Gießen zur Sicherung guter wissenschaftlicher Praxis“ niedergelegt sind, eingehalten.

Regarding the collaborative contributions of other scientists: PTP-tagged poly(A) polymerase and CPSF160 cell lines were generated by Christian Preußer. Recombinant poly(A) polymerases were expressed, purified and assayed for *in vitro* activity by Christian Preußer. RNAi-mediated knockdown of the poly(A) polymerases and following *in vivo* polyadenylation assays were performed by Christian Preußer. CPSF160-PTP TAP was done by Christian Preußer and mass spectrometry was carried out by Monika Raabe and Henning Urlaub (MPI Göttingen). DRBD4 knockdown and RNA-seq, including data analysis were performed by Marc Carrington and Steven Kelly (University of Cambridge; University of Oxford, respectively). Analysis of iCLIP and SELEX datasets as well as the integration of iCLIP and RNA-seq datasets were done by Lee-Hsueh Hung.

Gießen, den 7.7.2016
Henrik Koch